The Pennsylvania State University

The Graduate School

Department of Civil and Environmental Engineering

# EXAMINING CONCRETE PROPERTIES CONTAINING RECYCLED GLASS CULLET AS A 100% FINE AGGREGATE REPLACEMENT

A Thesis in

Civil Engineering

by

Jared Robert Wright



Submitted in Partial Fulfillment
of the Requirements
for the Degree of

Master of Science

August 2012

The thesis of Jared Wright was reviewed and approved* by the following:

Farshad Rajabipour
Assistant Professor of Civil and Environmental Engineering
Thesis Advisor

Jeffrey A. Laman
Professor of Civil Engineering

Shelley Stoffels
Associate Professor of Civil and Engineering

Peggy Johnson
Professor of Civil and Environmental Engineering
Head of the Department

*Signatures are on file in the Graduate School

## ABSTRACT

Over 600,000 tons of glass per year cannot be recycled into new glass. These glasses are subsequently stockpiled or landfilled. A ‘greener’ and more efficient use of this glass cullet is to find use in engineering materials. This thesis investigates the use of glass cullet as a 100% fine aggregate replacement in Portland cement concrete (glasscrete) systems.

Washed glass sand was produced in order to achieve a fineness modulus similar to natural sand for use in concrete. After mixture proportioning, the fresh and hardened properties of glasscrete were evaluated and compared to natural sand concrete on a basis of similar compressive strength or similar water-to-cementitious material ratio (w/cm). The objective was to create empirical data that would provide material engineers and suppliers design specifications on the proper methods of proportioning glasscrete mixtures. In order to mitigate the deleterious alkali-silica reaction resulting from the use of silica glass as a fine aggregate, a class F fly ash was used to replace 20% of cement by weight.

Fresh property testing showed that glasscrete has better workability than natural sand concrete. Hardened property testing showed that glasscrete needs a lower w/cm to reach similar design strengths. At similar strengths, glasscrete has an earlier initial and final set time, lower coefficient of thermal expansion, greater abrasion resistance, greater resistance to ion penetration, and lower water sorptivity. At similar w/cm, glasscrete has a lower linear coefficient of thermal expansion, greater resistance to chloride ion penetration than natural sand concrete, and a lower water sorptivity than natural sand concrete. However, glascrete is less abrasion resistant at the same w/cm.

This study concludes that glasscretes have adequate workability and can sustain loads necessary for field applications. Further research is necessary to examine the glass particle-cement paste interface.

# TABLE OF CONTENTS

LIST OF FIGURES ..... vi

LIST OF TABLES ..... x

ACKNOWLEDGEMENTS ..... xii

Chapter 1 Objectives and Organization ..... 1

1.1. Introduction ..... 1
1.2. Objectives and Scope ..... 2
1.3. Outline ..... 5

Chapter 2 Background ..... 7

2.1. Motivation ..... 7
2.2. Benefits ..... 8
2.3. Problems ..... 9
2.3.1. Alkali-Silica Reaction ..... 9
2.3.2. Alkali-Silica Reaction Mitigation ..... 11
2.4. Glass as a Coarse Aggregate ..... 13
2.5. Glass as a Fine Aggregate ..... 14

Chapter 3 Experimental Materials and Methodology ..... 18

3.1. Concrete Constituents ..... 18
3.1.1. Air ..... 19
3.1.2. Water ..... 19
3.1.3. Cement ..... 20
3.1.4. Fly Ash ..... 20
3.1.5. Chemical Admixtures ..... 21
3.1.6. Coarse Aggregate ..... 21
3.1.7. Natural Sand Fine Aggregate ..... 22
3.1.8. Glass Sand Fine Aggregate ..... 24
3.2. Mixture Proportioning (ACI 211.1) ..... 27
3.2.1. Preliminary Step: Design Input ..... 28
3.2.2. Step One: Choice of Slump ..... 29
3.2.3. Step Two: Choice of Maximum Size of Aggregate ..... 30
3.2.4. Step Three: Estimation of Mixing Water and Air Content ..... 31
3.2.5. Step Four: Selection of w/cm ..... 33
3.2.6. Step Five: Calculation of Cementitious Material Content ..... 35
3.2.7. Step Six: Estimation of Coarse Aggregate Content ..... 35
3.2.8. Step Seven: Estimation of Fine Aggregate Content ..... 36
3.2.9. Step Eight: Adjustments for Aggregate Moisture ..... 36
3.2.10. Step Nine: Trial Batch Adjustments ..... 37
3.3. Strength Based Testing ..... 38

3.4. Water to Cementitious Materiao (w/cm) Based Testing .....39
3.5. Testing Protocol.....39
3.5.1. ASTM C 143: Slump Test.....39
3.5.2. ASTM C 231: Plastic Air Content via the Pressure Method.....40
3.5.3. ASTM C 403: Time of Setting of Mortar .....41
3.5.4. ASTM C 39: Compressive Strength.....45
3.5.5. ASTM C 531: Coefficient of Thermal Expansion (COTE) .....48
3.5.6. ASTM C 944: Concrete Abrasion Resistance.....55
3.5.7. ASTM C 1202: Rapid Chloride Penetrability Test (RCPT).....58
3.5.8. ASTM C 1585: Water Sorptivity .....62

4. Chapter 4 Results and Discussion .....69

4.1. ACI 211.1 Mixture Proportioning .....69
4.2. Fresh Properties.....72
4.3. ASTM C 39: Compressive Strength.....73
4.4. ASTM C 403: Time of Setting of Mortar.....80
4.5. ASTM C 531: Coefficient of Thermal Expansion (COTE).....84
4.6. ASTM C 944: Concrete Abrasion Resistance .....86
4.7. ASTM C 1202: Rapid Chloride Penetrability Test (RCPT).....87
4.8. ASTM C 1585: Water Sorptivity.....88

5. Chapter 5 Conclusions and Future Research.....97

5.1. Conclusions .....97
5.2. Future Research.....98

REFERENCES .....100

# LIST OF FIGURES

Figure **1-1**: Glass cullet stockpile in West Virginia. ..... 2

Figure **1-2**: ACI 211.1 Portland cement concrete mixture design guide comparing w/cm to 28 day compressive strength (non-air entrained). ..... 5

Figure **2-1:** ASR crack manifestation (courtesy of FHWA).. ..... 10

Figure **2-2**: Results of ASTM C 1567 showing ASR expansion of glasscrete mortars containing fly ash (Shafaatian et al. 2012)). ..... 12

Figure **2-3**: Coarse glass aggregate cullet.. ..... 14

Figure **2-4**: Fine glass aggregate cullet. ..... 15

Figure **2-5**: Decorative concrete with the top layer of paste removed shown with various waste glass cullet sizes ..... 16

Figure **3-1**: Fly ash arrived is five (5) gallon buckets from the supplier ..... 21

Figure **3-2**: Coarse aggregate stockpile outside the lab. ..... 22

Figure **3-3**: 3000 revolution glass sand (left) and natural river sand (right) as used in production. ..... 23

Figure **3-4**: LA Abrasion Machine used to crush glass cullet to sand size ..... 24

Figure **3-5**: 1000 revolution glass sand used in production.. ..... 25

Figure **3-6**: Eirich S-1 counter current concrete mixer. ..... 29

Figure **3-7**: ACI 211.1 empirical relationship between w/cm and 28-compressive strength of non-air-entrained concrete ..... 34

Figure **3-8**: Batched concrete mixture ..... 37

Figure **3-9**: Slump cone dimensions ..... 40

Figure **3-10**: Type-B pressure meter used during study. ..... 41

Figure **3-11**: Humboldt H/4133 spring-reaction device used for time of setting measurements ..... 42

Figure **3-12**: Typical mortar time of setting specimen after testing is complete ..... 43

Figure **3-13**: ASTM C 403 specimen data shown on a plot of elapsed time (min) versus penetration resistance (lbs./in$^2$).. .....44

Figure **3-14**: Research sample determination of initial and final set times using a hand-fit approach. .....44

Figure **3-15**: Sample concrete specimen prior to compressive strength testing. .....46

Figure **3-16**: Sample concrete specimen post compressive strength testing. .....46

Figure **3-17**: Wet saw used to smooth, even, and dimension concrete specimens. .....47

Figure **3-18**: Boart Longyear model CM-625 with a CSI Model CS-100-2A Retrofit .....47

Figure **3-19**: Cement paste variation in COTE due to moisture content (Figure 2 from Emanuel and Hulsey 1977). .....49

Figure **3-20**: Idealized COTE curves for cement pastes with respect to moisture content and age of cement paste (Figure 3 from Emanuel and Hulsey 1977). .....49

Figure **3-21**: Variation of COTE due to RH (from Zoldners 1971). .....50

Figure **3-22**: Estimated expansion curves due to an increased temperature at different relative humidity values (Figure 6 from Bažant 1970). .....52

Figure **3-23**: Mold used to cast COTE mortar bars. .....53

Figure **3-24**: Humboldt model BG2600-16001 comparator with specimen loaded for measurement. .....55

Figure **3-25**: Abrasion resistance specimens. .....57

Figure **3-26**: ASTM C 944 setup. .....57

Figure **3-27**: 7 Corrosion of steel reinforcing bars in concrete (Courtesy of Matco Services, Inc.). .....58

Figure **3-28**: ASTM C 1202 RCPT six (6) hour test setup. .....60

Figure **3-29**: Sample overheat correction for RCPT. .....62

Figure **3-30**: Water absorption depiction during ASTM C 1585 (Adapted from Kelham 1988).. .....67

Figure **3-31**: Vinyl electricians tape exterior coating for ASTM C 1585. .....67

Figure **3-32**: Masonry waterproofing sealant to prevent moisture ingress and escape concrete-tape interface. .....68

Figure **3-33**: ASTM C 1585 water bath setup. ..... 68

Figure **4-1**: Glasscrete and concrete specimens during moist curing. ..... 69

Figure **4-2**: Compressive strength gain for G5,5.0" and N5,5.0" ..... 73

Figure **4-3**: Compressive strength gain for G4,5.0" and N4,5.0" ..... 74

Figure **4-4**: Compressive strength gain for G4,1.5" and N4,1.5" ..... 74

Figure **4-5**: Compressive strength gain for G4,5.0" and N0.48,5.0" ..... 75

Figure **4-6**: 7 day curves that provide w/cm changes for glasscrete to match concrete strengths. ..... 78

Figure **4-7**: 28 day curves that provide w/cm changes for glasscrete to match concrete strengths. ..... 79

Figure **4-8**: Penetration resistance vs. time of setting curves for G5,5.0" ..... 80

Figure **4-9**: Penetration resistance vs. time of setting curves for N5,5.0" ..... 81

Figure **4-10**: Penetration resistance vs. time of setting curves for G4,5.0" ..... 81

Figure **4-11**: Penetration resistance vs. time of setting curves for N4,5.0" ..... 82

Figure **4-12**: Penetration resistance vs. time of setting curves for G4,1.5" ..... 82

Figure **4-13**: Penetration resistance vs. time of setting curves for N4,1.5" ..... 83

Figure **4-14**: Penetration resistance vs. time of setting curves for N0.48,5.0" ..... 83

Figure **4-15**: G5,5.0" specimen one sorptivity. ..... 89

Figure **4-16**: G5,5.0" specimen two sorptivity. ..... 90

Figure **4-17**: G4,5.0" specimen one sorptivity. ..... 90

Figure **4-18**: G4,5.0" specimen two sorptivity ..... 91

Figure **4-19**: G4,1.5" specimen one sorptivity. ..... 91

Figure **4-20**: G4,1.5" specimen two sorptivity ..... 92

Figure **4-21**: N5,5.0" specimen one sorptivity. ..... 92

Figure **4-22**: N5,5.0" specimen two sorptivity. ..... 93

Figure **4-23**: N4,5.0" specimen one sorptivity. ..... 93

Figure **4-24**: N4,5.0" specimen two sorptivity.....94

Figure **4-25**: N4,1.5" specimen one sorptivity.....94

Figure **4-26**: N4,1.5" specimen one sorptivity.....95

Figure **4-27**: N0.48,5.0" specimen one sorptivity.....95

Figure **4-28**: N0.48,5.0" specimen two sorptivity.....96

Figure **4-29**: Coloration of concrete specimens after sorptivity testing.....96

## LIST OF TABLES

Table **1-1**: Naming system for mixtures .....4

Table **3-1**: Cement and Fly Ash oxide compositions.....20

Table **3-2**: Sieve Analysis for natural sand source.....23

Table **3-3**: Sieve analysis for fine glass sand .....27

Table **3-4**: Naming system for mixtures .....28

Table **3-5**: Sample values from Table 6.3.3 (ACI 211.1) relating the MSA and slump in order to find the water content of concrete ($lb/yd^3$) .....31

Table **3-6**: Sample values from Table 6.3.3 (ACI 211.1) relating the MSA and slump in order to find the water content of concrete ($lb/yd^3$) while using air entrainment.....31

Table **3-7**: Sample values from Table 6.3.6 (ACI 211.1) relating the MSA and the fineness modulus in order to find the coarse aggregate's apparent volume.....36

Table **3-8**: Target 7 day strengths. .....38

Table **3-9**: COTE ($10^{-6}$/°F) of various aggregate and cementitious mixtures in the saturated condition. (Courtesy of Mindess et al 2003, Meyers 1940, and Neville 1995) .....54

Table **3-10:** Qualitative description of concrete chloride ion penetrability. .....60

Table **4-1**: Research final mixtures (aggregates in oven dried condition) .....70

Table **4-2**: Research final mortar mixtures (aggregates in oven dried condition).....70

Table **4-3**: Chemical admixture proportioning (fluid ounces per pound of cementitious material) .....71

Table **4-4**: Chemical admixture proportioning (fluid ounces per cubic yard of concrete).....71

Table **4-5**: Strength gain for glasscrete and natural sand concrete (psi).. .....76

Table **4-6**: Coefficient of Variation (%) for glasscrete and natural sand concrete.....76

Table **4-7**: Range (%) of cylinder strengths of three (3) specimens for glasscrete and natural sand concrete.....76

Table **4-8**: ASTM C 403 time of setting values (hours: minutes).....80

Table **4-9**: COTE test results.....85

Table **4-10**: COTE ($10^{-6}$/°F) of various aggregate and cementitious mixtures in the saturated condition. (Courtesy of Mindess et al 2003; Meyers 1940; and Neville 1995). .....85

Table **4-11:** Average mass loss of three (3) specimens due to abrasion over six minutes.....86

Table **4-12**: RCPT results (Coulombs), bold-faced specimens overheated .....87

Table **4-13:** Sorptivity values ($10^{-4}$mm/sec$^{1/2}$)... .....89

# ACKNOWLEDGEMENTS

Let me begin by extending my appreciation to my thesis advisor and thesis committee chair, Dr. Farshad Rajabipour. His patience and interest in my development went well beyond the walls of CITEL. I express gratitude to Drs. Jeffrey Laman and Shelley Stoffels for participating as members of my thesis committee. Also, the financial support by the Hawaii DOT and FHWA under grant #HWY-L-2.6129 is acknowledged.

I would be remising without thanking Mr. Chris Cartwright, who unselfishly assisted me during the many trial and error loops associated with concrete testing. Others who assisted me in this process are, in no particular order, Mr. Alireza Akhavan, Mr. Seyed-Mohammad-Hadi (Afshin) Shafaatian, Mr. Hamed Maraghechi, Mr. Joe Reiter, Mr. Greg Braun, and Ms. Danielle Lombardi. Also, the assistance of Mr. Dan Fura could never be overlooked.

I would like to thank my brother for proving to be a reliable sounding board, sometimes even unwittingly. In addition, as always, I am indebted to my parents for their unfailing concern and wise counsel.

# Chapter 1: Objectives and Organization

## 1.1. Introduction

Portland cement concrete is the most widespread construction material in use today. Since the development of Ordinary Portland Cement (OPC) around the turn of the 19th Century, academia and industry have teamed in the search for ways to make concrete stronger, more durable, and more economical (Mindess et al 2003). Design standards and specifications (e.g. ACI 318; ACI 211.1; PCA Design Manual) have been created and expert committees have been formed in order to achieve these goals. The cement industry accounts for approximately 5% of the anthropogenic carbon emissions in the US (PCA 2012). The United State consumes 5.32MJ of energy per kilogram of cement produced (Mindess et al 2003). However, this energy is embodied in concrete throughout its long life cycle (PCA 2012; Mindess et al. 2003). Due to high greenhouse gas emission, energy consumption, and insatiable desire to consume virgin earth aggregates during the production of Portland cement concrete, a new push is focused on making the concrete industry more environmentally friendly. 'Greener' ways of producing concrete can be the use of supplementary cementitious materials (such as ground granulated blast-furnace slag, fly ash, silica fume, and glass powder) or the use of recycled aggregates.

Information gathered by the United States Environmental Protection Agency (USEPA) in 2010 states that 27.1% (3.13 million tons) of the 11.53 million tons of post-consumer glass (i.e. bottles and windows) generated per year by the United States is recycled (Municipal 2011). The remaining 72.9% of post-consumer glass is discarded along with other household wastes into landfills. Of the 3.13 million tons of glass collected for recycling, 80% is recycled into new glass

(Reindl 2003). The other 20% (approximately 600,000 tons/year) is subsequently stockpiled (Figure 1.1) or sent back to landfills. Other factors contributing to lowering the recycling rate of glass includes prohibitive transportation costs, color discrepancies, and deleterious organics along the glass surfaces (Reindl 2003). This research is focused on developing engineering specifications that allow recycling those 600,000 tons of glass as fine aggregate into concrete. This study will investigate the fresh and hardened properties of concrete while using recycled glass cullet as a 100% fine aggregate replacement (*glasscrete*). This study will also be used to develop design standards and specifications on how to proportion glasscrete to obtain desirable strength and durability.

Figure **1-1**: Glass cullet stockpile in West Virginia

## 1.2. Objectives and Scope

The main focus of this research is to provide material engineers and concrete suppliers for the state of Hawaii supplementary specifications for the safe and reliable use of recycled glass as an aggregate in Portland cement concrete. This study, therefore, investigates the relationship

between the water to cementitious material ratio (w/cm) and the compressive strength of glasscrete, in comparison to concrete made with natural sand. *ACI 211.1: Standard Practice for Selecting Proportions for Normal, Heavyweight and Mass Concrete (2009)* mixture proportioning methods were utilized in order to provide example glasscrete mixture proportions for adoption by commercial material suppliers. The fresh and hardened properties of these mixtures were then tested in order to evaluate the difference between glasscrete and natural sand concrete.

Table 1-1 provides a simple naming system for glasscrete and natural sand concrete mixtures to be compared throughout the study. The bulk of the research will compare properties of the two types of concrete at similar design compressive strengths. This is a typically replicated procedure that allows for a fundamental understanding of the concrete's composition versus strength that can then be expanded upon to improve the material's quality (Popovics 1990). Research results will be presented in the form of charts (similar to Figure 1-2) linking the compressive strength of glasscrete to a particular w/cm. This information will be collected for the compressive strengths in the range of 3000 lbs./in$^2$ to 6000 lbs./in$^2$ and will be very valuable to material suppliers when proportioning glasscrete mixtures. Research will also compare natural sand concrete and glasscrete at similar design w/cm ratios. The following tests are performed on all concrete mixtures:

- ASTM C 143: *Standard Test Method for Slump of Hydraulic-Cement Concrete*
- ASTM C 231: *Standard Test Method for Air Content of Freshly Mixed Concrete by the Pressure Method.*
- ASTM C 39: *Standard Test Method for Compressive Strength of Cylindrical Concrete Specimens*: to evaluate the strength development with age
- ASTM C 403: *Standard Test Method for Time of Setting of Concrete Mixtures by Penetration Resistance*

- ASTM C 531: *Linear Shrinkage and Coefficient of Thermal Expansion of Chemical-Resistant Mortars, Grouts, Monolithic Surfacings, and Polymer Concretes*
- ASTM C 944: *Abrasion Resistance of Concrete or Mortar Surfaces by the Rotating-Cutter Method*
- ASTM C 1202: *Electrical Indication of Concrete's Ability to Resist Chloride Ion Penetration*
- ASTM C 1585: *Measurement of Rate of Absorption of Water by Hydraulic-Cement Concrete*

Table **1-1**: Naming system for mixtures

| Mixture | Design Strength (ksi) | Design Slump | Fine Aggregate | Potential Applications |
|---|---|---|---|---|
| N5,5.0" | 5000 | 5.0" | Natural Sand | Building Frames and Bridge Decks |
| G5,5.0" | 5000 | 5.0" | Glass Sand | Building Frames and Bridge Decks |
| N4,5.0" | 4000 | 5.0" | Natural Sand | Building Frames and Bridge Decks |
| G4,5.0" | 4000 | 5.0" | Glass Sand | Building Frames and Bridge Decks |
| N4,1.5" | 4000 | 1.5" | Natural Sand | Pavements or Slip-Form Applications |
| G4,1.5" | 4000 | 1.5" | Glass Sand | Pavements or Slip-Form Applications |
| N0.48,5.0" | ? | 5.0" | Natural Sand | Building Frames and Bridge Decks |

These tests will provide adequate information in order to provide provisions and specifications for the use of glass sand in concrete systems by the concrete industry. Due to the environment in Hawaii, a mild freeze-thaw condition was considered and the mixtures were designed for a target air content of 3.0%. The resulting w/cm did not undergo further

modification based on durability criteria (e.g. chloride or sulfate exposure); but this can be done by the material designer by following ACI 211.1 provisions. Similar design procedures could be followed to design air entrained concrete for moderate or severe freeze-thaw conditions. In order to mitigate the alkali-silica reaction (ASR) resulting from the use of silica glass as fine aggregate, twenty percent (20%) of cement's weight is replaced with a Class F fly ash, as suggested by the work of Shafaatian et al. on ASR prevention in glasscrete mixtures ( 2012).

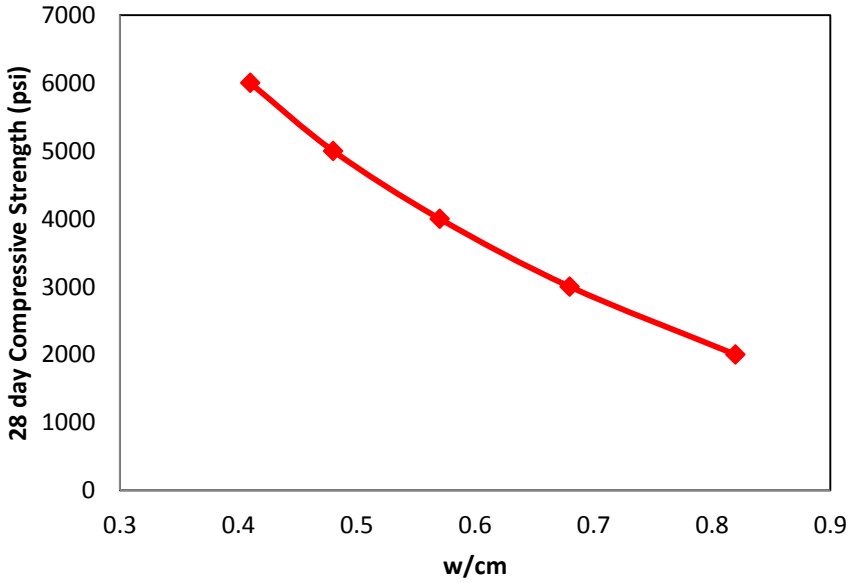


Figure **1-2**: ACI 211.1 Portland cement concrete mixture design guide comparing w/cm to 28 day compressive strength (non-air entrained)

### 1.3. Outline

This thesis is presented in four (4) remaining chapters. **Chapter 2** will provide the motivation and background on the use of recycled glass in concrete materials. **Chapter 3** discusses the materials and methods used throughout proportioning and testing of glasscrete and natural sand concrete mixtures. This chapter will also discuss the various theories behind the tests performed. **Chapter 4** presents the results and provides various discussions based on either a

comparison at similar design compressive strengths or similar w/cm. **Chapter 5** will provide the conclusions and suggestions for further research.

**Chapter 2**

# Chapter 2: Background

## 2.1. Motivation

One, out of many, definitions for the term ‘recycle’ offered from the Merriam-Webster Dictionary is ‘to adapt to a new use.’ Juxtapose that definition with another from the same dictionary, ‘to make ready for reuse,’ and the ideas are conflicting. Paper, for example, is commonly recycled in order to reuse as paper again in the future (this is often noted on the paper pad itself). Post-consumer soda-lime glass (e.g. bottles and window panes) are also recycled for reuse as glass products. However, due to economic constraints, as discussed below, not all post-consumer glass can be recycled into new glass and a significant portion ends up in stockpiles and landfills. Christian Meyer, in 2001, called for “Yankee ingenuity” to defy conventional recycling thought (Meyer 2001). Meyer wanted to recycle used glass as aggregate for use in concrete (known to many as ‘down-cycling’). Meyer planned to exploit this meaning of the term ‘recycle.’

The evolving denotation of the term ‘recycle’ comes as a necessity for the environment. Alarmingly low glass recycling rates mentioned in Chapter 1 (27% of 11.3 million tons) (Municipal 2011) contributed to crippling the world’s largest landfill, the Fresh Kills Landfill of Staten Island, New York. The Fresh Kills Landfill was subsequently closed in 2001 (Meyer 2001). This example of landfill area reduction leads to increased transportation costs to existing, operating landfills. Landfilling and disposal of glass is an acute issue for high density populations (e.g. northeastern US) and remote areas (e.g. Hawaii and the Rocky Mountain states).

These issues continue to make recycling a problem for states such as New York (Jin et al. 2000); which, along with Hawaii (Rajabipour 2010 et al.), Montana (Berry et al. 2011), Pennsylvania (Shafaatian et al. 2012; Maraghechi et al. 2012; Wartman et al 2004), and

Wisconsin (Polley et al. 1998), are all searching for alternative ways to recycle their glass. These states used their creativity to test the feasibility of using glass in concrete. Other nations such as Turkey (Topcu and Canbaz 2004; Turgut and Yahlizade 2009), South Korea (Park et al. 2004), The United Kingdom (Limbachiya 2009; Zhu and Byars 2005; Byars et al. 2004), Italy (Saccani and Bignozzi 2010), China (Kou and Poon 2009), and Australia (Shayan and Xu 2003) have reviewed the feasibility of using glass in concrete as well. Glass cullet has also been used and can perform well when used for road and pavement base layers, asphalt (glassphalt), landfill covers, reflective road strip materials, and salt/sand for deicing purposes (Wartman et al. 2004). The following sections will provide a discussion on the benefits of using recycled glass and a literature review of how different glass aggregates affect the fresh and hardened properties of concrete.

## 2.2. Benefits

The extensive use of glass across the nation allows for easy access to recycled glass cullet. Glass cullet is post-consumer broken down pieces of glass that cannot be reused in the bottling industry (Wartman el al. 2004). The use of glass cullet in concrete will both reduce the environmental costs of quarrying virgin natural aggregates and the transportation cost of shipping the quarried aggregates (Berry et al. 2011). Berry et al. also believes marketing glasscrete to the nation would help increase the rate of recycling glass (2011). The Leadership in Energy and Environmental Design (LEED) has recognized the use of recycled waste glass as an aggregate replacement and a number of LEED credits could be earned by use of recycled glass aggregates (LEED 2009). Also, European Standards have introduced specifications facilitating the use of natural, recycled, and manufactured aggregate materials (not necessarily glass) (Limbachiya 2009).

It is noted in prior research that simply replacing natural sand with waste glass may not provide a substantial economic benefit (Jin et al. 2000). However, the marginal cost benefit coupled with the abundance of environmental benefits hope to provide sound reasoning to use waste glass as an aggregate for many years to come (Jin et al. 2000; Berry et al. 2011). If a producer of over five (5) million 'blocks' of concrete (a feasible and often matched level) can replace 10% of aggregate with glass, then that single manufacturer could absorb ten thousand (10,000) tons of waste glass per year. Ten thousand tons is approximately 10% of the waste glass created by New York City annually (Jin et al. 2000).

## 2.3. Problems

Sugars, paper and other impurities present along the recycled glass cullet may negatively impact the strength of concrete. As such, it is important to properly wash the glass cullet and use magnetic and/or air separation devices to remove contaminants. (Polley et al. 1998; Rajabipour et al. 2009). The weak bond between the glass aggregate and cement paste may also reduce the concrete strength (Polley et al. 1998). Terro notes a difference in the glass aggregate's coefficient of thermal expansion (COTE) when compared to cement paste (2006). This may cause a differential expansion in the concrete (Terro 2006). A part of this study will be quantifying the COTE and other hardened properties of glasscrete.

### 2.3.1. Alkali-Silica Reaction

The overwhelming concern in using glass as an aggregate replacement in concrete is the potential for Alkali-Silica Reaction (ASR). ASR (Figure 2-1) is manifested by map cracking along the surface and through the volume of concrete. These cracks often exude a silica gel that

has been formed as a result of ASR (Mindess et al. 2003). Gel is formed when the alkali rich pore fluid of cement paste attacks the silicate aggregate. The aggregate structure is dissolved in the pore fluid and subsequently precipitates in the form of a silica gel. This gel has the capacity to swell in the presence of water and causes volumetric expansion and cracking of concrete (Mindess et al 2003, Hewlett 1998).

Figure **2-1**: ASR crack manifestation (courtesy of FHWA)

After years of postulation upon the origin of ASR in glasscrete systems, research by Rajabipour was able to locate the origin of ASR (2010). By utilizing Scanning Electron Microscopy (SEM), ASR was found to occur along the micro-cracks within the crushed glass cullet (Rajabipour 2010). Larger glass sand particles were found to have higher crack density, wider cracks, and more interconnected micro-cracks which resulted in a higher potential for ASR expansion. These intra-particle micro-cracks initiate during bottle crushing and will allow the alkali rich pore fluid of cement paste to penetrate into the glass particle and allow ASR to form in the interior of the glass (Rajabipour 2010). Additionally, no ASR was found to be forming along the interfacial transition zone (ITZ) (Rajabipour 2010).

Jin and Meyer tested aggregate batches with only similar color glass aggregate (2000). It was found that different color glasses react differently in terms of ASR (Zhu and Byars 2005; Jin

and Meyer 2000; Byars et al 2004). It was found that amber glass and green glass cullet were less reactive at the same proportions and sieve sizes than clear glass cullet. Green glass was found to be particularly less reactive when used as an aggregate replacement (Jin et al. 2000). However, results by Dhir et al. were contrary to these results showing green glass being the most expansive glass color (2009). Amber glass is created by adding iron oxide ($Fe_2O_3$) while creating the soda-lime glass. Green glass is created by adding chromium oxide ($Cr_2O_3$) while creating glass. The chemical bonding of these oxides to glass may result in different ASR gel compositions (Jin et al 2000; Dhir et al. 2009). Saccani and Bignozzi also suggest a strong influence between the glass chemical composition and subsequent susceptibility to ASR (2010). Rajabipour et al also states that additional testing showed that none of different glass colors were completely void of expansion (2009). It is likely that the costs associated with separating the multi-color glass cullet will make it difficult to mass produce single color glass cullet. This current study will therefore use a mixed color glass cullet throughout research.

### 2.3.2. Mitigation of Alkali-Silica Reaction

ASR can be mitigated using supplementary cementitious materials such as ground granulated blast furnace slag, fly ash, silica fume, or glass powder (Topcu et al 2008; Berry et al 2011). ASR can also be mitigated by annealing (healing the micro-cracks by heating) the glass (Maraghechi et al. 2012) or by use of lithium admixtures. ASR can be mitigated by controlling the alkalinity (pH levels) of concrete's pore solution, controlling the available moisture, or controlling the amount of reactive silica (Mindess et al. 2003). Controlling the alkalinity can be achieved by using low alkali cement or by using supplementary cementitious materials such as fly ash. As summarized by Shafaatian et al., fly ash may help in the mitigation of ASR by alkali binding, limiting mass transport, reducing aggregate dissolution rate, and improving tensile

strength of concrete (2012). Fly ash's ability to bind and dilute the alkalis in the concrete system is found to be its main and most productive mechanism for ASR mitigation (Thomas 2011). The moisture availability can be controlled by the w/cm. A lower w/cm will limit the supply of external water by reducing concrete permeability and therefore slow the ASR expansion rate within the concrete (Mindess et al. 2003). The silica variability from aggregate to aggregate causes the reaction to vary depending on aggregate mineralogy, internal porosity as well as other properties (Mindess et al. 2003).

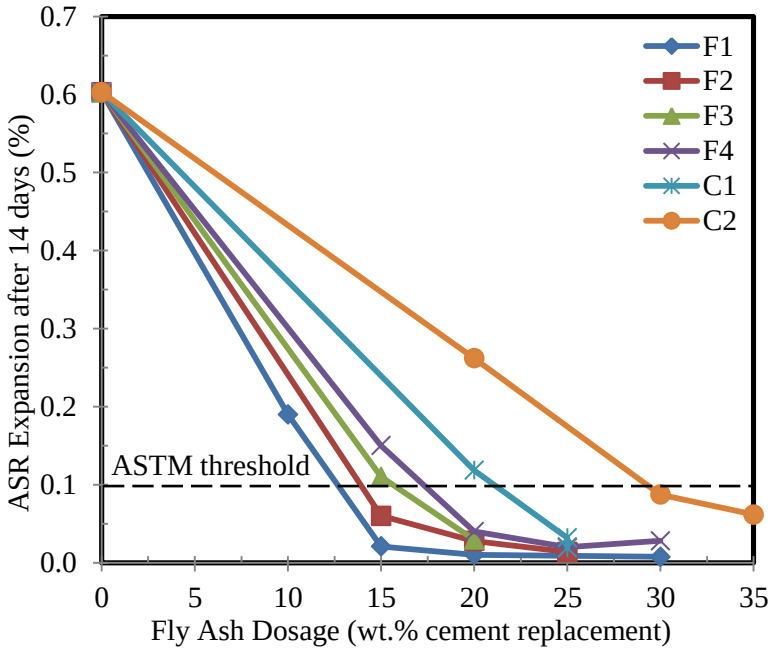


Figure **2-2**: Results of ASTM C 1567 showing ASR expansion of glasscrete mortars containing fly ash (Shafaatian et al. 2012)

Shafaatian et al. performed accelerated ASR testing on glasscrete mortar bars according to ASTM C 1567 (2012). Their results (Figure 2-2) are based on testing mortars containing one of six different ASTM C 618 fly ashes (4 class F fly ashes and 2 class C fly ashes). The results show that all fly ashes can reduce ASR expansion. However, to sufficiently mitigate ASR and to lower expansion below the ASTM threshold of 0.1%, different dosages were required for different fly

ashes. For example, while 15% F1 fly ash can sufficiently suppress ASR, 35% C2 fly ash is needed to do the same. In the present study, 20% F3 fly ash is used in all concrete mixtures to mitigate the risk of ASR. The oxide composition of this fly ash will be offered in Chapter 3.

## 2.4. Glass as a Coarse Aggregate

Coarse aggregates (Figure 2-3) are typically recognized as particles greater than the number 4 sieve (or 0.187 inch). Research has shown coarse glass aggregate can be hazardous to handle due to particularly sharp edges (Polley et al. 1998). The limited thickness (< ¼ inch) of glass bottles and window panes result in platy and needle shape particles when glass is crushed to coarse aggregate sizes. It it also difficult to coat the entire coarse glass particle with cement paste due to its irregular and complex shape. This leads to decreased workability of concrete (Polley et al. 1998; Terro 2006)

Coarse glass aggregate also performed poorly in concrete strength tests (Popovics 1987, Johnston 1974). Popovics found that the compressive strength results of concrete containing coarse glass aggregate were much lower than similar concretes made with aggregate from natural sources (1987). This has been attributed to the flat and elongated shape of coarse glass whose smoother and flatter surfaces have less chance to form constructive bonds and interfaces with cement paste (Polley et al. 1998).

Figure **2-3**: Coarse glass aggregate cullet

In summary, coarse glass aggregate is not suitable for use in concrete due to its negative impact on workability and strength of concrete. Therefore, this study focuses on use of glass as fine aggregate.

## 2.5. Glass as a Fine Aggregate

Fine aggregate (Figure 2-4) is generally characterized as aggregates between the sizes of 0.187 in and 0.003 in (#4 and #200 sieve). Most specifications limit the amount of aggregate passing the #100 sieve due to an increase in the water demand to attain workable concrete (Mindess et al. 2003).

Tests have shown promise for the use of fine glass aggregate in concrete systems (Polley et al. 1998; Jin et al. 2000; Kou and Poon 2009). Fine glass aggregate demonstrate shape characteristics similar to crushed natural sand (both angular with an aspect ratio close to 1); this

was also discussed by Wartman et al. (2004). Concrete workability is generally comparable if not better when compared to natural sand mixes (Polley et al. 1998; Topcu and Canbaz 2004; Kou and Poon 2009; Terro 2006). Strength tests were noted to perform better than coarse glass aggregate tests and vary depending on fine glass volume content when compared to natural sand aggregate concrete mixtures (Polley et al 1998, Topcu and Canbaz 2004).

Figure **2-4**: Fine glass aggregate cullet

Polley et al. noted that glasscrete properties such as compressive strength were adversely affected by glass cullet that was unwashed (1998). This may be due to waste particles such as plastics and paper, as well as organics along the glass surfaces that cause retardation in hydration of cement and a weak bond between the glass aggregate and cement paste. Polley et al. note a variability in the compressive strength of concrete containing fine glass aggregate (1998). Their research shows ranges from 25% strength loss to a 5% strength gain when glasscrete is compared to natural sand concrete mixtures (Polley et al. 1998). They researched the use of glass as a partial

fine aggregate replacement and not a full sand replacement in concrete; and concluded by stating that more research is necessary to completely understand the variances in glasscrete mixtures depending on glass sand volume content (Polley et al. 1998). It should be noted that this current study uses glass sand as a 100% fine aggregate replacement.

The slump may remain the same at a lower dosage of plasticizer for glasscrete when compared to natural sand concrete (Kou and Poon 2009). This may be due to weaker cohesion between the glass and fresh cement paste due to the smooth and impermeable surfaces of glass (Kou and Poon 2009). Kou and Poon also observed adequate segregation resistance in glasscrete mixtures (2009). Polley et al. found glasscrete to be workable when implemented in the field (1998). Alternatively, the angularity of the glass surfaces may reduce the slump. The time of setting of glasscrete may increase with an increasing volume percentage of glass sand (Terro 2006).

Figure **2-5**: Decorative concrete with the top layer of paste removed shown with various waste glass cullet sizes

The low water absorption of glass may increase the freeze-thaw resistance and lower the permeability of concrete (Maraghechi 2010). Also, the low porosity and absorption of glass sand has shown to reduce drying shrinkage (Kou and Poon 2009). The low porosity can also reduce the chloride penetrability and therefore be more resistant to chloride induced corrosion (Kou and Poon 2009). These durability benefits may allow glass to be used in high-performance concretes (Meyer 2001). Glass has a low thermal conductivity and could reduce the costs of heating and air conditioning when used as an aggregate in concrete building envelopes. The varying colors of the glass can be used for aesthetic purposes in architectural concrete (such as flooring and countertops) as shown in Figure 2-5 (Maraghechi 2010).

# Chapter 3: Experimental Materials and Methodology

This chapter will present detailed information on the materials and the experimental methods used throughout the research to achieve the objectives outlined in Chapter 1. The goal is to utilize ACI 211.1 to create glasscrete and natural sand concrete mixtures to achieve similar compressive strengths. Another goal is to create glasscrete and natural sand concrete with similar w/cm. After mixtures have been created, this study will compare the fresh and hardened properties of glasscrete to natural sand concrete. Basic concepts and theory behind the various tests will be expanded upon.

Fresh property testing will consist of slump (ASTM C 143), plastic air content (ASTM C 231), and time of setting (ASTM C 403). Hardened property testing will consist of compressive strength (ASTM C 39), coefficient of thermal expansion (ASTM C 531), abrasion resistance (ASTM C 944), rapid chloride penetration resistance (ASTM C 1202), and water sorptivity (ASTM C 1585). In addition to discussing the tests above, this section will discuss the concrete constituents, procurement, and mixture proportioning procedure.

## 3.1. Concrete Constituents

The following sections will discuss the constituents that were used in proportioning the concrete throughout this research. The basic concrete constituents are coarse aggregate, fine aggregate, water, air, cement, and fly ash. Plasticizers and air entraining admixtures were also used throughout this study. The coarse aggregate, water, cement, and fly ash did not differ in properties across the natural sand concrete and glasscrete mixtures. However, the fine aggregate's

properties change due to glass being used as a 100% fine aggregate replacement for glasscrete systems.

### 3.1.1. Air

Air is a main part of the cement paste matrix and accounts for the isolated air pockets that are entrapped in the cement paste during mixing and placement of concrete (Mindess et al. 2003). In addition, well-dispersed fine air voids can be entrained inside cement paste by using air entraining admixtures and these can allow for expansion of ice during the freezing and thawing cycles (Mindess et al. 2003). While entrained air improves the freeze-thaw durability of concrete, both entrapped air and entrained air reduce the strength of concrete (Du and Folliard 2005). The air content, theory behind air entrainment and other parameters related to air void systems in concrete will be discussed further throughout this chapter. The concrete mixtures created in this study are for a mild freeze-thaw environment in Hawaii. Therefore, the design air content of glasscrete and natural sand concrete was maintained at 3.0%.

### 3.1.2. Water

Experimental testing was meant to replicate industrial scale production of concrete as closely as possible; therefore, ordinary tap water was used throughout experimentation. Water was typically batched in one gallon water jugs, five to ten minutes prior to mixing to prevent evaporation. The water faucet was allowed to run continuously in order to allow the water to remain at constant temperature for a particular single mixture.

### 3.1.3. Cement

ASTM C 150 Type I Portland cement was used throughout experimentation. The cement was procured from a supplier in Nazereth, PA. Table 3-1 provides information on the oxide composition of the cement. Type I cement has a specific gravity of 3.15.

Table **3-1**: Cement and Fly Ash oxide compositions

| Oxide | Cement | Fly Ash |
|---|---|---|
| CaO | 62.5 | 3.81 |
| $SiO_2$ | 19.9 | 49.20 |
| $Al_2O_3$ | 5.44 | 23.34 |
| $Fe_2O_3$ | 2.26 | 14.72 |
| $Na_2O$ | 0.30 | 0.69 |
| $K_2O$ | 0.89 | 1.78 |
| MgO | 2.31 | 1.03 |
| MnO | 0.09 | 0.03 |
| $TiO_2$ | 0.29 | 1.03 |
| $SO_3$ | 4.93 | 1.47 |
| $P_2O_5$ | 0.23 | 0.35 |
| LOI | 0.86 | 2.55 |
| $Na_2O_{eq}$ | 0.89 | 1.86 |

### 3.1.4. Fly Ash

Past research based on mortar bars containing 100% glass sand (ASTM C 1567) suggested the use of a locally available class F fly ash at a dosage of 20% replacement of Portland cement by weight to mitigate ASR in glasscrete (Shafaatian et al. 2012). Typical Class F fly ash used in this research had a specific gravity of 2.4. Fly ashes range in size, geometry, and composition (Quan 2011, Shafaatian et al 2012); therefore, the same fly ash with an oxide content

shown in Table 3-1 was used throughout this study. Figure 3-1 shows the typical laboratory storage of fly ash.

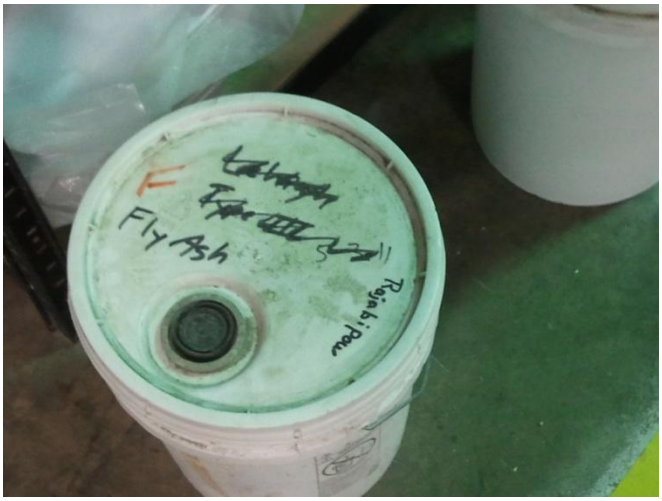


Figure **3-1**: Fly ash arrived is five (5) gallon buckets from the supplier

### 3.1.5. Chemical Admixtures

Both a super plasticizer and an air-entraining admixture were used during this study. The super plasticizer was Glenium® 7710 manufactured by BASF and was used to achieve a consistent workability across the varying mixtures. The air-entraining admixture was MB-AE™ 90, also manufactured by BASF. The air entrainer was used to obtain the desired air content and distribute the air bubbles evenly through the cement paste.

### 3.1.6. Coarse Aggregate

Coarse aggregates are shown in Figure 3-2. This aggregate stockpile complied with ASTM C 33 for a #57 type aggregate. The maximum size aggregate (MSA) was 1.0" and all

aggregate smaller than the #4 sieve were expelled via a wet sieving procedure. The coarse aggregate was a locally available crushed limestone. The aggregate was batched at oven dried conditions (mixed at room temperature) and used both for glasscrete and natural sand concrete mixtures. The aggregate properties were as follows:

- Dry-Rodded Unit Weight (DRUW): 95.51 lbs/ft$^3$
- Oven-Dried Specific Gravity: 2.80
- Absorption Capacity: 0.60%

Figure **3-2**: Coarse aggregate stockpile outside the lab

### 3.1.7. Natural Sand Fine Aggregate

Natural sand aggregate (as seen is juxtaposed to glass sand in Figure 3-3) used throughout this research adhere to ASTM C 33 for use as a fine aggregate in concrete. The fineness modulus for the sand was measured as 2.93. The aggregate size distribution is provided

in Table 3-2 below. The sand was batched at oven dried conditions (mixed at room temperature) throughout the study. The natural sand properties were as follows:

- Oven-Dried Specific Gravity: 2.60
- Absorption Capacity: 0.96%

Table **3-2**: Sieve Analysis for natural sand source

| Sieve Size | Cumulative % Retained |
|---|---|
| 3/8" | 0 |
| #4 | 2 |
| #8 | 22 |
| #16 | 38 |
| #30 | 55 |
| #50 | 81 |
| #100 | 95 |
| FM (ASTM C 125) | 2.93 |

Figure **3-3**: 3000 revolution glass sand (left) and natural river sand (right) as used in concrete production

### 3.1.8. Glass Sand Fine Aggregate

The glass was procured from a local recycling company that provided sacks of clear glass cullet and mixed color glass cullet (green, amber, orange, blue, etc.). In order to facilitate an ease of production while maintaining color consistency, a distribution of two (2) pounds of mixed color cullet to one (1) pound of clear cullet was followed while crushing the glass into sand size. The following process was followed to produce fine glass sand aggregate.


Figure **3-4**: LA Abrasion Machine used to crush glass cullet to sand size

1. Obtain recycled glass cullet ranging in size from 1/16 inch to 1 inch.
2. Wash glass cullet thoroughly using a wet sieve approach to expel deleterious materials such as paper and organics. (Similar to approach by Polley et al. (1998)).
3. Place glass cullet in stainless steel trays inside oven and heat until all water has evaporated.
4. Remove oven dried glass cullet and allow it to cool to room temperature.

5. Place approximately 20 lbs. of glass cullet in a standard Los Angeles (LA) Abrasion Machine (Figure 3-4)
6. Two different revolution quantities were used to obtain glass sand, as described below:
    a. Rotate approximately 20 lbs. of glass cullet in the LA Abrasion Machine for 1000 revolutions. Remove all glass aggregate from the LA Abrasion Machine. Expel all glass particles retained on sieve number 4 or greater. Please view Figure 3-5 for a final product.
    b. Rotate a different 20 lbs. batch of glass cullet in the LA Abrasion Machine for 3000 revolutions. Remove all glass particles retained on sieve #4 and passing sieve #100. A wet sieve procedure is employed in order to remove aggregate passing the #100 sieve. After the process is complete, oven dry the aggregate until the water is completely removed. Please view Figure 3-3 for a final product and its juxtaposition to natural sand.
7. Allow separate containers to store the aggregate of the 1000 revolutions and the aggregate of the 3000 revolutions.

Figure **3-5**: 1000 revolution glass sand used in production

A trial and error approach was used to fine tune details of the glass sand preparation procedure. The resulting data showed that by blending the 1000 revolution glass aggregate and 3000 revolution glass aggregate on a 50/50 basis, the aggregate size distribution comparable to the natural sand (Table 3-2) can be obtained. The fineness modulus is also similar at approximately 3.00. Table 3-3 shows the aggregate size distribution of recycled glass sand measured at several times throughout research.

The aggregate was batched at oven dried conditions (mixed at room temperature). Table 3-3 shows a combined fineness modulus of between 3.08 and 2.91 that passes ASTM C 33 standards. The FM is defined (ASTM C 125) as the sum of the cumulative percentages retained on the standard sieves between the numbers four (#4) and one-hundred (#100) divided by one-hundred (100). According to ASTM C 33, the FM may fluctuate within 0.20 for a given concrete mixture design. Since the FMs of natural sand concrete and glasscrete were 2.93 and 3.06 are within 0.20 of each other, the FM of 3.00 was used in design of concrete mixtures throughout this study.

The fine aggregate gradation is known to have a large impact on the workability of concrete by affecting the water demand as well as the particle packing of aggregates which determines the required paste content (Neville 1995, Mindess et al. 2003). Although the FM is a rough estimate of the consistency across mixtures, its simplicity in evaluation and rudimentary properties provide concrete suppliers a basis for quality control of workability (Mindess et al. 2003).

The properties of the glass sand were as follows:

- Oven Dried Specific Gravity: 2.53
- Absorption Capacity: 0.00%

Table **3-3**: Sieve analysis for fine glass sand

| | 5/24/2011 | | | 6/7/2011 | | |
|---|---|---|---|---|---|---|
| Sieve Size | Cumulative % Retained (1000 Revs) | Cumulative % Retained (3000 Revs) | Overall % Retained | Cumulative % Retained (1000 Revs) | Cumulative % Retained (3000 Revs) | Overall % Retained |
| (3/8) in | 0 | 0 | 0 | 0 | 0 | 0 |
| #4 | 0 | 0 | 0 | 0 | 0 | 0 |
| #8 | 21 | 15 | 18 | 24 | 14 | 19 |
| #16 | 46 | 40 | 43 | 44 | 40 | 42 |
| #30 | 66 | 64 | 65 | 64 | 64 | 64 |
| #50 | 82 | 85 | 83.5 | 84 | 88 | 86 |
| #100 | 93 | 100 | 96.5 | 92 | 100 | 96 |
| FM | 3.08 | 3.04 | 3.06 | 3.08 | 3.06 | 3.07 |

| | 9/20/2011 | | | 12/12/2011 | | |
|---|---|---|---|---|---|---|
| Sieve Size | Cumulative % Retained (1000 Revs) | Cumulative % Retained (3000 Revs) | Overall % Retained | Cumulative % Retained (1000 Revs) | Cumulative % Retained (3000 Revs) | Overall % Retained |
| (3/8) in | 0 | 0 | 0 | 0 | 0 | 0 |
| #4 | 0 | 0 | 0 | 0 | 0 | 0 |
| #8 | 25 | 9 | 17 | 18 | 10 | 14 |
| #16 | 50 | 35 | 42.5 | 41 | 38 | 39.5 |
| #30 | 67 | 62 | 64.5 | 69 | 59 | 64 |
| #50 | 86 | 85 | 85.5 | 84 | 80 | 82 |
| #100 | 97 | 100 | 98.5 | 96 | 100 | 98 |
| FM | 3.25 | 2.91 | 3.08 | 3.08 | 2.87 | 2.98 |

### 3.2. Mixture Proportioning (ACI 211.1)

ACI 211.1 provides a multi-step process for proportioning normal, heavy weight, and mass concrete mixtures. This section will review the ACI 211.1 steps and provide insight into what particular proportioning choices were made throughout this research. Mixture proportions

for all seven (7) mixtures outlined in Table 1-1 from page 3 (reintroduced as Table 3-4) are provided in the results section.

Table **3-4**: Naming system for mixtures

| Mixture | Design Strength (ksi) | Design Slump | Fine Aggregate | Potential Applications |
|---|---|---|---|---|
| N5,5.0" | 5000 | 5.0" | Natural Sand | Building Frames and Bridge Decks |
| G5,5.0" | 5000 | 5.0" | Glass Sand | Building Frames and Bridge Decks |
| N4,5.0" | 4000 | 5.0" | Natural Sand | Building Frames and Bridge Decks |
| G4,5.0" | 4000 | 5.0" | Glass Sand | Building Frames and Bridge Decks |
| N4,1.5" | 4000 | 1.5" | Natural Sand | Pavements or Slip-Form Applications |
| G4,1.5" | 4000 | 1.5" | Glass Sand | Pavements or Slip-Form Applications |
| N0.48,5.0" | ? | 5.0" | Natural Sand | Building Frames and Bridge Decks |

Mixing was performed according to ASTM C 192 using a standard Eirich S-1 counter-current concrete mixer (Figure 3-6). This mixer allowed for full depth continuous shearing of the fresh concrete in order to allow for optimum mixing.

### 3.2.1. Preliminary Step: Design Input

Before proportioning can begin, it is important to understand the design restrictions. Often, concrete production will be limited by the material availability (aggregate, cement, admixtures, etc.), environmental exposure conditions, as well as the structural design requirements. The mixture designer needs to understand all these parameters in order to correctly create a concrete mixture. For this research, G5,5.0", N5,5.0", G4,5.0", and N4,5.0" are to be proportioned for use in building frames and bridge decks. These mixtures will have a workability

of five (5.0) inches and a design air content of three (3.0) percent. G4,1.5" and N4,1.5" are to be proportioned for use in slip-form applications such as pavements. These mixtures will have a workability of one and one-half (1.5) inches and a design air content of three (3.0) percent. Considering the mixtures are to be implemented for in-land applications in Hawaii, mild freeze thaw conditions and no corrosion risk was assumed. Exposure to a mild freeze thaw condition includes indoor or outdoor applications where the concrete is not exposed to freezing or deicing salts (ACI 211.1).

Figure **3-6**: Eirich S-1 counter current concrete mixer

### 3.2.2. Step One: Choice of slump

Slump is an indirect measure of the workability of concrete. Workability typically represents the work and energy required to place, compact, and finish concrete. Concrete mixtures with similar slumps may be used for similar applications (Mindess et al. 2003).

Workability is dependent on the binder content, fineness of cement and supplementary cementitious material, volume of entrained air, and maximum size, grading, and particle shape of aggregates. The slump of a concrete mixture can provide insight into the quality control of the concrete such as aggregate segregation (Mindess et al. 2003). In a field construction job, corrective actions are implemented if the concrete does not have the specified slump, this can manifest in the addition of a plasticizer. It is against standard ASTM and ACI procedures to induce a greater slump by adding more water to the fresh concrete system due to its severe negative impact on the strength and durability of hardened concrete. The slump values used for this study are five (5.0) inches or one and one-half (1.5) inches, as mentioned previously.

### 3.2.3. Step Two: Choice of Maximum Size of Aggregate

The maximum size aggregate (MSA) is the largest sieve size through which 100% of the aggregate would pass. The MSA is typically governed by design parameters such as the concrete member dimensions, reinforcing bar spacing, or pre-tensioning strand placement. Other design standards such as the ACI 318.11 Building Code have specifications for the MSA based on member dimensions (2011). However, when these restrictions are not in place, it is standard to choose a well graded aggregate gradation that will allow for the largest MSA possible. Larger aggregates have less surface area and therefore need less cement paste to achieve a desired workability (ACI 211.1; Mindess et al. 2003). Larger aggregates would in turn need less mixing water to have a greater workability (Walker 1960). On the other hand, research has shown that a smaller MSA may results in a greater compressive strength (Walker 1960). The local crushed limestone coarse aggregate used in this study has a MSA of one (1.0) inch.

### 3.2.4. Step Three: Estimation of Mixing Water and Air Content

Since the workability of concrete is directly related to the paste content, MSA, aggregate shape and texture, as well as chemical and mineral admixtures used, tables have been created in ACI 211.1 that allow designers to quantify their interrelation (Neville 1995). In the previous steps, the choice of slump (in inches) and MSA (in inches) were made. In this step, the designer uses the slump and MSA to identify a required mixing water content that has been empirically found to yield a concrete of desired slump (ACI 211.1). Table 3-5 shows a sample relation between the MSA and slump. Table 3-6 shows how that sample relationship changes if air entraining admixtures are implemented.

Table **3-5**: Sample values from Table 6.3.3 (ACI 211.1) relating the MSA and slump in order to find the water content of non-air-entrained concrete (lbs./yd$^3$)

| | | MSA, in | | |
|---|---|---|---|---|
| | | 1/2 in | 3/4 in | 1 in |
| Slump, in | 1 to 2 | 335 | 315 | 300 |
| | 3 to 4 | 365 | 340 | 325 |
| | 6 to 7 | 385 | 360 | 340 |

Table **3-6**: Sample values from Table 6.3.3 (ACI 211.1) relating the MSA and slump in order to find the water content of concrete (lbs./yd$^3$) while using air entrainment

| | | MSA, in | | |
|---|---|---|---|---|
| | | 1/2 in | 3/4 in | 1 in |
| Slump, in | 1 to 2 | 295 | 280 | 270 |
| | 3 to 4 | 325 | 305 | 295 |
| | 6 to 7 | 345 | 325 | 310 |

All concrete entraps air during its placement; these typically take the form of larger air bubbles that are greater than 0.002 inches (Neville 1995). It is known throughout literature (Mindess et al. 2003; Neville 1995) that concrete systems with larger MSA's have less entrapped air because there is less cement paste and mortar necessary to coat the larger coarse aggregate surface area. However, air is a necessity in creating a durable concrete that can withstand harsh freezing and thawing conditions. Therefore, air content is often increased by the use of air entraining admixtures that allow formation of well dispersed spherical air bubbles throughout the concrete (Neville 1995). These widespread air voids dispersed throughout the concrete will allow pore water across the entire concrete system room to expand into during freezing cycles (Neville 1995). This expansion of water into the air void system relieves the concrete system of tensile stresses that may form in the matrix and therefore can mitigate cracking (Mindess et al. 2003). If the air voids were not well dispersed, cracking will occur before these stresses can be relieved. Total fresh air content will be measured using the pressure method outlined in ASTM C 231. Other methods for measuring the fresh air content are the gravimetric method (ASTM C 138) and the volumetric method (ASTM C 173) (Mindess et al. 2003).

The concrete proportioning in this study will be for natural sand concrete and glasscrete with design air content of three percent (3.0%) which corresponds to a mild exposure to freezing and thawing condition and deicing salts. Experiments (ASTM C 231) were conducted in order to evaluate the necessity for using air entraining admixtures in order to attain this desired air content. After a trial and error process, the proper amount of air entrainer was determined for each mixture.

### 3.2.5. Step Four: Selection of w/cm

When discussing the compressive strength of concrete, it is commonplace to mention the twenty-eight (28) day compressive strength as the standard bearer for representing the strength. In this step, ACI 211.1 offers w/cm values that would correspond empirically to an associated twenty-eight (28) day compressive strength as shown in Figure 1-2 on page 4 (reintroduced as Figure 3-7). The designer uses this as a first approximation and subsequently refines and adjusts the w/cm based on trial batch results to achieve the required strength (ACI 211.1). Each job is different; therefore the designer may need to tweak ACI 211.1 codes in order to achieve the desired strength and durability (Mindess et al. 2003). ACI 211.1 also mentions that their design should be used simply as a guide to begin the mixture proportioning.

It is understood that a lower w/cm would result in greater compressive strengths than higher w/cm at the same age (Figure 3-7). It is also understood that increasing the air content will reduce the strength of the concrete (Neville 1995, Mindess et al. 2003). Step four takes this into account by reducing the w/cm for mixtures that incorporate air entraining admixtures. Supplementary cementitious materials such as fly ash will reduce the early age strength of concrete as well (Neville 1995). Fly ash's hydration products are similar to Portland cement's; however, fly ash requires a higher pH in order to begin its chemical reaction (Fraay et al. 1989, Neville 1995). Over time, the hydrating cement particles allow for the pH in the system to rise and create an environment for fly ash to react (Neville 1995).

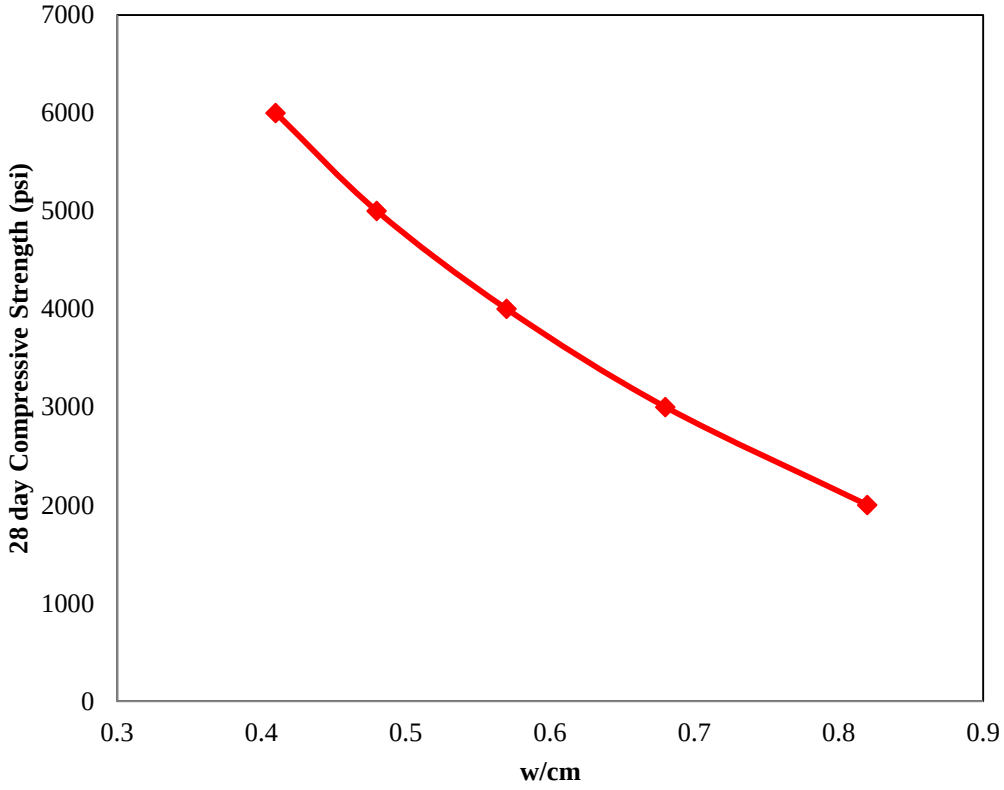


Figure **3-7**: ACI 211.1 empirical relationship between w/cm and 28-compressive strength of non-air-entrained concrete

Popovics (1982) provided a literature review comparing the compressive strength of concretes containing fly ash to plain OPC concrete at 28 days using analytical formulas. A main conclusion of his paper states the importance of experimental investigations in order to fully quantify fly ash's effect on concrete strength. Therefore, a trial and error approach was followed.

ACI 211.1 and ACI 318 also offer design criteria for freeze/thaw resistance, corrosion, and sulfate resistance. Codes require the w/cm to be reduced to limit the ingress of moisture or deleterious elements such as chlorides and sulfates. Due to Hawaii's mild freeze/thaw conditions and low risk of corrosion for in-land applications, this study does not take those criteria into effect. However, concrete designers can adjust the w/cm for applications where risk of corrosion or sulfate attacks is a concern. Also, ACI 318-11 Building Code specifies the incorporation of the

standard deviation of the concrete's compressive strength in order to achieve desired reliability in compressive strength of concrete. This study will provide insight into the standard deviation and coefficient of variation of strength for glasscrete mixtures.

### 3.2.6. Step Five: Calculation of cementitious materials content

Steps three and four provided the concrete mixture's water content and water to cementitious materials ratio, respectively. This step takes those two values and yields the cementitious materials content. Considering prior research by Shafaatian et al. (2012) outlined earlier in this chapter and in Chapter 2, the present study used Class F fly ash to replace 20% of cement by weight in order to mitigate the risk of the alkali silica reaction.

### 3.2.7. Step Six: Estimation of coarse aggregate content

The interaction between the coarse aggregate and the fine aggregate will directly affect the workability and mechanical properties of concrete (Mindess et al. 2003). Well graded coarse aggregates of similar MSA's will provide satisfactory workability of fresh concrete when the aggregate volume is based on an oven dry-rodded unit weight (ACI 211.1). The workability of the concrete is also dependent of the FM of sand (Mindess et al. 2003, Neville 1995). Therefore, this step provides a table that outputs the apparent volume of coarse aggregate per unit volume of concrete based on the fineness modulus of sand and the MSA of the coarse aggregate. The MSA for this study is 1.0 inches and the FM is 3.00. Table 3-7 provides a coarse aggregate volume of 0.65 per unit volume of concrete (e.g. 1 $yd^3$)

.

Table **3-7**: Sample values from Table 6.3.6 (ACI 211.1) relating the MSA and the fineness modulus in order to find the coarse aggregate's apparent volume

| | | Fineness Modulus | | | |
|---|---|---|---|---|---|
| | | 2.40 | 2.60 | 2.80 | 3.00 |
| MSA, in | 1/2 | 0.59 | 0.57 | 0.55 | 0.53 |
| | 3/4 | 0.66 | 0.64 | 0.62 | 0.60 |
| | 1 | 0.71 | 0.69 | 0.67 | 0.65 |

### 3.2.8. Step Seven: Estimation of fine aggregate content

ACI 211.1 'Absolute Volume Method' volumetrically proportions concrete to one (1) cubic yard. The constituents making up concrete will account for a certain percentage of the total volume of the concrete, typically shown in cubic feet. This percentage is based on previously measured weights and specific gravities. Fine aggregate is typically considered a filler material and will make-up the remaining volume of concrete not consumed by air, water, cementitious materials (cement and fly ash), and coarse aggregate (Mindess et al. 2003). It is important to note the specific gravity of fly ash is different than cement and therefore adjust the filler content accordingly.

### 3.2.9. Step Eight: Adjustments for aggregate moisture

Mixture proportions typically designate aggregate in two separate states; oven-dried (OD) and saturated surface dry (SSD) (Mindess et al. 2003). OD aggregate have all their moisture removed and SSD aggregate have all their internal pores filled with moisture yet have no excess water on their surface (Mindess et al. 2003). Most coarse and fine aggregates have inherent moisture absorption capacity (tendency to move from OD to SSD). This study decided to test all

aggregates in the oven-dried condition; therefore, the oven-dried aggregate's absorption capacity needs to be accounted for in the mixture design. This addition of water would allow the aggregates sufficient water to fill their internal pores completely before the remaining water can be used by the cementitious materials to hydrate (Mindess et al. 2003).

Figure **3-8**: Batched concrete mixture

### 3.2.10. Step Nine: Trial batch adjustments

After estimating the mixture proportions for the specified design, a trial batch is prepared and tested to evaluate exact properties of concrete. Adjustments often will be made to any number

of the previous proportioning steps in order to bring the concrete properties to specification. Concrete specifications often stipulate desired workability, strength, and durability. This step is utilized to make sure these specifications are met. The dosage of chemical admixtures such as plasticizers and air-entrainers may be adjusted here in order to attain desired properties. Adjustments in the w/cm can result in achieving the specified strength. Figure 3-8 presents a typical batched mixture for this study (as well as this paper's author).

### 3.3. Strength Based Testing

One focus of this research was to attain natural sand concrete and glasscrete mixtures that yielded comparable 7 day and 28 day compressive strengths at similar workability (slump) and fresh air contents. This was achieved by mix proportioning according to ACI 211.1 followed by casting trial batches to check strength and fresh properties of concrete. The w/cm and chemical admixture dosages were adjusted as needed to achieve target strength, slump, and air content. Table 3-8 shows 7 day strength aims with assumed 25% to 33% strength increase from 7 days to 28 days.

Table **3-8**: Target 7 day strengths

| | N5,5.0" | G5,5.0" | N4,1.5" | G4,1.5" | N4,5.0" | G4,5.0" |
|---|---|---|---|---|---|---|
| 7 day target (lbs./in$^2$) | 3800 | 3800 | 3000 | 3000 | 3000 | 3000 |
| 28 day target (lbs./in$^2$) | 5000 | 5000 | 4000 | 4000 | 4000 | 4000 |
| Target Air Content (%) | 3.0 | 3.0 | 3.0 | 3.0 | 3.0 | 3.0 |
| Target Slump (") | 5.0 | 5.0 | 1.5 | 1.5 | 5.0 | 5.0 |

After correctly proportioning concrete and glasscrete to have comparable strengths at 7 days and 28 days, further testing was conducted. The further testing provided greater insight into the mechanical and durability properties of glasscrete and natural sand concrete at various strengths and w/cm.

## 3.4. Water to Cementitious Material (w/cm) Based Testing

Another focus of this study was testing glasscrete and natural sand concrete at the same w/cm. After creating glasscrete mixtures using the strength based approach, ACI 211.1 was followed in order to create a natural sand concrete mixture at the same w/cm as G4,5.0". The fresh and hardened properties of glasscrete and natural sand concrete would therefore be compared at the same w/cm.

## 3.5. Testing Protocol

Fresh property testing consisted of slump (ASTM C 143), plastic air content (ASTM C 231), and time of setting (ASTM C 403). Hardened property testing consisted of compressive strength (ASTM C 39), coefficient of thermal expansion (ASTM C 531), abrasion resistance (ASTM C 944), rapid chloride penetration resistance (ASTM C 1202), and water sorptivity (ASTM C 1585).

### 3.5.1. ASTM C 143: Slump Test

The oldest and most widely used test to qualitatively define workability is the slump test (Mindess et al. 2003). The slump test is performed on freshly mixed concrete. The plastic

concrete is filled into the frustum of a cone (dimensions shown in Figure 3-9) in three (3) separate layers. Each layer is rodded 25 times with a 5/8-inches diameter steel rod. After the mold is lifted vertically, the slump is determined by measuring the vertical height difference between the slump cone and the center of the base of the concrete specimen.

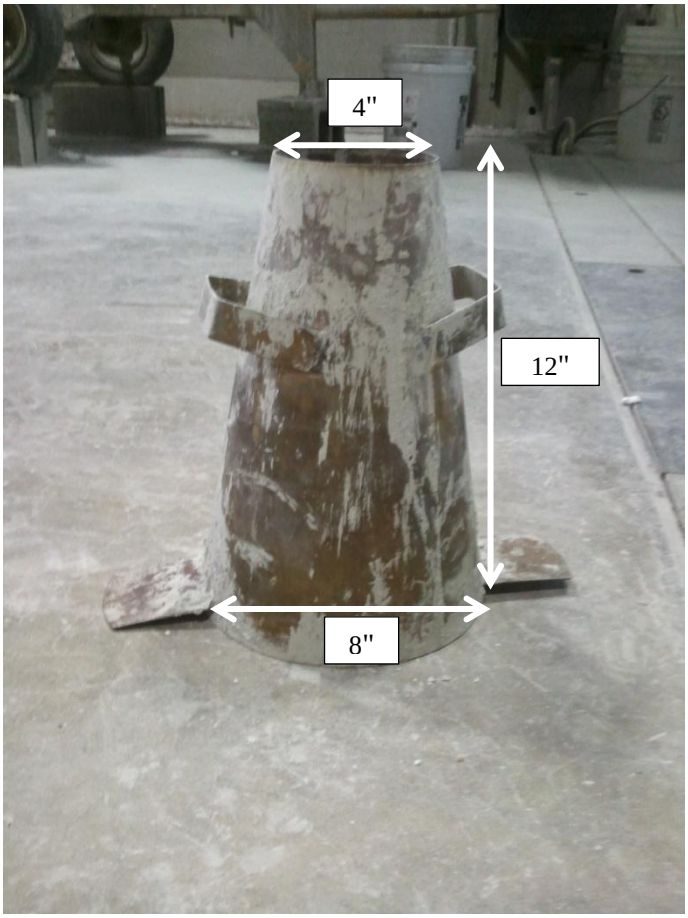


Figure **3-9**: Slump cone dimensions

### 3.5.2. ASTM C 231: Plastic Air Content via the Pressure Method

ASTM C 231 measures the total air content of freshly mixed concrete. The plastic concrete is consolidated in a measuring bowl (Figure 3-10) in three (3) layers, with 25 rods of 5/8-in rod for each layer. After the lid is assembled to the measuring bowl and the bleed water is

added through the side petcocks, pressure is applied to concrete specimen. It is assumed that the change in volume occurs entirely through the compression of air. Therefore, after the pressure is released, the air content can be read as the total air content of the concrete specimen.


Figure **3-10**: Type-B pressure meter used during study

### 3.5.3. ASTM C 403: Time of Setting of Mortar

ASTM C 403 provides information on the initial and final set time of the various natural sand concrete and glasscrete mortars. The initial set time of mortar is defined as the time when mortar loses its plastic consistency and will deform under loading (Hewlett 1998). The final set time of mortar is defined as the time when mortar can begin to sustain a load (Hewlett 1998). Mortars were tested in order to isolate the fine aggregate variable and its interaction with the concrete paste. Mortar was proportioned using similar method to ACI 211.1. The results section

(Chapter 4) will elaborate on the paste and aggregate content of the mortars. The mortar was placed into a six (6) inch diameter plastic cylinder that was cut in order to have a maximum height of six (6) inches. This cylinder was subsequently filled with mortar in three layers and compacted using a vibrating table between each step. The cylinder was placed in the moist cure room for the duration of testing, only removed to take measurements. Three separate specimens were tested for each mixture.


Figure **3-11**: Humboldt H/4133 spring-reaction device used for time of setting measurements

Measurements were performed by using the spring-reaction device seen in Figure 3-11. This Humboldt H/4133 version allows for a needle with a bearing diameter of ¼ inch to be thrust into the setting mortar (Figure 3-12) in order to attain a pressure/resistance reading. The needle shall be forced to penetrate one (1) inch into the mortar. Upon penetrating the mortar, the spring-reaction will provide a force reading in pounds. This force reading (lbf) will be divided by the penetration area in order to find the penetration resistance in psi. Initial setting is the time where

penetration resistance is equal to 500psi and final set time occurs when the penetration resistance is equal to 4000psi. The needle diameter yields a penetration area of 0.049 square inches.

The time of setting clock begins at the moment water comes into contact with cementitious materials. The initial reading occurs two to three (2-3) hours post contact, with subsequent readings occurring at thirty (30) minute intervals or whenever deemed suitable. It is important to realize that at least six (6) penetrations are necessary to create a penetration resistance versus time curve that can be used to find the initial and final time of setting. Also, one reading shall be less than or equal to 500psi and one reading shall be greater than or equal to 4000psi in order to properly capture the setting characteristics of the mortar mixture.

Figure **3-12**: Typical mortar time of setting specimen after testing is complete

After at least six (6) penetration points are recorded, the results are shown as a plot with the elapsed time (in minutes) on the horizontal axis and the penetration resistance (in psi) on the vertical axis. The plot is then fit to a power function. If the regression coefficient is greater than or equal to 0.98 ($R > 0.98$, $R^2 > 0.96$), the power function can be used to determine the initial and final set times. The initial and final set times are found for penetration resistance values corresponding to 500 lbs./in$^2$ or 4000 lbs./in$^2$, respectively. The average results of the three specimens tested are reported. If the regression coefficient is less than 0.98, the initial and final

set time will be hand-fit by linear interpolation between each two consecutive data points. Figure 3-13 shows a sample time of setting relationship from ASTM C 403. Figure 3-14 offers a sample hand-fit curve from this research.

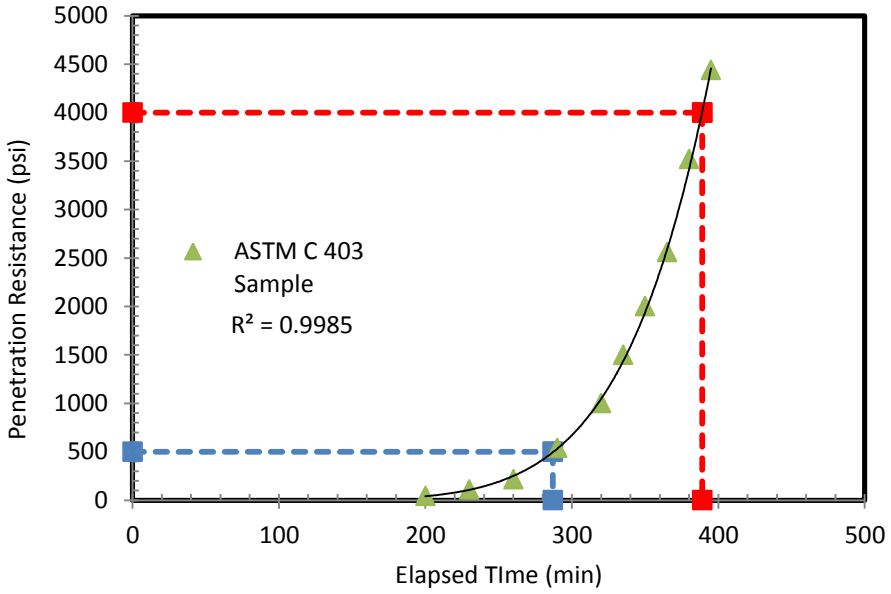


Figure **3-13**: ASTM C 403 sample data shown on a plot of elapsed time (min) versus penetration resistance (lbs./in$^2$)

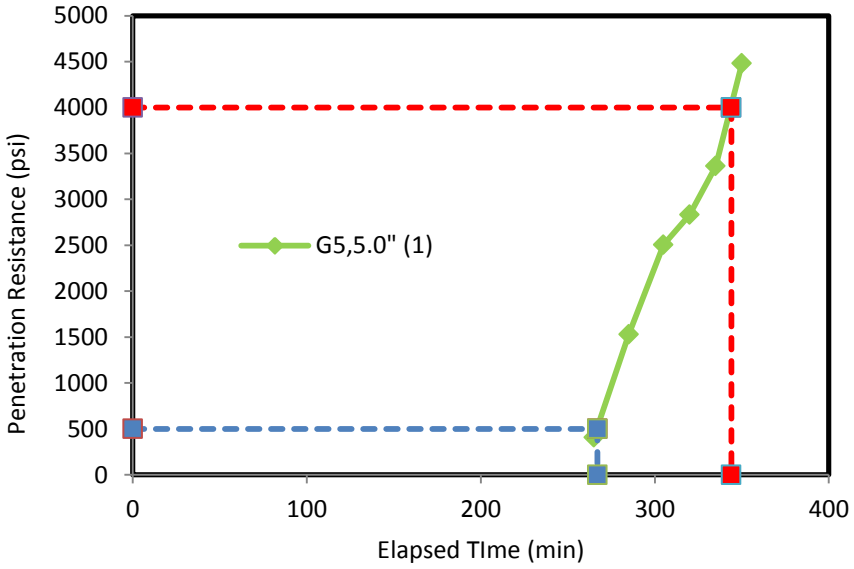


Figure **3-14**: Research sample determination of initial and final set times using a hand-fit approach

### 3.5.4. ASTM C 39: Compressive Strength

This test measures the uniaxial, unconfined, compressive strength of concrete specimens. The specimens are either cast cylindrically or are cored in order to attain the necessary shape and dimensions. All cylinders used during this work were cast cylindrically. Cylinders with a length to diameter ratio (*l/d*) of two (2) were used throughout this research. This simple ratio has fostered a level of consistency in compressive strength testing over the last century. This ratio also allows for the restraint provided by the steel end retaining ring to have a relatively small and consistent contribution to the compressive strength of concrete specimens (Bartlett 1994). Figure 3-15 and Figure 3-16 present the correct placement of the steel end retaining ring. Neoprene pads were placed inside the steel end caps in order to distribute the load evenly across the concrete's cross-section.

All cylinders tested were cast with the following dimensions: four (4) inches in diameter and eight (8) inches in length. The cylinders were cast in three (3) layers and compacted via 25 rods at each layer. All specimens were moist cured for the duration of their lifetime (until moments before testing). The tops were smoothed with a diamond cut wet saw (Figure 3-17) to provide an even surface for loading.

The cylinders were tested for each mixture at one (1), three (3), seven (7), twenty-eight (28), and ninety (90) days. For each mixture and age, three (3) duplicate cylinders were tested in accordance with ASTM C 39. The cylinders were tested using a Boart Longyear model CM-625 with a CSI Model CS-100-2A Retrofit (Figure 3-18) allowing for an instantaneous readout of the load imposed on the specimen. According to the standard, a rate of 35+/-7 (psi/sec) was applied to the cylinder. Both a load (in lbf) and load rate (lbf per square inch) were recorded.

Figure **3-15**: Sample concrete specimen prior to compressive strength testing

Figure **3-16**: Sample concrete specimen post compressive strength testing

Figure **3-17**: Wet saw used to smooth, even, and dimension concrete specimens


Figure **3-18**: Boart Longyear model CM-625 with a CSI Model CS-100-2A Retrofit

### 3.5.5. ASTM C 531: Coefficient of Thermal Expansion (COTE)

Thermal properties of concrete are important for the design of concrete structures when the structure is exposed to sustained high temperatures, used for thermal insulation, or used for fire protection (Mindess et al. 2003). In addition, COTE has a significant impact on thermal cracking tendencies of mass concrete and concrete members at early ages (ACI 231). The coefficient of thermal expansion quantifies the thermal strain of concrete in response to a unit increase or decrease in temperature. As concrete hydrates, it warms due to heat of hydration. Concrete often sets near its peak temperature. As the concrete cools to ambient temperature, it undergoes thermal contraction. Thermal contraction results tensile stress development and cracking when concrete is restrained (e.g. pavements or bridge decks). A larger COTE results in a greater the thermal contraction and a higher the risk of cracking (Won 2005).

In the present study, the COTE was determined for each mixture, both in saturated conditions as well as oven dry conditions, using mortar bars. Mortar bars (1×1×10 inches) were used to focus on the fine aggregate's role on the COTE and limits the temperature gradients that could develop in larger prisms containing coarse aggregate. Variability in field conditions as well as the importance of moisture content to cement paste's reaction to strain development precipitated the need to test the COTE at different moisture contents. Research by Zoldners (1971) showed a significant increase in the COTE at relative humidity (RH) between 40% and 80%, peaking at 50-70% RH for cement pastes. Emanuel and Hulsey (1977) investigated moisture content's link to COTE further and found similar results in a comprehensive literature review (Figure 3-19). Emanuel and Hulsey found minimum COTE values occurring at 100% saturation and 0% saturation, typically lowest at 100% saturation (Figures 3-19 and 3-20). Research has also shown that the age of cement paste plays a role in the COTE, reducing when

paste is older than six (6) months (Figure 3-20). As the concrete mature, it may become less porous, thus allowing for less moisture to be affected by changes in temperature.

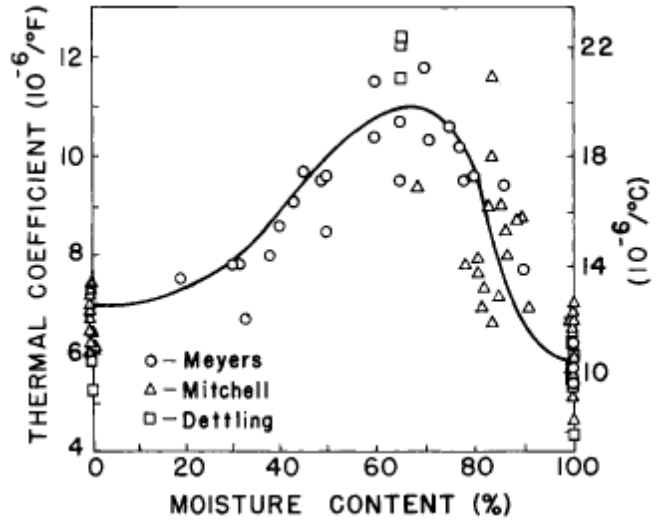


Figure **3-19**: Cement paste variation in COTE due to moisture content (Figure 2 from Emanuel and Hulsey 1977)

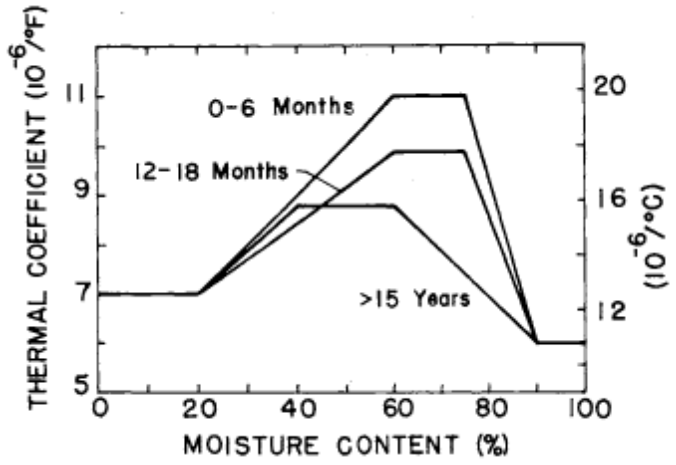


Figure **3-20**: Idealized COTE curves for cement pastes with respect to moisture content and age of cement paste (Figure 3 from Emanuel and Hulsey 1977)

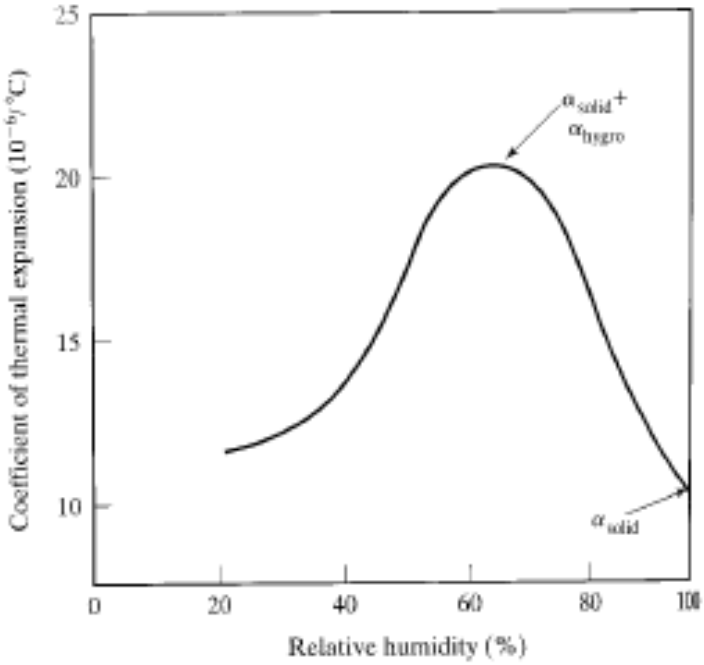


Figure **3-21**: Variation of COTE due to RH (from Zoldners 1971)

Equation 3-1 shows the relationship between the measured COTE and the COTE measured due to the presence and absence of hygrothermal expansion (also shown qualitatively in Figure 3-21):

$$\alpha_{actual} = \alpha_{solid} + \alpha_{hygro} \quad (3\text{-}1)$$

Where

$\alpha_{actual}$ = measured coefficient of thermal expansion ($10^{-6}$/°C)

$\alpha_{solid}$ = measured in the absence of hygrothermal change ($10^{-6}$/°C)

$\alpha_{hygro}$ = measured coefficient of hygrothermal expansion ($10^{-6}$/°C)

Hygrothermal expansion or contraction can be qualitatively expressed as a volume change due to a change in the internal relative humidity through a temperature increase or decrease (Mindess et al. 2003). The Laplace equation (equation 3-2) and the Kelvin equation (equation 3-3) combine to provide the Kelvin-Laplace equation (equation 3-4) that shows temperature increases will cause the water to expand and the surface tension of water to decrease within capillary pores. This will

increase the radius to curvature of the meniscus, increase the RH, and increase in pore fluid pressure. This pore fluid pressure would cause expansion in the concrete (Meyers 1950; Bažant 1970; Summarized by Grasley 2003). The reverse is true upon cooling.

$$p_v - p_l = \frac{2\sigma}{r} \tag{3-2}$$

Where

$p_v$ = vapor pressure

$p_l$ = liquid pressure

$\sigma$ = surface tension of water

$r$ = radius of curvature of the meniscus

$$\frac{2\sigma}{r} = \frac{\ln(RH)\,RT}{v} \tag{3-3}$$

Where

$\sigma$ = surface tension of water

$r$ = radius of curvature of the meniscus

$RH$ = internal relative humidity of concrete

$R$ = universal gas constant

$T$ = temperature

$v$ = molar volume of water

$$p_v - p_l = \frac{\ln(RH)\,RT}{v} \tag{3-4}$$

Concrete with 0% or 100% RH do not experience these changes in relative humidity and would therefore show less expansion. Equation 3-4 shows the pressure difference between the vapor and liquid would go to zero when the moisture content is 0%. The COTE has been postulated to be dependent on pure thermal dilation, thermal shrinkage or swelling, and relative humidity changes (Meyers 1950; Bažant 1970; and Sellevold and Bjøntegaard 2006). Bažant offers a relationship

that shows the maximum hygrothermic dilation at a RH of 70% (1970). He continues to estimate that the maximum and minimum thermal expansion would occur at 70% RH and 0% RH, respectively (Figure 3-22). This study will therefore test a saturated sample that represents a specimen closest to 50%-70% RH and a dry sample that represents a specimen closest to 0% RH in order to find the maximum and minimum COTE values, respectively. Neville states that the value determined for a saturated sample can represent a 'true' COTE (1995).

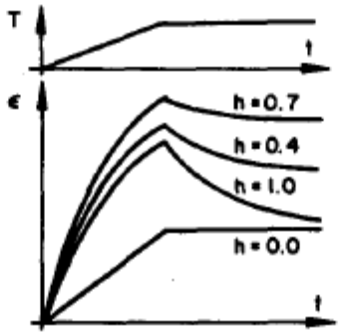


Figure **3-22**: Estimated expansion curves due to an increased temperature at different relative humidity values (Figure 6 from Bažant 1970)

The COTE differs between the aggregate and cement paste that makes up the mortar mixture (Neville 1995). Table 3-9 offers COTE for various aggregates and cementitious mixtures. Cement paste generally has a larger COTE in the range of 23°C to 100°C (Emanuel and Hulsey 1977). Hobbs also found the COTE reduced significantly with an increase in aggregate volume (1971); this can also be seen in Table 3-9. Large differences in coefficients of thermal expansion between the aggregate and the paste may cause differential expansion in the mortar and therefore cause cracking in the specimen (Mindess et al. 2003). Correct characterization of the COTE can help limit early-age cracking, as well as fatigue cracking and joint spalling on concrete pavements (Tanesi et. al 2012). Mortars were mixed according to ASTM C 305 and cast in molds similar to Figure 3-23. The dimensions of the mold were according to ASTM C 490 as follows: effective length of 10.0", depth 1.0", and width of 1.0". The ends of the specimens were cast with nickel

alloy studs to facilitate length measurements. The studs have a coefficient of thermal expansion of 7.2E-06/°F which was accounted for in the COTE calculations.

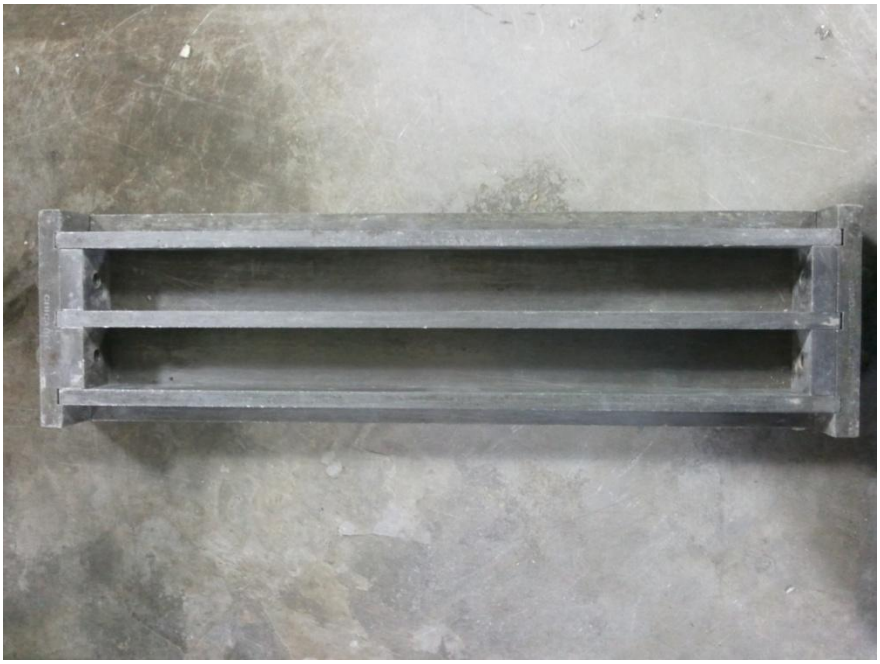

Figure **3-23**: Mold used to cast COTE mortar bars

Testing began after the specimens have been moist cured for fourteen (14) days. The results from four (4) duplicate prisms were used and averaged to determine the COTE of each mixture in the saturated or oven-dry condition. The saturated specimens were heated from room temperature (23°C) to a temperature of 80°C while fully submerged in water. After at least sixteen (16) hours at 80°C, the specimens' length measurements were recorded using a Humboldt model BG2600-16001 comparator (Figure 3-18) by taking mortar bars out of the 80°C bath one by one and measuring their length. The measurements were recorded to the nearest 0.0001". The specimens were then submerged back into the water bath and cooled to a temperature of 60°C. After at least sixteen (16) hours at 60°C, the specimens' length measurements were recorded. This temperature cycle (60°C to 80°C and reverse) continued until specimens reached constant lengths at both 60°C and 80°C.

Table **3-9**: COTE ($10^{-6}$/°F) of various aggregate and cementitious mixtures in the saturated condition. (Courtesy of Mindess et al 2003, Meyers 1940, and Neville 1995)

| | |
|---|---|
| Basalt | 3.3-4.4 |
| Granite | 4.0-5.0 |
| Limestone | 3.3 |
| Sandstone | 6.1-6.7 |
| Quartzite | 6.1-7.2 |
| Soda-Lime Glass | 4.0-5.0 |
| Concrete | 4.1-7.3 |
| Steel | 11.0-12.0 |
| 100% paste | 10.3 |
| 50% paste | 7.5 |
| 25% paste | 6.2 |

The dry specimens were first conditioned at a temperature of 23°C and a relative humidity of 50% after 14 days of moist curing. After at least sixteen (16) hours at 23°C, the specimens' length measurements were recorded using the digital comparator (Figure 3-24). After measurements have been taken, the specimens were moved to a 100°C oven. After at least sixteen (16) hours at 100°C, the specimens' length measurements were recorded and the specimens were placed back at 23°C, 50%RH ambient. This temperature cycle (23°C to 100°C and reverse) repeated until the specimens reached a consistent mass and length both at 23°C and 100°C.

The COTE is determined using Equation 3-5 below

$$COTE = \frac{Z - Y - W}{T(W - X)} \tag{3-5}$$

Z = length of mortar bar, including studs, at elevated temperature, in

Y = length of stud expansion, in $= X * T * k$, where k is the linear coefficient of thermal expansion per °F of the studs

W = length of bar, including studs, at lower temperature, in.

T = temperature change, °F

X = length of the two studs at lower temperature, in.

Figure **3-24**: Humboldt model BG2600-16001 comparator with specimen loaded for measurement

### 3.5.6. ASTM C 944: Concrete Abrasion Resistance

Abrasion resistance is an important parameter to quantify wearing durability of concrete floors, pavements, and bridge decks. Abrasion is quantified as the repeated frictional rubbing (attrition) that is typically associated with pavements or industrial floors (Mindess et al. 2003). Abrasion resistance is therefore the ability of the concrete to resist this attrition. Aggregate-cement paste bond tends to have a significant impact on the abrasion resistance of the concrete system. The bond between the aggregate and the cement binder could be the weakest point and tend to be the fastest abrading part of concrete. The aggregate type also plays a role in the

abrasion resistance of concrete. Although, if the w/cm is low enough, the cement paste can form a strong binder around the aggregates which makes the abrasion resistance less dependent on the aggregate type (Mindess et al. 2003). The surface finishing is also important to the abrasion resistance of concrete (Mindess et al. 2003). The abrasion resistance of concrete is taken as a whole instead of by parts considering the abrasion resistance of the aggregate (LA Abrasion Test) tends to be a measure of the aggregate's affinity to break while being handled (Mindess et al. 2003, Neville 1995). It is important to incorporate the paste-aggregate bond when quantifying the abrasion resistance (Mindess 2003).

For the purposes of this test, the specimens were cut in order to have diamond cut surfaces tested for every specimen. This ensures quality control across all the specimens. This test was conducted on three (3) one (1.00) inch thick concrete disks cut from an interior section of a six inch by twelve inch (6"×12") concrete cylinder as seen in Figure 3-25. This cylinder was moist cured for twenty-seven (27) days. After moist curing, the concrete cylinder was cut to the previously described disk dimensions and allowed to air-dry for twenty-four (24) hours. This technique was employed to limit the effect of mass loss due to moisture loss.

For the abrasion resistance test, disk specimens were loaded onto a drill press and secured in place with set of large clamps. These clamps hold the specimen in place while two rotating cutters are lowered on top of the specimen. These rotating cutters are free to spin on the concrete surface while carrying a vertical load of 44 lbf. The cutters are spinning at 200 revolutions per minute. The concrete specimens were abraded three (3) separate times for two (2) minute durations. The specimens' mass is determined before the initial abrasion and after each successive interval. The test setup is shown in Figure 3-26. The results report the overall mass loss.

Figure **3-25**: Abrasion resistance specimens

Figure **3-26**: ASTM C 944 setup

### 3.5.7. ASTM C 1202: Rapid Chloride Penetrability Test

The ability of concrete to resist penetration from aggressive elements (i.e. chloride ions) is a key component to the durability of reinforced concrete. External chloride ions (i.e. due to the application of deicing salts or from marine environments) can penetrate through the concrete's cover layer and cause corrosion of the steel reinforcing bars (Figure 3-27) (Berke 1988). The steel corrosion (rust) products have a larger volume of up to seven (7) times the volume of original steel. This volume expansion can cause large tensile stresses inside the concrete and result in cracking and spalling (Berke et al. 1988).

Figure **3-27**: Corrosion of steel reinforcing bars in concrete (Courtesy of Matco Services, Inc.)

To evaluate the resistance of concrete mixtures against penetration of chloride ion, ASTM C 1202 was performed. Four by eight inch (4"×8") concrete cylindrical specimens were prepared and moist cured for 24 days. This test requires a considerable amount of preparation time; therefore, in order to test the specimens at 28 days, preparation began at 24 days. After curing, the specimens were cut into two (2) inch thick disks from the center of the specimen.

Then, epoxy resin was applied to the exterior sides of the cylinder to prevent lateral moisture loss. After the epoxy resin dried, the concrete specimens were subjected to a vacuumed drying inside a desiccator for three (3) hours. After three (3) hours, the desiccator was partially filled with de-aired (boiled) water to submerge all specimens. The vacuum was allowed to run for an additional one (1) hour. Next, the vacuum was shut off and the specimens were allowed to soak for an additional eighteen (18) hours. This procedure is intended to fully saturate the concrete pores with water. The specimens were subsequently removed and loaded into two (2) half cells made of Plexiglas and sealed via silicone (Figure 3-28). Each half cell had a reservoir that was filled with a solution of either 3.0% $NaCl$ or 0.3 $N$ $NaOH$ . After the silicone was allowed to dry overnight, thus concluding the 4 day preparation process, the cells were filled with the aforementioned solutions and subjected to a 60V DC voltage across the specimens' cross-section. The voltage was applied for six (6) hours with the measurements recorded automatically every thirty (30) minutes by the RLC Instrument Co. model 164A Test Set Power Supply. Two (2) specimens of each mixture were tested at an age of 28 days. Please review figure 3-28 for more information.

The charge passed (in Coulombs) was recorded. These values were adjusted by converting the charge passed through the diameter of the tests specimen (4 inches) to the equivalent charge passed through a standardized diameter (3.75 inches) using Equation 3-6. This allows the standard to classify concrete's susceptibility to ion penetration using the qualitative descriptions provided in Table 3-10.

$$Q_{3.75} = Q_{4.0} * \left(\frac{3.75}{4.0}\right)^2 \quad (3\text{-}6)$$

$Q_{3.75}$ = charge passed (coulombs) through a 3.75-in diameter specimen.

$Q_{4.0}$ = charge passed (coulombs) through a 4.0-in diameter specimen

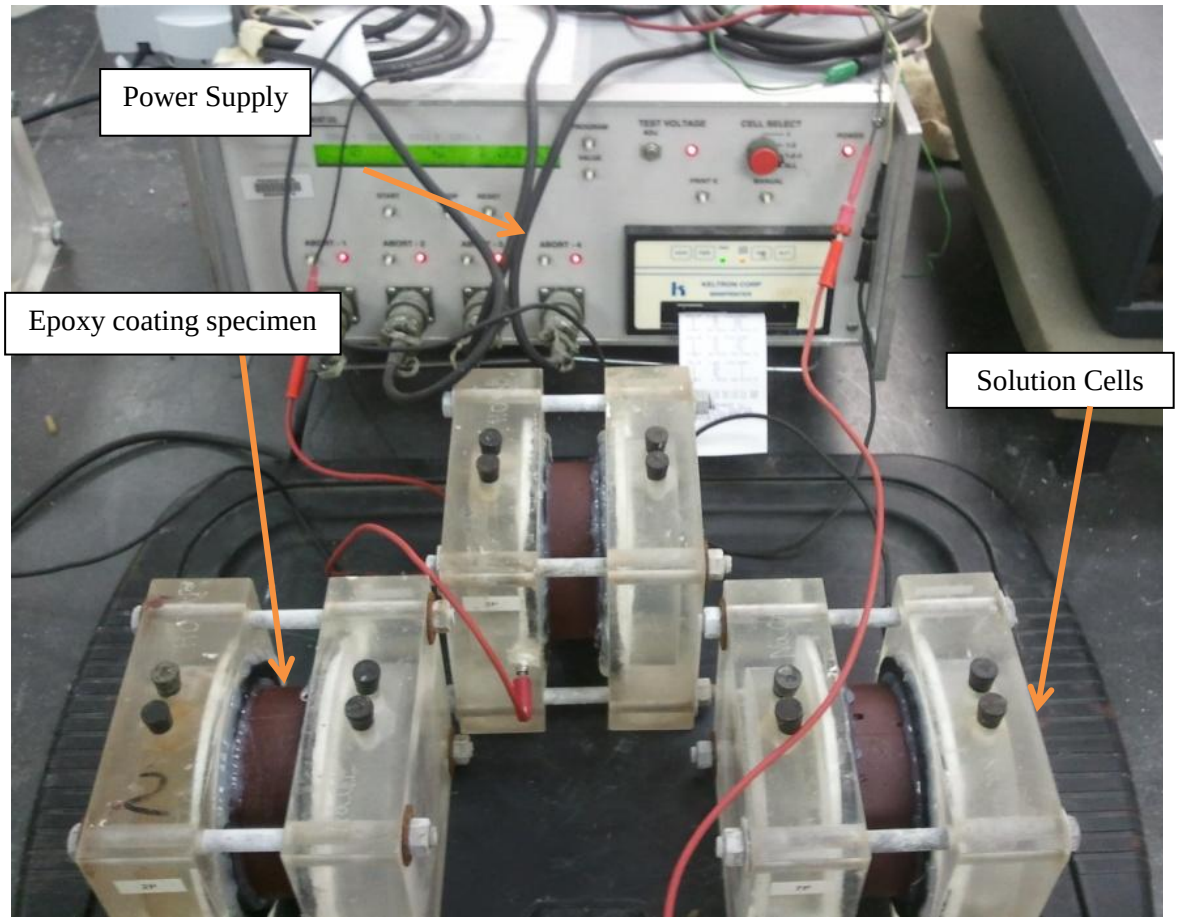


Figure **3-28**: ASTM C 1202 RCPT six (6) hour test setup

Table **3-10:** Qualitative description of concrete chloride ion penetrability

| Charge Passed (coulombs) | Chloride ion Penetrability |
|---|---|
| >4000 | High |
| 2000-4000 | Moderate |
| 1000-2000 | Low |
| 100-1000 | Very Low |
| <100 | Negligible |

Concrete with a higher w/cm will have a greater volume of capillary pores and thus allow for easier penetration of moisture and ions. Similarly, higher w/cm concretes will allow a larger magnitude of electrical current to pass through its cross-section at a given voltage (Stanish et al. 1997). This will produce heat thus increasing the temperature in the solution cells and across the

concrete specimen (Stanish et al.1997). The increase in temperature then serves as a positive feedback, leading to an increase in the current and the charge passed (Mindess et al. 2003). This artificial increase in the charge passed will distort the results. During the test, the temperatures of the solutions were monitored periodically using thermometers to ensure that they do not exceed 190°F (90°C). In addition, when the current exceeded 300mA at the test's conclusion, the RCPT values were corrected to account for overheating. The RCPT values are corrected based on the current passed during the first thirty (30) minutes of testing (Mindess 2003). The new ASTM C 1760 test method allows for the use of electrical current passing during the first one (1) minute of the test. Please see Figure 3-29 for a sample correction for overheating.

Concrete standards and literature suggest mitigation ion ingress by reducing the w/cm (Berke et al. 1988; Ozyildirim and Halsted 1988). In addition, other durability factors such as freeze thaw resistance need to be considered. Fly ash has been found to reduce the ion penetrability of concrete. Fly ash reduces the porosity and generates a finer pore structure through pozzolanic reactions which results in consumption of capillary water and formation of additional solid C-S-H phase. In addition, fly ash can reduce the RCPT results by reducing the alkalinity and electrical conductivity of the pore solution (Malek and Roy 1987; Ozyildirim and Halsted 1988).

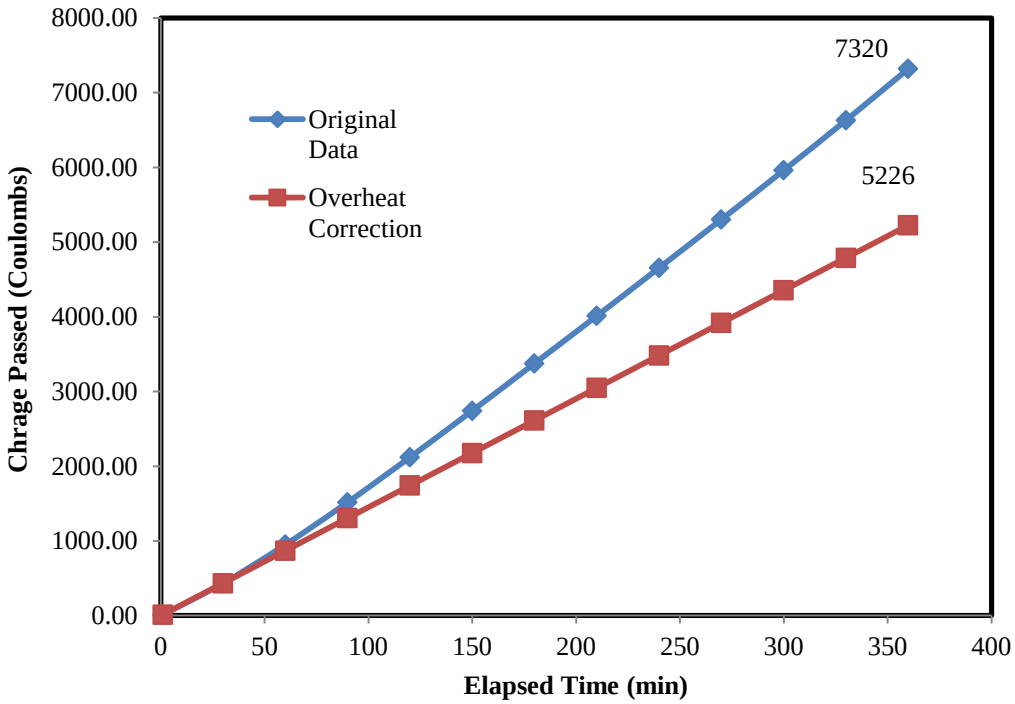


Figure **3-29**: Sample overheat correction for RCPT

### 3.5.8. ASTM C 1585: Water Sorptivity Test

The water sorptivity of concrete is governed by the capillary forces that allow moisture to ingress into the unsaturated concrete system via suction (Hall 1989; Martys and Ferraris 1997; DeSouza et al. 1997; Hall and Hoff 2002; Castro et al. 2011). The term sorptivity encompasses both absorption and desorption and therefore allows the coefficient value to be used interchangeably for both processes (Philip 1957). The initial sorption of the concrete cover is typically governed by the larger capillary pores while secondary sorption is governed by the much smaller gel pores (Martys and Ferraris 1997). A typical cut-off in pore sizes between capillary pores and gel pores is ten (10) nanometers; with capillary pores larger and gel pores smaller (Mindess et al. 2003). This difference in suction forces could show a marked change in

the initial sorptivity and secondary sorptivity values (Martys and Ferraris 1997; Castro et al. 2011). Tests have shown (Martys and Ferraris 1997; Castro et al. 2011) that concrete's initial six (6) hours of water contact will be governed by capillaries while the next eight (8) hours are governed by gel pore suction. Sorptivity testing is also dependent on the relative humidity and moisture content of the specimen prior to testing (Castro 2011). The pore volume created by higher w/cm will also affect the sorptivity of concrete (Mindess et al. 2003). This study ran sorptivity tests to the ASTM standard as described in the procedure below. Moisture intake is shown in Figure 3-30.

Concrete was cast in four by eight (4"×8") inch concrete cylinders and allowed to moist cure for twenty-eight (28) days. After curing, the cylinders were cut into two (2) inch disks allowing two (2) specimens for each mixture. The specimens were then conditioned by being placed in an environmental chamber at 50°C and 80% RH for three (3) days. After three (3) days, the specimens were individually packaged in sealable plastic containers and maintained at a temperature of 23°C for a minimum of fifteen (15) days to allow for the internal redistribution of moisture throughout the specimen (Castro et al. 2011). The specimens used for this study were maintained at 23°C for twenty (20) days. After proper conditioning, the exterior of the specimens were coated with vinyl electricians tape (Figure 3-31) to prevent air and moisture loss from the perimeter. Also, the top of the specimens were covered with a plastic sheet (Figure 3-31) to allow only water to ingress through the bottom while allowing the air to escape into the plastic sheet without allowing drying to occur from the top surface. In order to mitigate moisture ingress through the sides of the concrete, a commercially available masonry waterproofing sealer was placed at the interface of the concrete and vinyl electricians tape (the white substance in Figures 3-31 and 3-32). Although the seal may not be completely air tight, it was deemed acceptable for testing. Mass recordings of the specimen were then performed at predetermined intervals and

reported accordingly. These measures allow only the bottom face of the concrete cylinder to be freely exposed to a moisture bath (Figure 3-33).

The absorption represents the volumetric flux of absorbed water and can be measured using equation 3-7 from ASTM C 1585.

$$I = \frac{m_t}{a * d} \tag{3-7}$$

I = absorption, mm

$m_t$ = change in specimen mass in grams, at time t

a = exposed area of the specimen, $mm^2$

d = density of water, $g/mm^3$

$$I(t) = St^{0.5} \tag{3-8}$$

I = absorption, mm

t = time, min

S = sorptivity coefficient, $mm/min^{0.5}$

The sorptivity coefficient of concrete (S in equation 3-8) is attained by plotting the absorption (mm) versus the square root of time ($sec^{1/2}$) (Hall 1989). The following derivation shows the linear relationship between absorption (I) and the square root of time ($t^{1/2}$) (Kelham 1988). Flow through a porous medium is represented by Darcy's Law (equation 3-9).

$$q = \frac{\left(\kappa A \rho \frac{dP}{dx}\right)}{\eta} \tag{3-9}$$

$Q$ = mass flow rate of the fluid

$K$ = intrinsic permeability of the medium

$A$ = cross sectional area

$\rho, \eta$ = density and viscosity of the fluid

$\frac{dP}{dx}$ = pressure gradient

The Laplace equation (3-10) provides the relationship between capillary pore pressure and the surface tension and radius of curvature.

$$\Delta P_{capillary} = \frac{2\sigma}{r} \tag{3-10}$$

$\Delta P_{capillary}$ = pressure difference in capillary pore

$\sigma$ = surface tension of water

$r$ = radius of curvature of the meniscus

Suction begins immediately after the specimen is placed into contact with water. This process is shown in Figure 3-24. Pressure gradients develop within the concrete system. The concrete-water interface is represented by $P_w$, the concrete-air interface is represented by $P_a$, while the water-air interface within the concrete is represented by $P_{iw}$ or $P_{ia}$ depending which side of the capillary interface the pressure is being calculated (equation 3-11).

$$\Delta P_{capillary} = P_{ia} - P_{iw} \tag{3-11}$$

It is assumed that capillary pressures will be the dominant driving force and hydrostatic pressure differences may be ignored. Also, the concrete is assumed to be homogenous and $\Delta P_{capillary}$ will be independent of I. The volume flow rate of water ($V_w$) at the air-water interface can be shown in equation 3-12 (for incompressible fluids). As well, the volume flow rate of air ($V_a$) at the interface can be represented by equation 3-13

$$V_w = \frac{q_w}{\rho} = \frac{\kappa A}{\eta_w}\left(\frac{P_w - P_{iw}}{I}\right) \tag{3-12}$$

$$V_a = \frac{\kappa A}{\eta_a}\left(\frac{P_{ia} - P_a}{L - I}\right)\left(\frac{P_{ia} - P_a}{2P_{ia}}\right) \tag{3-13}$$

The term $\left(\frac{P_{ia}-P_a}{2P_{ia}}\right)$ represents the compressibility of air and therefore the approximation $P_{ia} = P_a$ can be assumed for the majority of the concrete specimen. The hydrostatic pressures that are ignored allow $P_a = P_w$. Therefore, equation 3-14 shows the new representation of the change in capillary pressure and equation 3-15 shows the new representation of $V_w$.

$$\Delta P_{capillary} = P_w - P_{iw} \tag{3-14}$$

$$V_w = \frac{\kappa A}{\eta_w}\left(\frac{\Delta P_{capillary}}{I}\right) \tag{3-15}$$

The volume of water necessary to saturate a concrete specimen can be represented by equation 3-16.

$$dV = (dI)A * z \tag{3-16}$$

z = effective porosity

The rate of increase of I is therefore represented by the integral in equation 3-17

$$\int dI = \int \frac{V_w}{Az}\,dt = \int \frac{\kappa \Delta P_{capillary}}{Iz\eta_w}\,dt \tag{3-17}$$

Solving for the integral provides equation 3-18.

$$I(t) = \left(\frac{2t\kappa \Delta P_{capillary}}{z\eta_w}\right)^{0.5} \tag{3-18}$$

This shows the absorption (I(t)) in linearly dependent on the square root of time. The sorptivity coefficient is therefore represented in equation 3-19 and the final form used throughout this study is simplified to equation 3-20.

$$S = \left(\frac{2\kappa \Delta P_{capillary}}{z\eta_w}\right)^{0.5} \tag{3-19}$$

$$I(t) = St^{0.5} \tag{3-20}$$

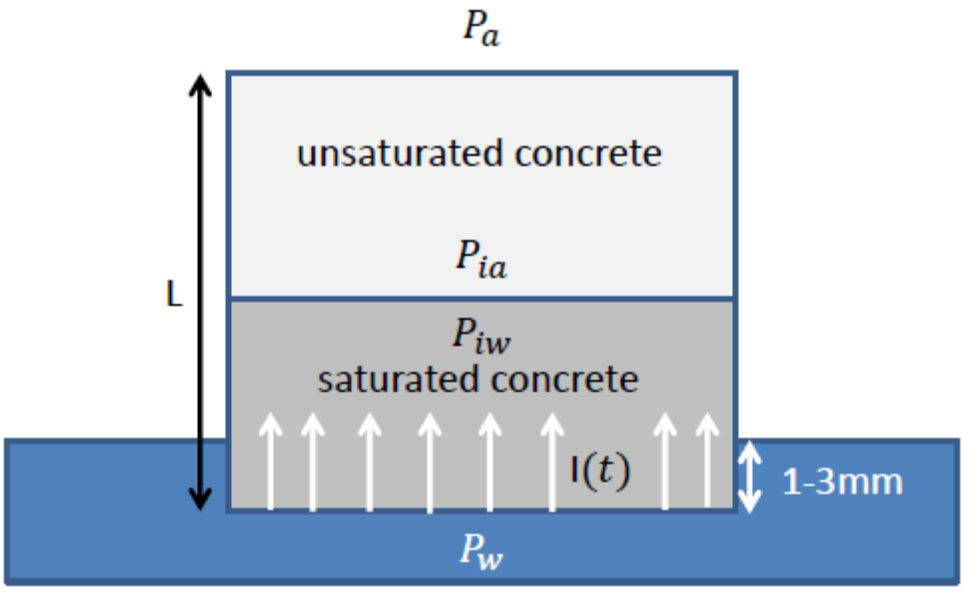


Figure **3-30**: Water absorption depiction during ASTM C 1585 (Adapted from Kelham 1988)

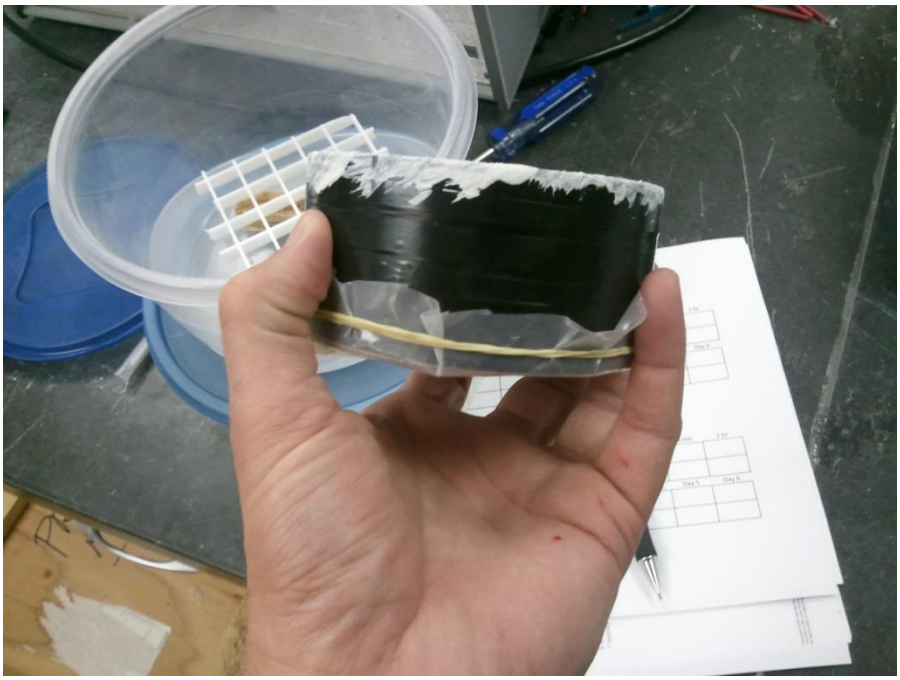

Figure **3-31**: Vinyl electricians tape exterior coating for ASTM C 1585

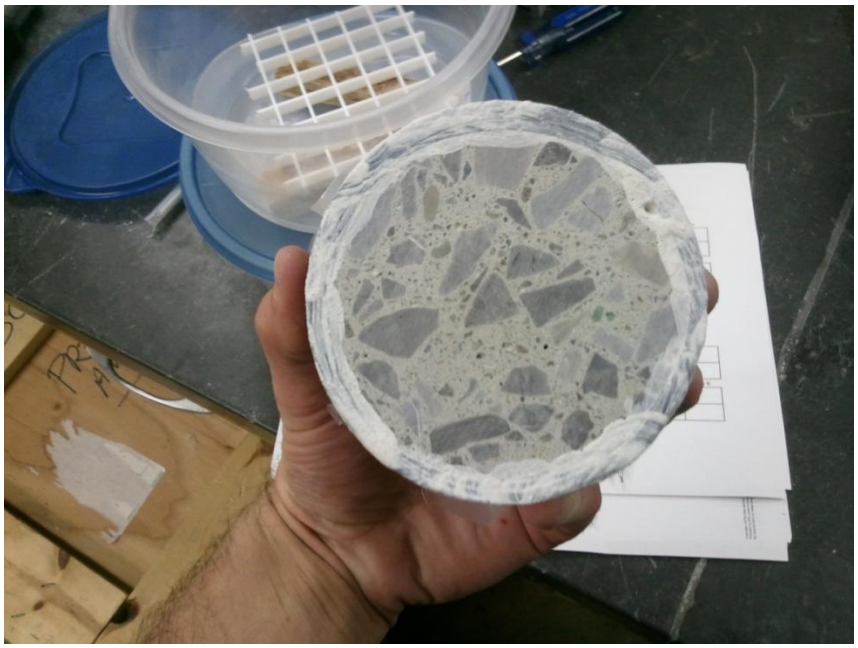

Figure **3-32**: Masonry waterproofing sealant to prevent moisture ingress through the interface between concrete and vinyl electricians tape.

Figure **3-33**: ASTM C 1585 water bath setup

**Chapter 4**

# Chapter 4: Results and Discussion

This chapter will provide the results and discussion regarding the mixture proportioning of the natural sand concrete and glasscrete mixtures. The results for each mixture are shown for mixture proportioning and testing of fresh and hardened properties of concrete.

## 4.1. ACI 211.1 Mixture Proportioning

Table 4-1 shows the final mixture proportioning results for each mixture after trial batch adjustments. Up to five (5) trial batches were made for each mix in order to match the target slump, air content, and compressive strengths. Figure 4-1 shows a few of the cylinder specimens in the moist curing room that were used for strength measurements. It can be seen in Table 4-1 that to achieve similar compressive strength, the w/cm needs to be reduced for glasscrete mixtures. Table 4-2 shows the mortar mixture proportions. The mortar mixtures were attained after the concrete mixtures were properly proportioned. This will be discussed further in the next section.

Figure **4-1**: Glasscrete and concrete specimens during moist curing

Table **4-1**: Research final concrete mixtures (aggregates in oven dried condition)

| | N5,5.0" | G5,5.0" | N4,1,5" | G4,1,5" | N4,5.0" | G4,5.0" | N0.48,5.0" |
|---|---|---|---|---|---|---|---|
| Design 28 day f'c (lbs./in$^2$) | 5000 | 5000 | 4000 | 4000 | 4000 | 4000 | ? |
| Design Slump (") | 5.0" | 5.0" | 1.5" | 1.5" | 5.0" | 5.0" | 5.0" |
| Design Air Content (%) | 3.0 | 3.0 | 3.0 | 3.0 | 3.0 | 3.0 | 3.0 |
| Cement (lbs./yd$^3$) | 539.1 | 590.5 | 421.0 | 450 | 424.6 | 504.2 | 504.2 |
| Fly Ash (lbs./yd$^3$) | 134.8 | 147.6 | 105.3 | 112.5 | 106.1 | 126.0 | 126.0 |
| Water Content (lbs./yd$^3$) | 310 | 310 | 300 | 270 | 302.5 | 302.5 | 302.5 |
| Coarse Aggregate (lbs./yd$^3$) | 1676.2 | 1676.2 | 1676.2 | 1676.2 | 1676.2 | 1676.2 | 1676.2 |
| Fine Aggregate (lbs./yd$^3$) | 1285.9 | 1193.8 | 1442.2 | 1446.4 | 1431.9 | 1305.8 | 1344 |
| w/cm | 0.46 | 0.42 | 0.57 | 0.48 | 0.57 | 0.48 | 0.48 |
| Paste Content (%) | 0.34 | 0.35 | 0.30 | 0.29 | 0.31 | 0.32 | 0.32 |
| Measured Slump (in) | 4.5-5.5 | 4.5-5.5 | 1.5-1.75 | 1.25-1.50 | 4.5-5.5 | 4.5-5.5 | 4.5-5.5 |
| Measured Air Content (%) | 2.0-4.0 | 2.0-4.0 | 2.0-4.0 | 2.0-4.0 | 2.0-4.0 | 2.0-4.0 | 2.0-4.0 |
| Measured 28 day f'c (lbs./in$^2$) | 5420 | 5060 | 4040 | 4240 | 4200 | 4070 | 4750 |

Table **4-2**: Research final mortar mixtures (aggregates in oven dried condition)

| | N5,5.0" | G5,5.0" | N4,1,5" | G4,1,5" | N4,5.0" | G4,5.0" | N0.48,5.0" |
|---|---|---|---|---|---|---|---|
| Cement (lbs.) | 539.1 | 590.5 | 421.0 | 450 | 424.6 | 504.2 | 504.2 |
| Fly Ash (lbs.) | 134.8 | 147.6 | 105.3 | 112.5 | 106.1 | 126.0 | 126.0 |
| Water Content (lbs.) | 310 | 310 | 300 | 270 | 302.5 | 302.5 | 302.5 |
| Fine Aggregate (lbs) | 1285.9 | 1193.8 | 1442.2 | 1446.4 | 1431.9 | 1305.8 | 1344 |
| Paste Content (%) | 0.53 | 0.55 | 0.50 | 0.48 | 0.48 | 0.51 | 0.51 |

A major task was finding the correct dosage of chemical admixtures (plasticizer and air-entrainer) to use in each mixture. The results are shown in Tables 4-3 and 4-4. Testing showed

that for natural sand concrete mixtures, the proper amount of super-plasticizer to add is 0.007fl.oz./lb. of cementitious material to 0.074fl.oz./lb. of cementitious material. The lower range was used for the 1.5" slump mixture and the higher range for the 5.0" slump mixtures. Testing showed for glasscrete mixtures, the proper amount of super-plasticizer to add is 0.007fl.oz./lb. of cementitious material to 0.038fl.oz./lb. of cementitious material. The lower range was used for the 1.5" slump mixture and the higher range for the 5.0" slump mixtures. These values are well within and even below the dosage range recommended by the admixture manufacturer (BASF) of 0.02fl.oz./lb. to 0.15fl.oz./lb. The plasticizer was mixed with the batch water prior to mixing concrete.

Table **4-3**: Chemical admixture proportioning (fluid ounces per pound of cementitious material)

| | N5,5.0" | G5,5.0" | N4,1.5" | G4,1.5" | N4,5.0" | G4,5.0" | N0.48,5.0" |
|---|---|---|---|---|---|---|---|
| w/cm | 0.46 | 0.42 | 0.57 | 0.48 | 0.57 | 0.48 | 0.48 |
| Plasticizer | 0.058 | 0.038 | 0.007 | 0.007 | 0.074 | 0.037 | 0.061 |
| Air-entrainer | 0.005 | 0.005 | 0.002 | 0.002 | 0.006 | 0.005 | 0.005 |

Table **4-4**: Chemical admixture proportioning (fluid ounces per cubic yard of concrete)

| | N5,5.0" | G5,5.0" | N4,1.5" | G4,1.5" | N4,5.0" | G4,5.0" | N0.48,5.0" |
|---|---|---|---|---|---|---|---|
| w/cm | 0.46 | 0.42 | 0.57 | 0.48 | 0.57 | 0.48 | 0.48 |
| Plasticizer | 190 | 136 | 18 | 19 | 190 | 115 | 187 |
| Air-entrainer | 15 | 17 | 19 | 19 | 15 | 15 | 15 |

Testing was also performed to determine the dosage of an air-entraining admixture. Testing showed that for natural sand mixtures, the proper amount of air-entraining admixture to add is 0.002fl.oz./lb. of cementitious material to 0.006fl.oz./lb. of cementitious material. The lower range was used for the 1.5" slump mixture and the higher range for the 5.0" slump mixtures. Testing showed for glass sand mixtures, the proper amount of air-entraining admixture to add is 0.002fl.oz./lb. of cementitious material to 0.005fl.oz./lb. of cementitious material. The lower range was used for the 1.5" slump mixture and the higher range for the 5.0" slump

mixtures. These values are well within the range the recommended dosages by the admixture manufacturer (BASF) of 0.002fl.oz./lb. to 0.040fl.oz./lb. The air entrainer was added to a separate portion of the batch water prior to mixing concrete.

## 4.2. Fresh Properties

In order to achieve a similar slump of five inches, glasscrete required on average 30% to 40% less super plasticizer than the natural sand concrete mixtures (Table 4-4). The super plasticizer demand was similar to achieve a slump of 1.5". Previous studies have reported either an increase or a decrease of slump when fine glass aggregates were used as a natural sand substitution (Rajabipour et al. 2009; Polley et al. 1998). Field workers noted that glasscrete mixtures demonstrated adequate workability and showed little problems with finishing (Polley et al. 1998). This study's results agree with Kou and Poon on improving workability and reducing super plasticizer demand when glass sand is used (2009). The glass aggregate's smooth surfaces in comparison with rough surfaces of natural sand can result in lower surface area at similar particle sizes. The lower sand surface area can lead to better workability at similar paste content. Also, the smooth glass surface may produce a reduction in friction with the fresh cement paste and cause greater workability. At the same time, glass's angularity may reduce workability. This study observed that for glasscrete and natural sand concrete mixtures with similar target 28 day strengths and five inch slump, glasscrete can achieve its designed slump with the use of less plasticizer. At the same w/cm, glasscrete also requires less plasticizer to reach five inch slump (Table 4-4).

The fresh air content of concrete mixtures was measured according to ASTM C 231. The target air content of 3.0% was attained via trial and error with multiple mixtures (Table 4-4). It can be seen that glasscrete and natural sand concrete mixtures with similar design slumps require

approximately the same amount of air entrainer. Regardless of the mixture, air entrainer was necessary to attain the designed fresh air content.

### 4.3. ASTM C 39: Compressive Strength

Using trial batches, mixture proportions were adjusted using seven (7) days compressive strengths. After finalizing the proportions, larger mixtures were batched that allowed the testing of the concrete's compressive strength at 1, 3, 7, 28, and 90 days. For each mixture, three (3) duplicate specimens were tested. Table 4-5 provides strength results for the various mixtures tested. Figures 4-2, 4-3, 4-4, and 4-5 are also provided to show the strength gain over time for each mixture. The coefficient of variation and range of acceptability percentages are offered in Tables 4-6 and 4-7. Please note error bars were not included because they were too small to appear on the figures.

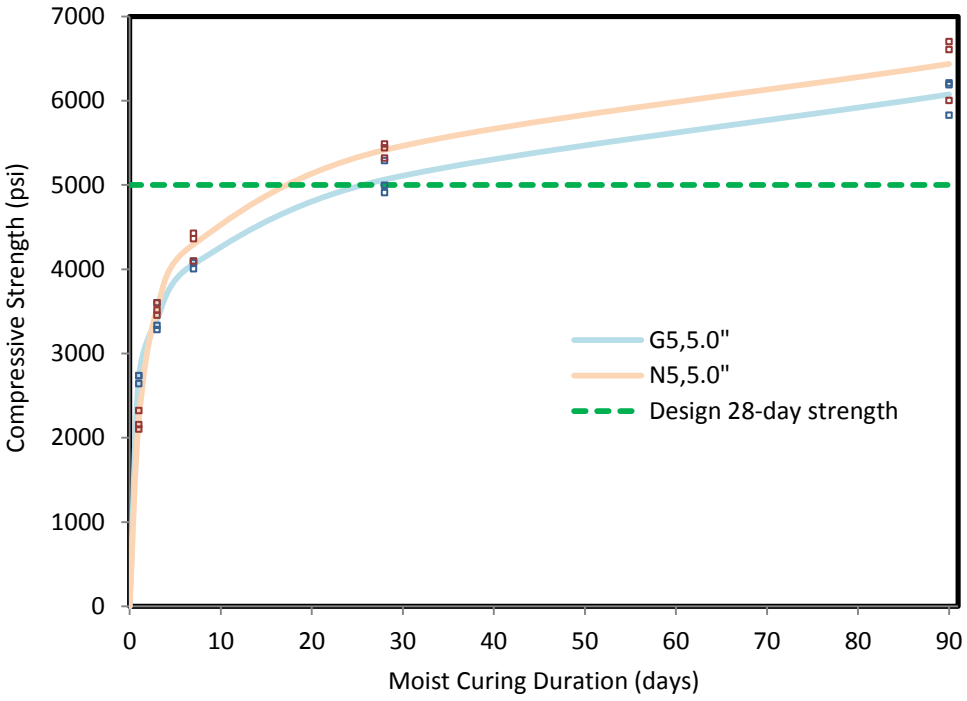

Figure **4-2**: Compressive strength gain for G5,5.0" and N5,5.0"

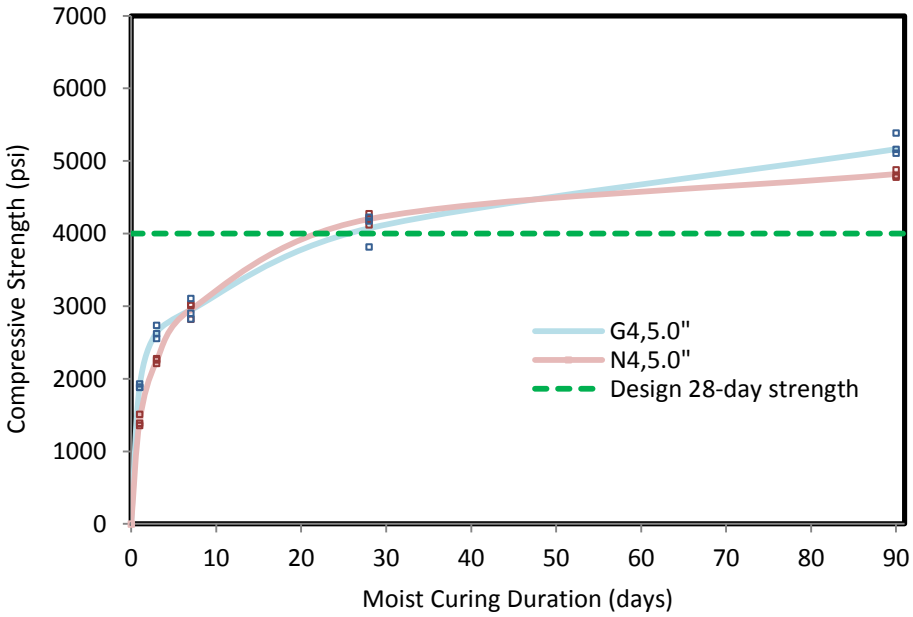


Figure **4-3**: Compressive strength gain for G4,5.0" and N4,5.0"

.

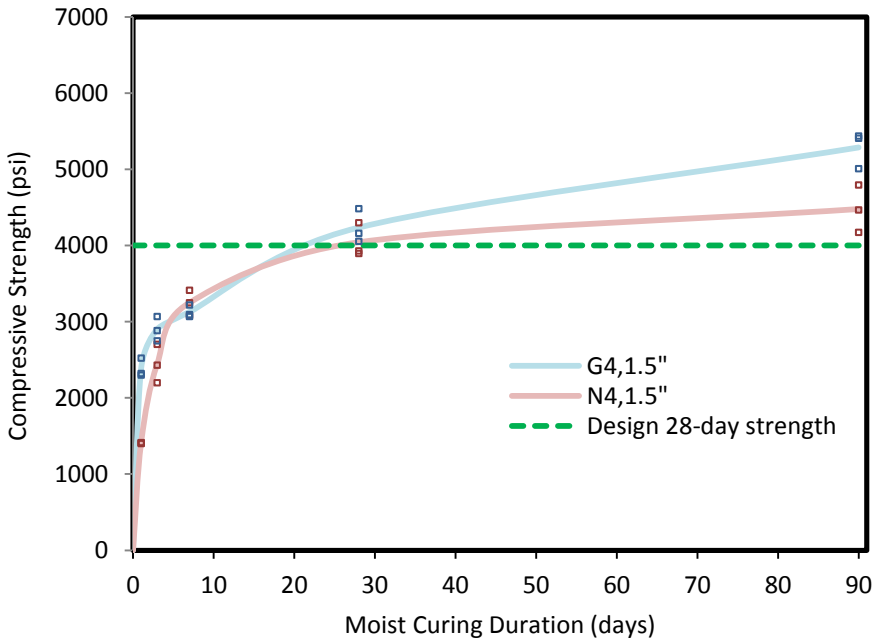


Figure **4-4**: Compressive strength gain for G4,1.5" and N4,1.5"

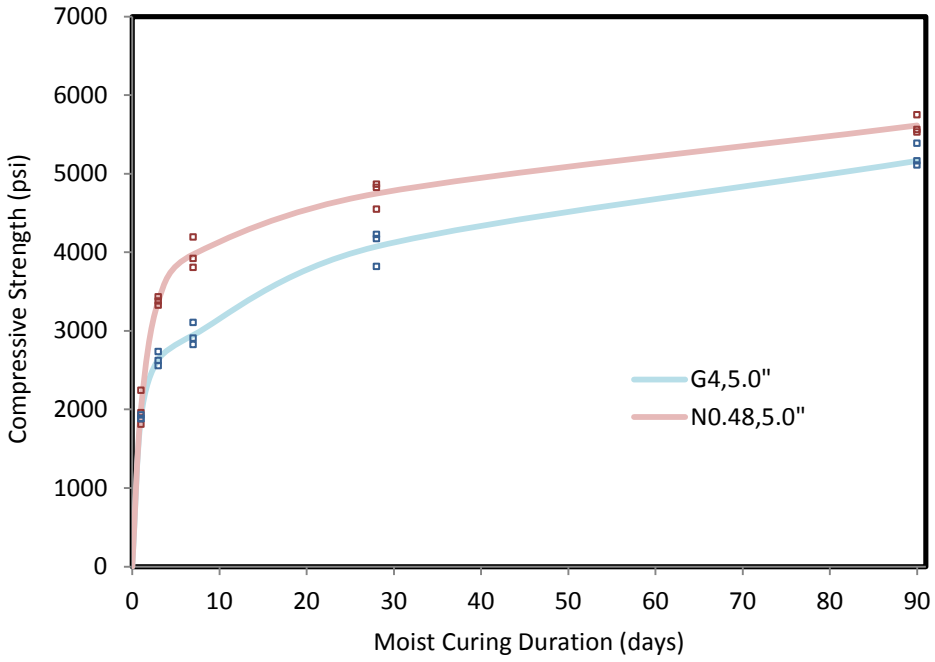


Figure **4-5**: Compressive strength gain for G4,5.0", N4,5.0", N0.48,5.0"

Figures 4-2, 4-3, and 4-4 and Table 4-5 show glasscrete mixtures require a lower w/cm to achieve the same 28 day compressive strength as natural sand concrete mixtures. Those tables and figures also show that glasscrete mixtures have a greater initial strength due to lower w/cm. Natural sand concrete may eventually gains a similar or greater strength. Lower w/cm concrete has lower paste porosity, allowing the specimen to sustain a greater load earlier (Mindess et al. 2003). However, as the concrete matures, the weak bond of glass aggregate to hydrated cement paste becomes the weak link causing glasscrete to fail at a lower load. When comparing natural sand to glass sand, natural sand may allow for a better bond between itself and the cement paste due to a greater surface roughness or more absorption capacity.

Table **4-5**: Compressive strength at various ages for glasscrete and natural sand concrete (lbs./ft$^2$)

| | N5,5.0" | G5,5.0" | N4,1.5" | G4,1.5" | N4,5.0" | G4,5.0" | N0.48,5.0" |
|---|---|---|---|---|---|---|---|
| w/cm | 0.46 | 0.42 | 0.57 | 0.48 | 0.57 | 0.48 | 0.48 |
| 1 day | 2190 | 2700 | 1410 | 2380 | 1420 | 1900 | 2010 |
| 3 day | 3520 | 3410 | 2250 | 2900 | 2250 | 2640 | 3380 |
| 7 day | 4290 | 4060 | 3250 | 3130 | 2950 | 2950 | 3970 |
| 28 day | 5420 | 5060 | 4040 | 4240 | 4200 | 4070 | 4750 |
| 90 day | 6440 | 6070 | 4480 | 5290 | 4820 | 5160 | 5610 |

Table **4-6**: Coefficient of Variation (%) for glasscrete and natural sand concrete

| | N5,5.0" | G5,5.0" | N4,1.5" | G4,1.5" | N4,5.0" | G4,5.0" | N0.48,5.0" |
|---|---|---|---|---|---|---|---|
| w/cm | 0.46 | 0.42 | 0.57 | 0.48 | 0.57 | 0.48 | 0.48 |
| 1 day | 4.3 | 1.7 | 0.3 | 4.2 | 4.8 | 1.2 | 9.0 |
| 3 day | 1.7 | 4.1 | 8.4 | 4.5 | 1.2 | 2.8 | 1.3 |
| 7 day | 3.3 | 1.0 | 4.2 | 2.1 | 3.2 | 4.0 | 4.1 |
| 28 day | 1.3 | 3.2 | 4.5 | 4.3 | 1.5 | 4.4 | 3.0 |
| 90 day | 4.8 | 2.9 | 5.6 | 3.7 | 0.9 | 3.2 | 1.7 |
| Avg. | 3.1 | 2.6 | 4.6 | 3.8 | 2.3 | 3.1 | 3.8 |

Table **4-7**: Range (%) of cylinder strengths of three (3) specimens for glasscrete and natural sand concrete

| | N5,5.0" | G5,5.0" | N4,1.5" | G4,1.5" | N4,5.0" | G4,5.0" | N0.48,5.0" |
|---|---|---|---|---|---|---|---|
| w/cm | 0.46 | 0.42 | 0.57 | 0.48 | 0.57 | 0.48 | 0.48 |
| 1 day | 10.1 | 3.6 | 0.7 | 9.2 | 4.8 | 2.7 | 21.6 |
| 3 day | 4.1 | 9.3 | 20.6 | 10.9 | 1.2 | 6.9 | 3.2 |
| 7 day | 6.3 | 2.3 | 10.3 | 4.8 | 3.2 | 9.6 | 9.8 |
| 28 day | 3.1 | 7.5 | 10.0 | 10.1 | 1.5 | 10.0 | 6.7 |
| 90 day | 10.9 | 6.3 | 13.8 | 8.2 | 0.9 | 7.7 | 3.9 |

The coefficient of variation of cylinder strength results are offered in Table 4-6. ASTM C 39 suggests the coefficient of variation shall be less that 3.2%. In addition, ASTM C 39 suggests

the acceptable range of difference between individual cylinder strength results shall be no greater than 10.6% of the mean value for three (3) cylinders (Table 4-7). These precision values are valid for 4.0"×8.0" cylinders between the compressive strengths of 2500 lbs./in$^2$ and 4700 lbs./in$^2$. In this study most of the strength results comply with the precision statement of ASTM. However, some values fall outside the suggested precision values for the coefficient of variation and acceptable range of cylinder strength (comparing three (3) cylinders). This may be a function of using unbounded caps instead of bonded caps. Also, plastic reusable cylindrical molds were used to cast the specimens. Over time, these molds' geometrical shape may deform causing concave ends (Mindess et al. 2003). However, all specimens dimensions were measured prior to testing and conformed to the 2:1 length:diameter relationship after the ends were smoothed with a diamond cut wet-saw. Since precision errors occurred across all mixtures; the cylindrical molds, compressive machine calibration, and steel end restraining ring with neoprene pad should be investigated for possible replacement. Considering the variability of natural sand concrete shown in Table 4-5, glasscrete mixtures do not increase the variability of concrete mixtures. Regardless of the precision values, it is clearly demonstrated that 100% glass sand concrete systems need a reduction in w/cm to reach similar design 28 day strengths of natural sand concrete.

The results shown in Table 4-5 and Figure 4-5 compare the strength development of glasscrete and natural sand concrete. These results show that glasscrete mixtures show a lower strength at all ages at similar a w/cm of 0.48. This difference in strengths at the same w/cm may be attributed to make-up of the glass-paste interface. Figures 4-6 and 4-7 provide correlations between w/cm and compressive strength at 7 days or 28 days for glasscrete and natural sand concrete mixtures. Figure 4-7 also shows ACI 211.1 recommended relationship between w/cm and compressive strength based on empirical data for concrete with 100% Portland cement. It should be noted that the natural sand concrete created in this study used 20% fly ash and attained compressive strength values similar to the ACI 211.1 recommendations. Such figures can serve as

design tools to proportion concrete mixtures containing recycled glass fine aggregate to achieve a target compressive strength. Regression coefficients offered are for a power function regression.

It was observed that glasscrete mixtures at all ages, (especially 90 day test specimens) exhibit a 'progressive' failure. This failure is manifested by small pop-outs of concrete that break off along the final fourth of loading. The cylinder continues to hold load and will not fail immediately upon initial pop-outs. Periodically, unused specimens were cut in half with a wet saw to qualitatively examine the possible segregation. No segregation was noted.

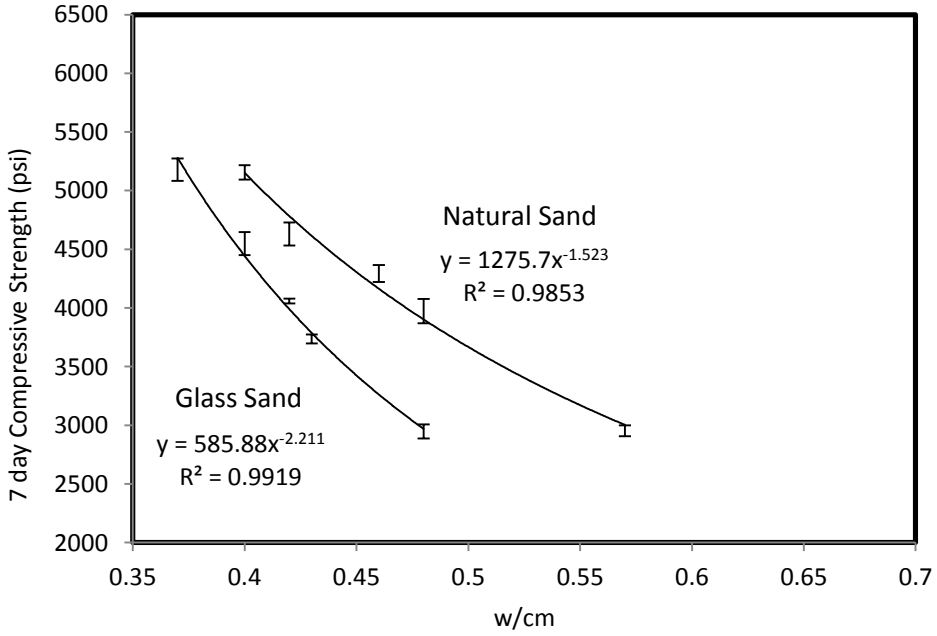


Figure **4-6**: 7 day curves that provide w/cm changes for glasscrete to match concrete strengths

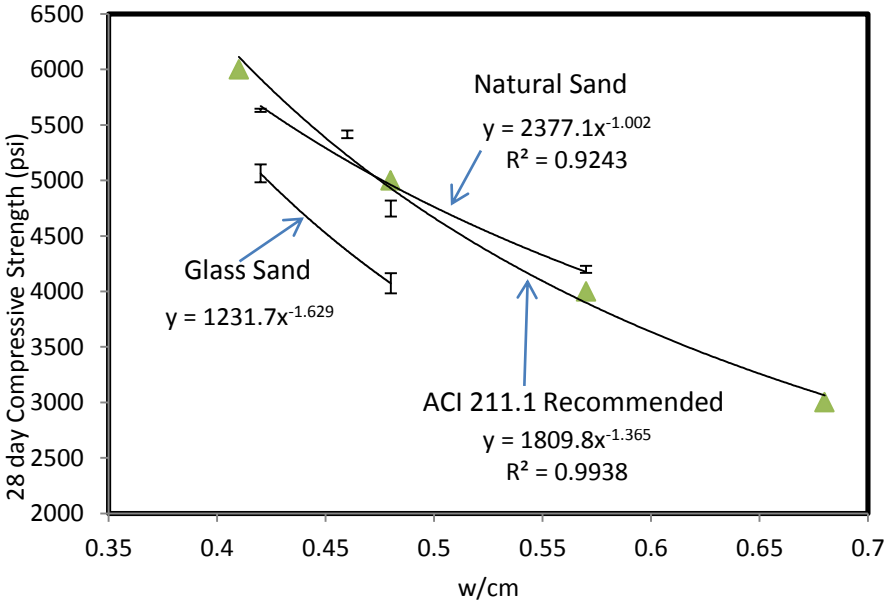


Figure **4-7**: 28 day curves that provide w/cm changes for glasscrete to match concrete strengths

### 4.4. ASTM C 403: Time of Setting

The data in Table 4-8 shows glass sand mixtures have earlier initial and final set times when compared to their natural sand counterpart at the similar strengths. This can be attributed to the lower w/cm glasscrete mixtures setting faster due to lower initial capillary porosity. Figure 4-8 through Figure 4-14 provide information on the time of setting for each mixture. Plots that show a power regression coefficient of correlation $R < 0.98$ ($R^2 < 0.96$) are hand-fit (shown in Chapter 3) to find the initial and final set. The data presented in Table 4-8 are the average initial and final set times for 3 identical specimens for each mixture.

The values shown in Table 4-7 show glasscrete also sets quicker than natural sand concrete at the same w/cm. This differs from tests performed by Terro (2006). More research is necessary to better quantify this observation.

Table **4-8**: ASTM C 403 time of setting values

| | N5,5.0" | G5,5.0" | N4,1.5" | G4,1.5" | N4,5.0" | G4,5.0" | N0.48,5.0" |
|---|---|---|---|---|---|---|---|
| w/cm | 0.46 | 0.42 | 0.57 | 0.48 | 0.57 | 0.48 | 0.48 |
| Paste Content (%) | 53.0 | 54.9 | 50.6 | 47.8 | 48.1 | 51.0 | 51.0 |
| Initial Set (hr:min) | 4:40 | 4:25 | 6:30 | 5:05 | 5:50 | 5:10 | 5:45 |
| Final Set (hr:min) | 6:20 | 5:45 | 8:25 | 6:40 | 7:30 | 6:40 | 7:10 |

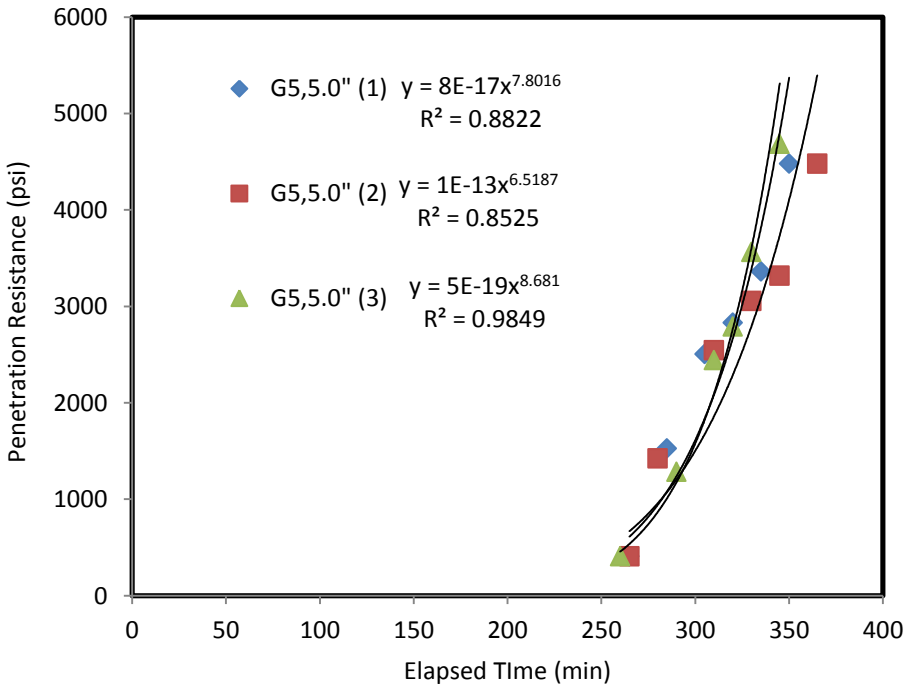


Figure **4-8**: Penetration resistance vs. time of setting curves for G5,5.0"

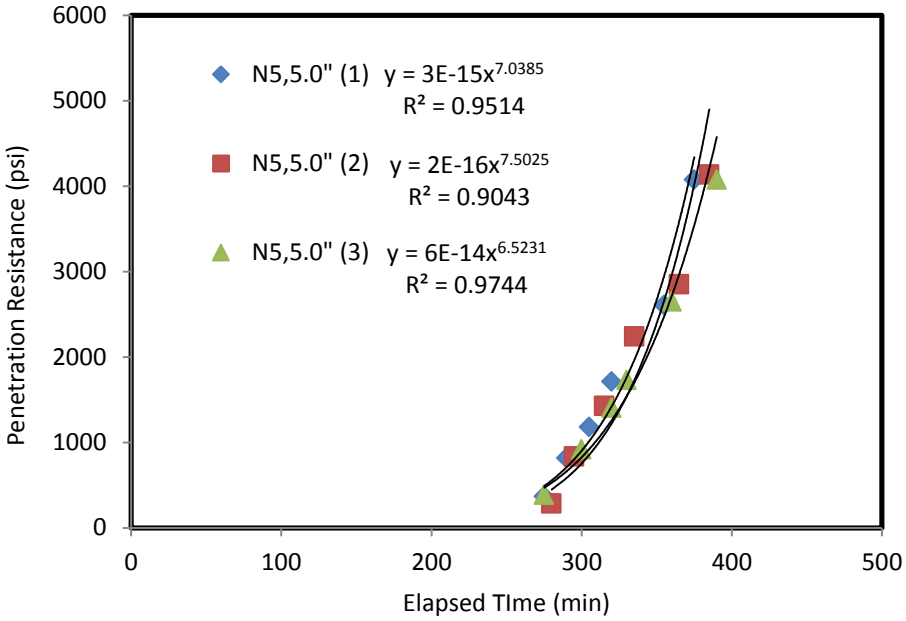


Figure **4-9**: Penetration resistance vs. time of setting curves for N5,5.0"

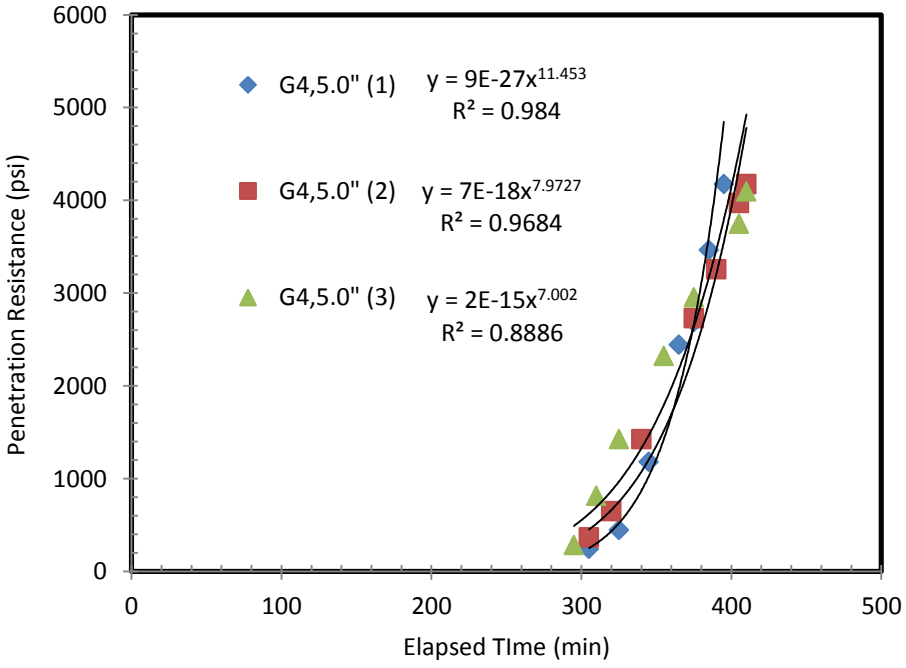


Figure **4-10**: Penetration resistance vs. time of setting curves for G4,5.0"

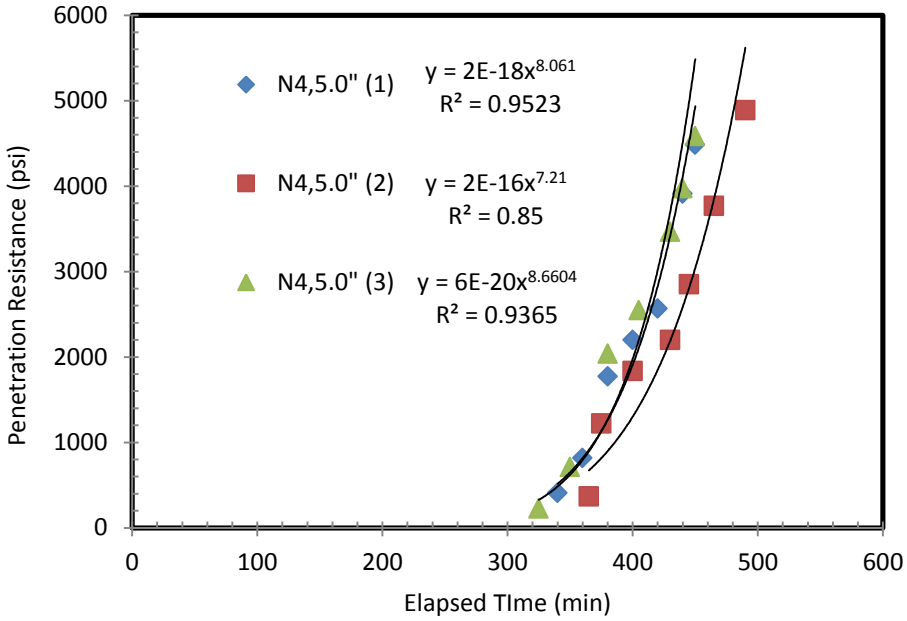


Figure **4-11**: Penetration resistance vs. time of setting curves for N4,5.0"

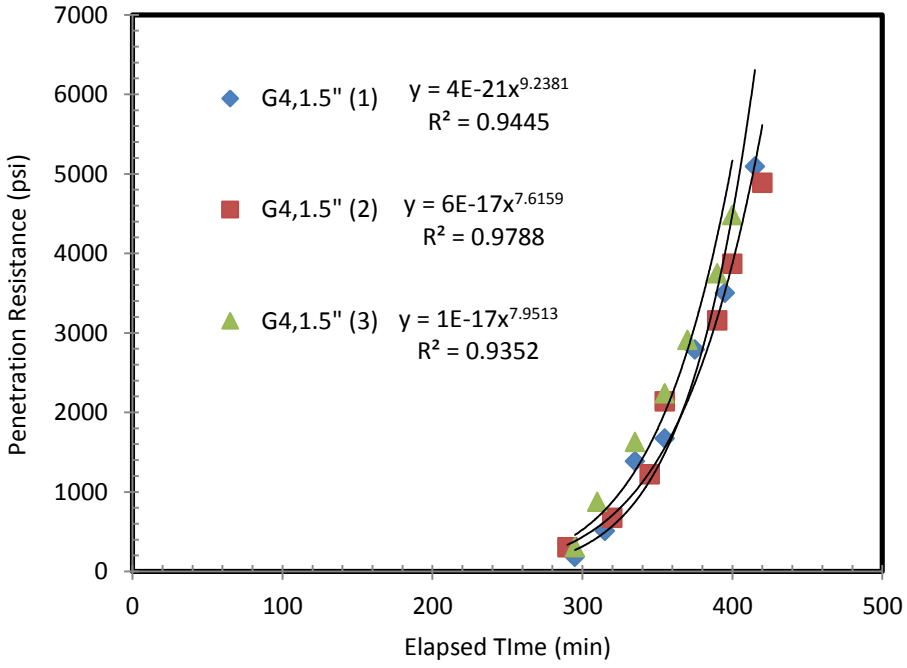


Figure **4-12**: Penetration resistance vs. time of setting curves for G4,1.5"

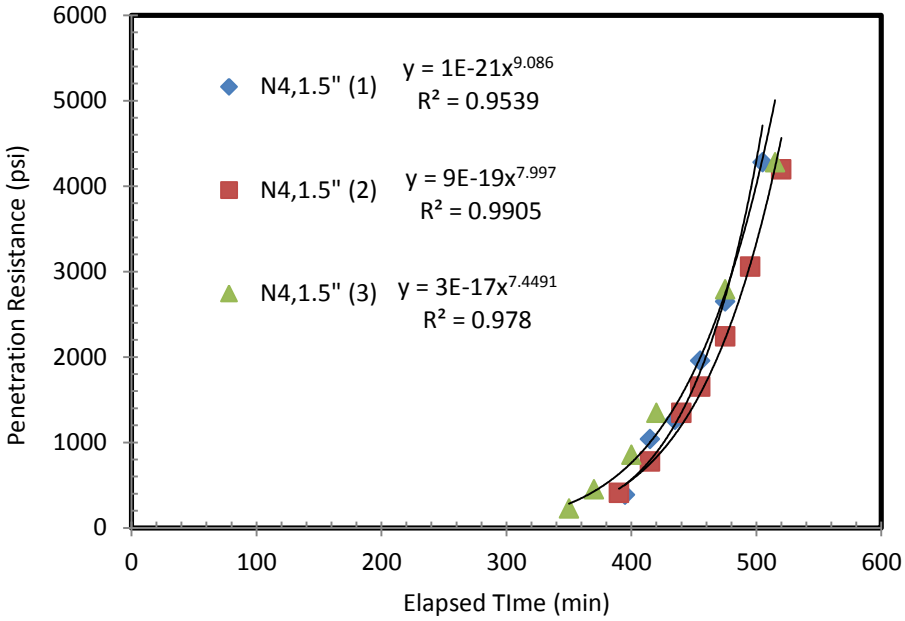


Figure **4-13**: Penetration resistance vs. time of setting curves for N4,1.5"

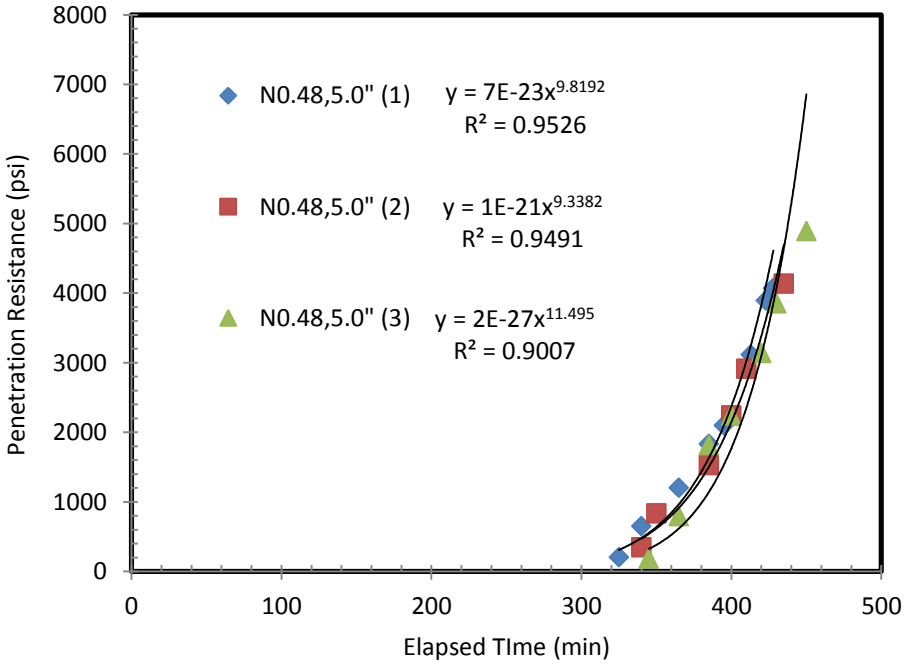


Figure **4-14**: Penetration resistance vs. time of setting curves for N0.48,5.0"

## 4.5. ASTM C 531: Coefficient of Thermal Expansion

The results in Table 4-9 follow a pattern that shows a greater COTE when specimens are tested in the saturated condition. This was expected considering the internal relative humidity of the saturated mortars would allow for a greater change in pore water pressure during the heating and cooling phases. The saturated specimen allows for a consistent relative humidity (and change in relative humidity) and is a more accurate representation of the actual COTE of field conditioned concrete. However, measuring the COTE at the dry condition is also important to evaluate the effect of drying on COTE.

Natural sand mixtures tend to have a greater COTE at the same design strength despite having slightly lower paste contents. Of all minerals, the mineral quartz has the greatest COTE. Therefore, aggregate containing high quantities of quartz (sandstone and quartzite) would exhibit greater volume change upon thermal changes than aggregate containing lower quantities of quartz (Table 3-9 reintroduced as Table 4-10). Algorithms have been created to quantify the aggregate COTE based on the mineralogy of the aggregates (Dossey et al. 1994). These algorithms back-calculate the various minerals' effect on COTE based on measured aggregate COTE and mineralogy (Dossey et al. 1994). It was recognized that quartz contributed the greatest to the COTE of various rock aggregates (Dossey et al. 1994). It should be noted that Dossey et al. took care to differentiate the various forms of $SiO_2$ present in different aggregate sources (1994). The mineralogy of the river sand and glass sand used during this study could be properly defined using quantitative X-Ray Diffraction techniques.

Table 4-9 also shows that at the same w/cm ratio and relative paste content, natural sand concrete has a greater COTE than glasscrete. This may be contributed to natural aggregates higher COTE and greater propensity to increase in volume. These wet and dry values offered in

Table 4-8 should be considered a representation of the relative difference in COTE between glasscrete and natural sand concrete.

Table **4-9**: COTE test results

| Mixture | w/cm | Paste Content (%) | Wet ($10^{-6}$/°F) | Dry ($10^{-6}$/°F) | Wet/Dry |
|---|---|---|---|---|---|
| N5,5.0" | 0.46 | 53.0 | 5.79 | 3.95 | 1.47 |
| G5,5.0" | 0.42 | 54.9 | 4.13 | 3.20 | 1.29 |
| N4,1.5" | 0.57 | 50.6 | 5.79 | 4.54 | 1.28 |
| G4,1.5" | 0.48 | 47.8 | 5.43 | 3.09 | 1.76 |
| N4,5.0" | 0.57 | 48.1 | 4.99 | 4.53 | 1.10 |
| G4,5.0" | 0.48 | 51.0 | 5.20 | 3.30 | 1.58 |
| N0.48,5.0" | 0.48 | 51.0 | 5.48 | 3.22 | 1.70 |

Table **4-10**: COTE ($10^{-6}$/°F) of various aggregate and cementitious mixtures in the saturated condition. (Mindess et al 2003; Meyers 1940; and Neville 1995)

| | |
|---|---|
| Basalt | 3.3-4.4 |
| Granite | 4.0-5.0 |
| Limestone | 3 3 |
| Sandstone | 6.1-6.7 |
| Quartzite | 6.1-7.2 |
| Soda-Lime Glass | 4.0-5.0 |
| Concrete | 4.1-7.3 |
| Steel | 11.0-12.0 |
| 100% paste | 10.3 |
| 50% paste | 7.5 |
| 25% paste | 6.2 |

## 4.6. ASTM C 944: Concrete Abrasion Resistance

The results presented in Table 4-11 show glasscrete mixtures typically offer a greater abrasion resistance than their natural sand concrete counterparts at the same design strength. Glasscrete's w/cm is lower in each comparison. A lower w/cm is known to create a stronger cement matrix than higher w/cm (Neville 1995, Mindess et al. 2003). At the same w/cm, glasscrete is less abrasion resistant. According to basic LA Abrasion tests, glass has a greater mass loss than typical rock aggregate (Wartman et al. 2004). However, concrete abrasion resistance is more concerned with the bond characteristics between the aggregates and the cement paste (Neville 1995, Mindess et al. 2003). Glass's inability to create a strong bond with its surrounding hydrated cement paste will lead to the entire system being more susceptible to abrasion. The coefficient of variation do not differ significantly between glasscrete and natural sand concrete.

Table **4-11**: Average mass loss of three (3) specimens due to abrasion over six minutes

| | N5,5.0" | G5,5.0" | N4,1.5" | G4,1.5" | N4,5.0" | G4,5.0" | N0.48,5.0" |
|---|---|---|---|---|---|---|---|
| w/cm | 0.46 | 0.42 | 0.57 | 0.48 | 0.57 | 0.48 | 0.48 |
| Mass loss (g) | 0.90 | 0.77 | 0.93 | 0.80 | 1.27 | 0.97 | 0.60 |
| COV (%) | 11.1 | 7.5 | 16.4 | 14.4 | 24.1 | 19.6 | 6.0 |

## 4.7. ASTM C 1202: Rapid Chloride Penetration Test

The RCPT results (Table 4-12) demonstrate that all glasscrete mixtures have a greater resistance to chloride penetration than natural sand concrete mixture at similar design compressive strengths. This was expected considering natural sand concrete's higher w/cm allows for a larger volume of capillary pores in the paste (Mindess et al. 2003). These pores allow ions to pass through the concrete at a greater rate. Results show that glasscrete also has a greater

resistance to chloride penetration at the same w/cm when compared to natural sand concrete mixtures. It is understood that glass aggregates have little to no porosity comparing to natural aggregates. Since glass sand is replacing a natural sand aggregate and therefore creating more volume of concrete that is impermeable, it would be expected that glasscrete mixtures would provide a greater resistance to chloride ion penetration. It is worth mentioning that the pozzolanic reactions of the glass sand can be considered to have an effect creating more C-S-H that would provide a less porous medium for ions to travel.

Table **4-12**: RCPT results (Coulombs), bold-faced mixtures overheated

| | N5,5.0" | G5,5.0" | **N4,1.5"** | G4,1.5" | **N4,5.0"** | G4,5.0" | N0.48,5.0" |
|---|---|---|---|---|---|---|---|
| w/cm | 0.46 | 0.42 | 0.57 | 0.48 | 0.57 | 0.48 | 0.48 |
| Charge passed (Coulombs) | 3220 | 2320 | 5040 | 1920 | 4480 | 2540 | 3080 |
| Ion penetration resistivity | Moderate | Moderate | High | Moderate to Low | High | Moderate | Moderate |
| COV (%) | 16.91 | 2.84 | 16.96 | 5.36 | 5.15 | 14.47 | 10.32 |

### 4.8. ASTM C 1585: Sorptivity

The initial sorptivity of glasscrete shown in Table 4-13 is lower than natural sand concrete at the same design twenty-eight day strength by a factor of 2 to 4. The secondary sorptivity of glasscrete is lower than natural sand concrete at the same design twenty-eight day strength also by a factor of 2 to 4. This is expected considering concrete with a lower w/cm will produce less capillary pores per volume of cement paste (Mindess et al. 2003). Less capillary porosity results in less moisture intake. Glasscrete also absorbs less water at the same w/cm than

natural sand concrete. As shown in equation 3-19 (reintroduced as equation 4-1) the sorptivity depends on the permeability of the medium and its effective porosity (Kelham 1988).

$$S = \left(\frac{2\mathrm{K}\Delta P_{capillary}}{z\eta_w}\right)^{0.5} \tag{4-1}$$

Results shown in Figure 4-15 through Figure 4-28 follow the theory provided in Chapter 3 and shown in equation 4-1. Concrete with a lower w/cm will have a lower permeability; therefore, concrete's with a lower w/cm would be expected to absorb less water. Also, the moisture content greatly affects the effective porosity of the concrete specimen. Recent tests by Castro have shown a large dependence on the relative humidity of the specimen (2011). The specimens were conditioned to ASTM 1585 standard; however, studies show ASTM C 1585 may not condition the specimens long enough and it is hinted that the standard may soon be under review for changes (Castro 2011).

Upon breakdown of the testing setup (30 days after initial moisture contact), all specimens that had w/cm greater than 0.48 were observed to have a moist coloration to their top cover (the non-water touching face). These specimens with a much higher w/cm would tend to consume more water. Specimens below a w/cm equal to 0.48 did not show moisture rise at their top cover. Specimens with a w/cm equal to 0.48 vary in appearance and did not show a trend with respect to fine aggregate source. This observation also provides information on the relative capillary rise of greater w/cm when compared to lower w/cm values. This can be seen in Figure 4-29

It is recognized that all initial and secondary sorptivity values have a correlation coefficient ($R > 0.98$, $R^2 > 0.96$) within their individual test that allows for their values to be considered valid.

Table **4-13**: Sorptivity values ($10^{-4}$mm/sec$^{1/2}$)

| | N5,5.0" | G5,5.0" | N4,1.5" | G4,1.5" | N4,5.0" | G4,5.0" | N0.48,5.0" |
|---|---|---|---|---|---|---|---|
| w/cm | 0.46 | 0.42 | 0.57 | 0.48 | 0.57 | 0.48 | 0.48 |
| Paste Content | 0.34 | 0.35 | 0.30 | 0.29 | 0.31 | 0.32 | 0.32 |
| Initial Sorptivity | 13.3 | 6.74 | 34.6 | 9.23 | 37.4 | 10.0 | 15.8 |
| Final Sorptivity | 11.7 | 5.46 | 28.1 | 9.25 | 26.8 | 6.41 | 13.8 |

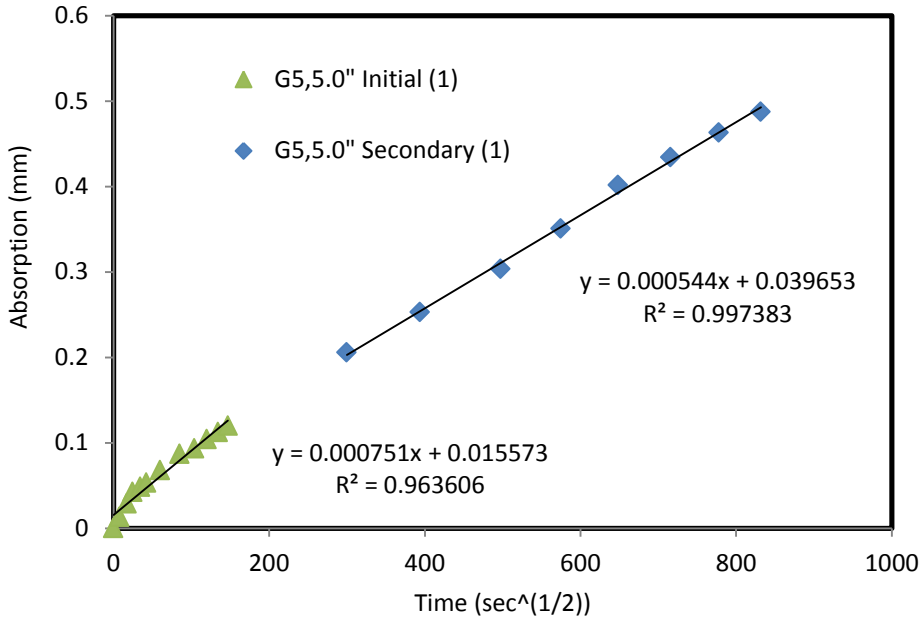


Figure **4-15**: G5,5.0" specimen one sorptivity

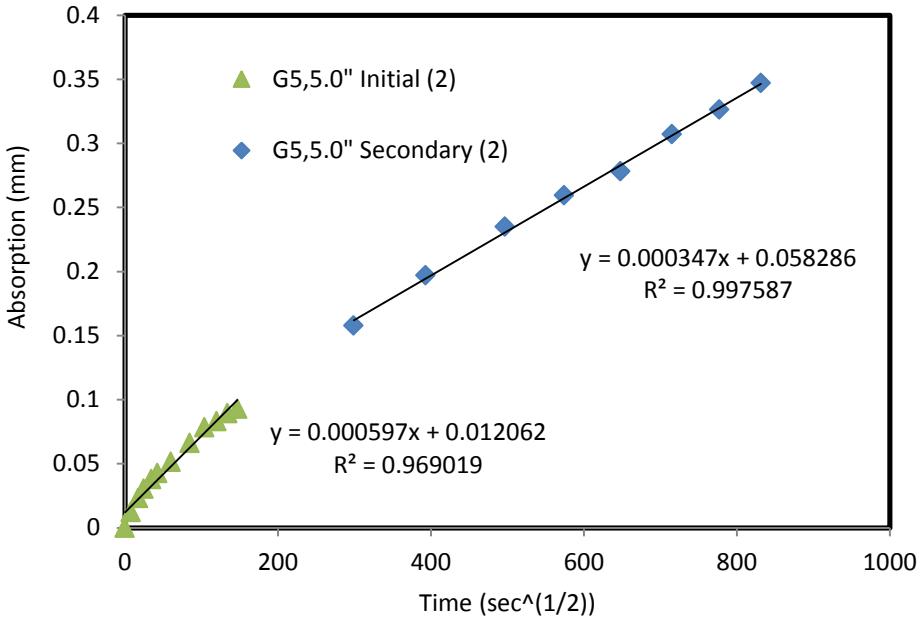


Figure **4-16**: G5,5.0" specimen two sorptivity

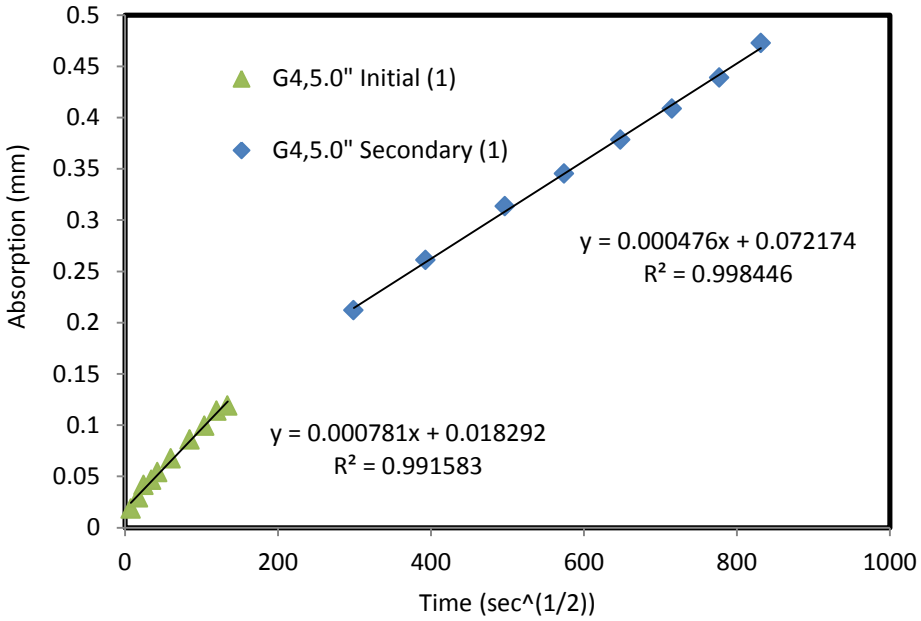


Figure **4-17**: G4,5.0" specimen one sorptivity

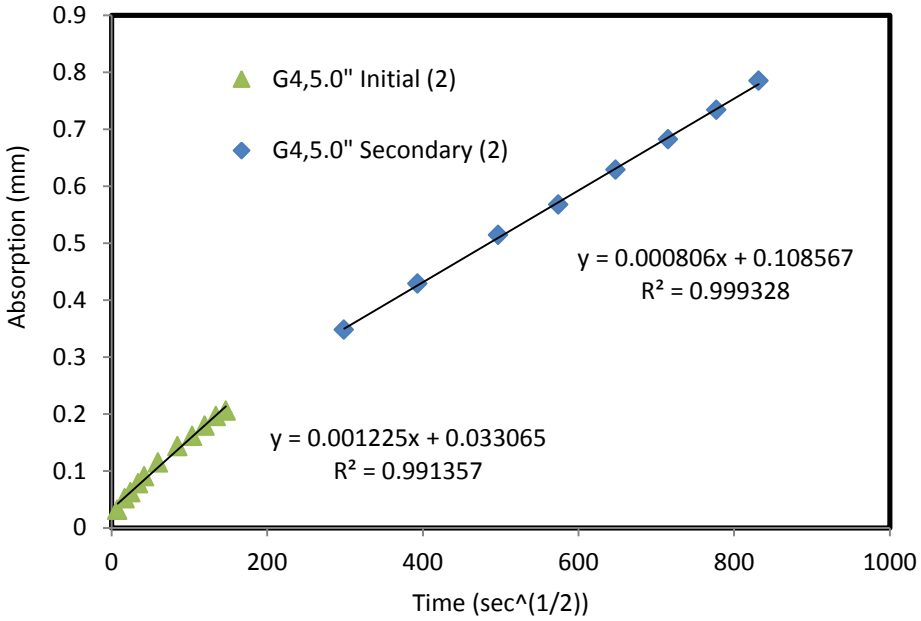


Figure **4-18**: G4,5.0" specimen two sorptivity

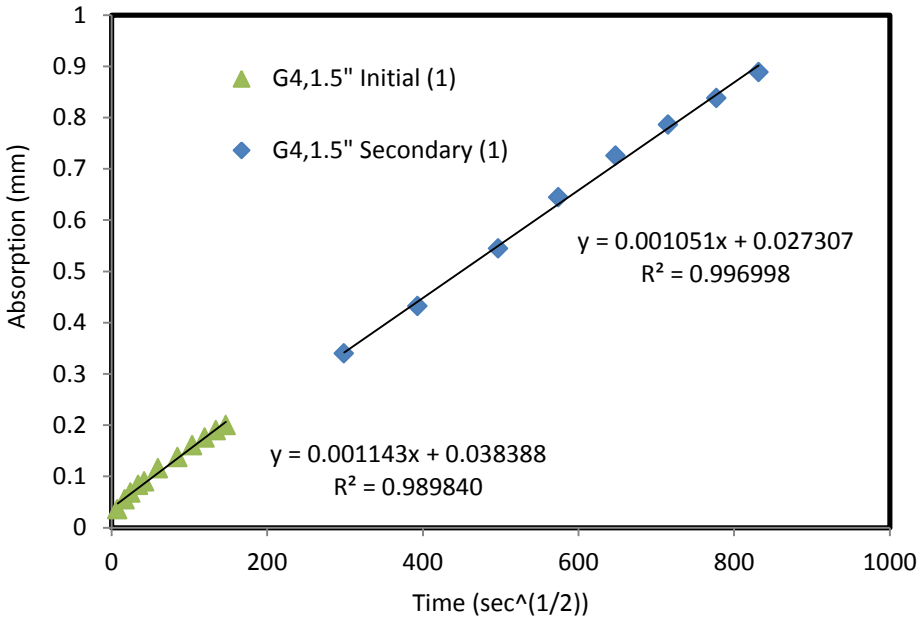


Figure **4-19**: G4,1.5" specimen one sorptivity

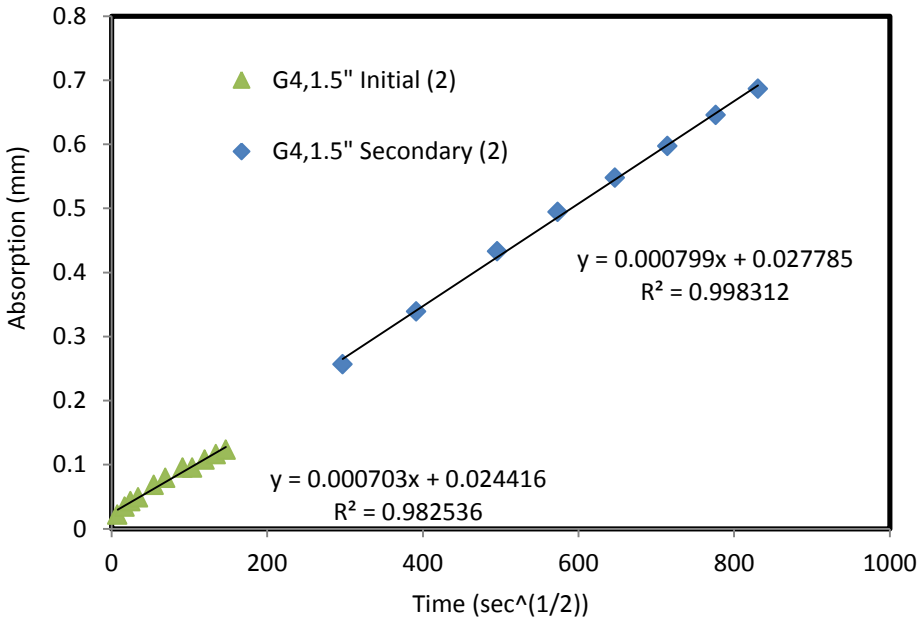


Figure **4-20**: G4,1.5" specimen two sorptivity

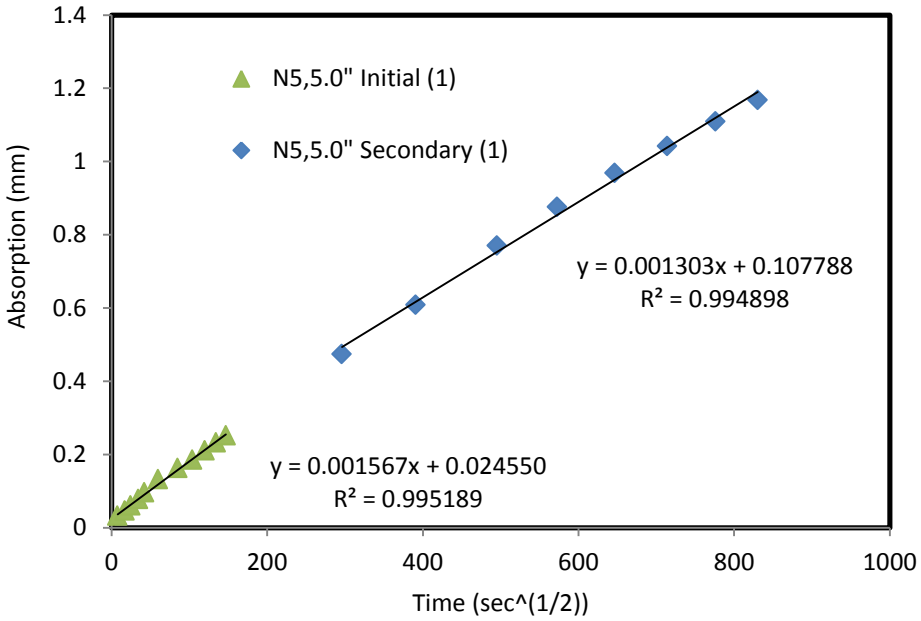


Figure **4-21**: N5,5.0" specimen one sorptivity

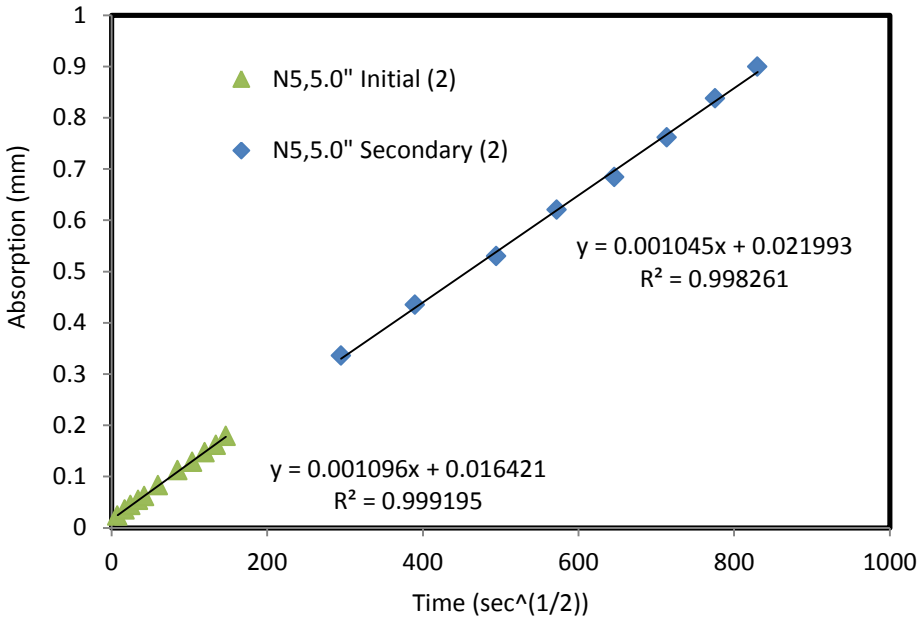


Figure **4-22**: N5,5.0" specimen two sorptivity

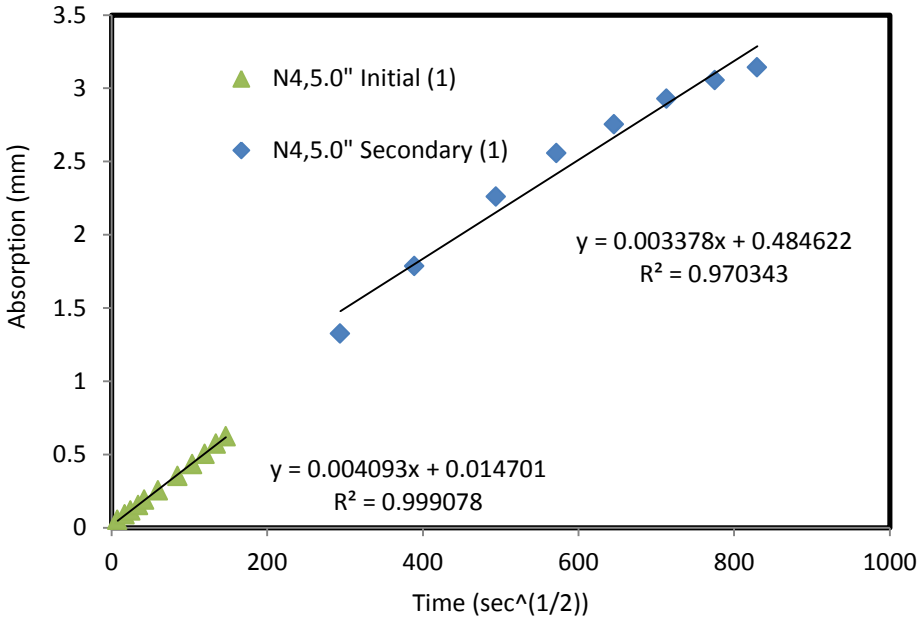


Figure **4-23**: N4,5.0" specimen one sorptivity

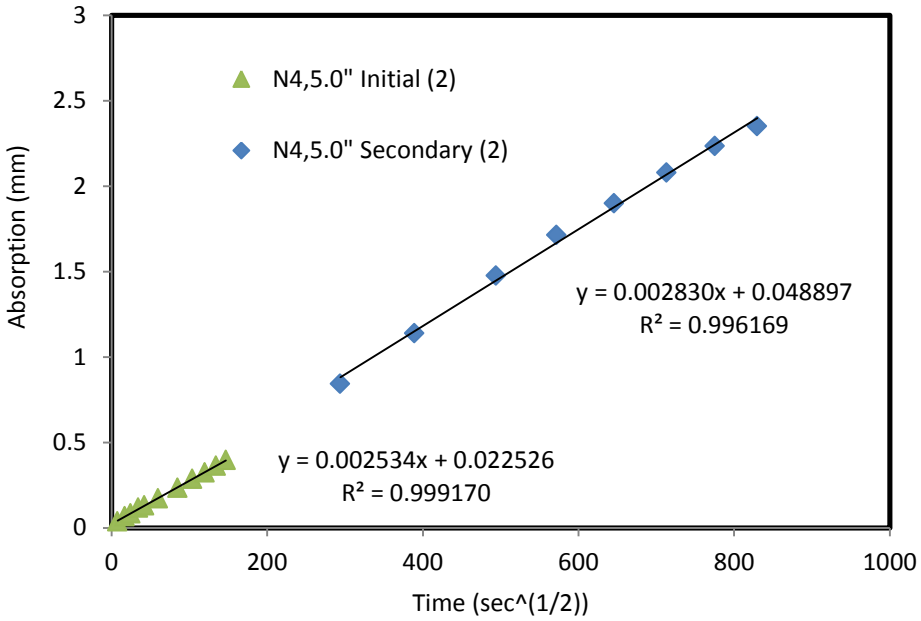


Figure **4-24**: N4,5.0" specimen two sorptivity

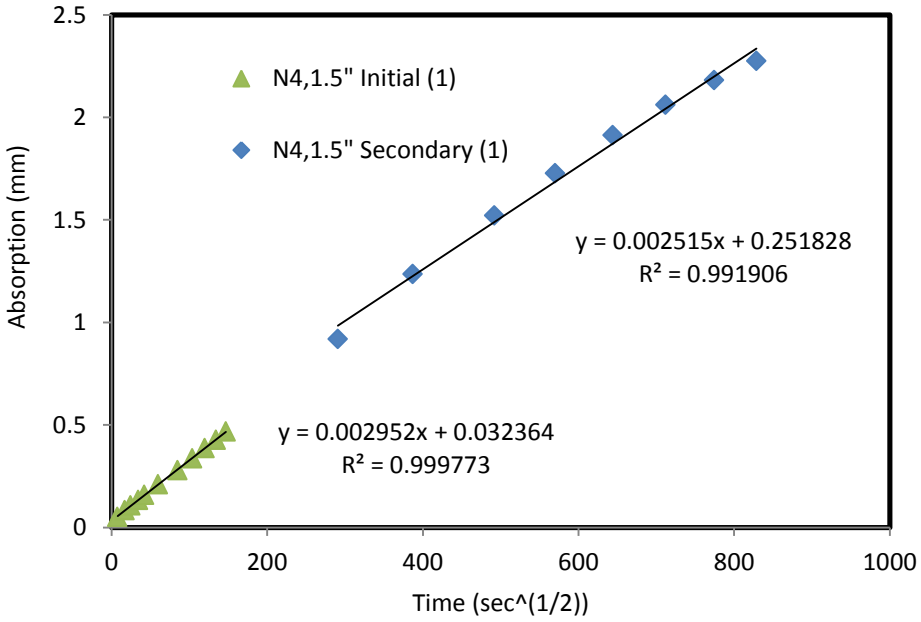


Figure **4-25**: N4,1.5" specimen one sorptivity

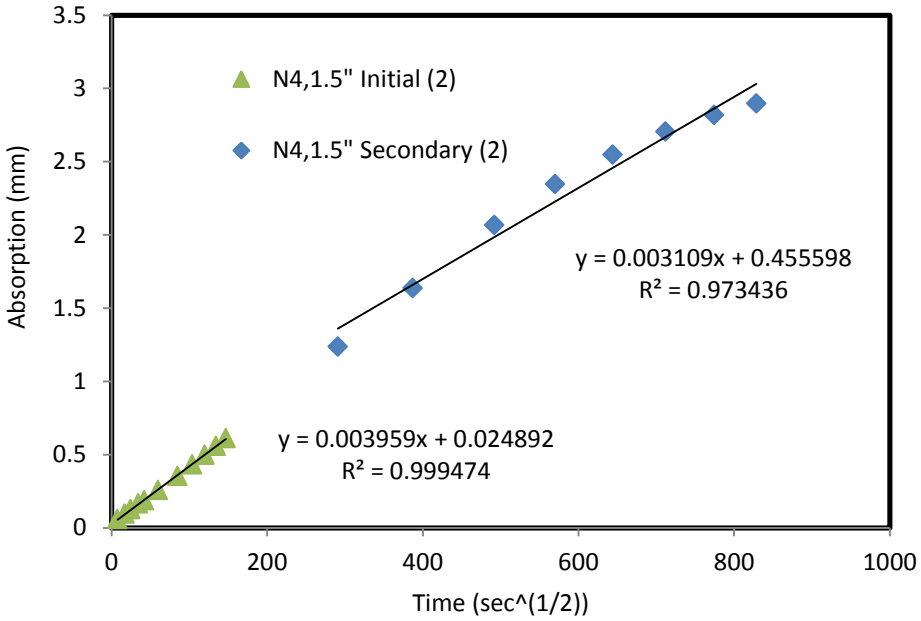


Figure **4-26**: N4,1.5" specimen one sorptivity

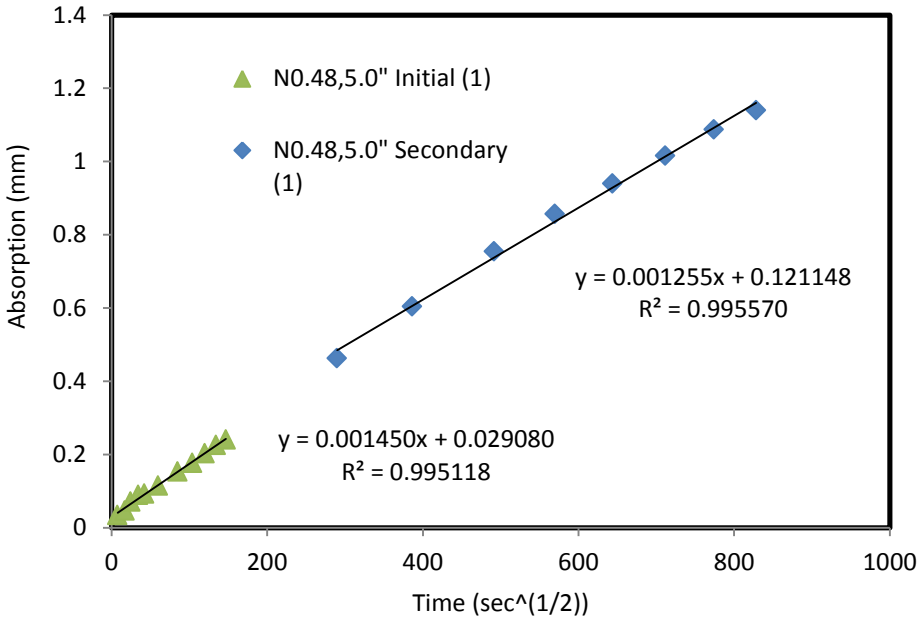


Figure **4-27**: N0.48,5.0" specimen one sorptivity

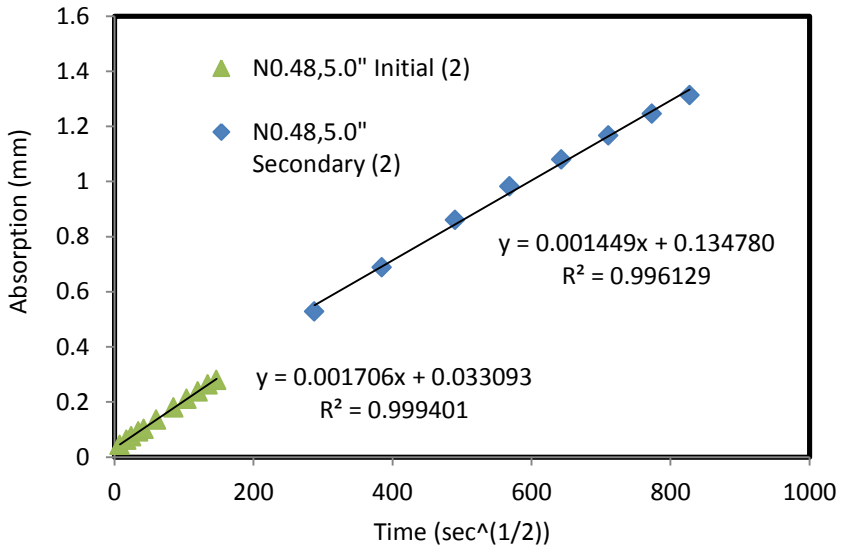


Figure **4-28**: N0.48,5.0" specimen two sorptivity


Figure **4-29**: Coloration of concrete specimens after sorptivity testing

# Chapter 5: Conclusions and Future Research

## 5.1. Conclusions

This study has shown that glasscrete (concrete with 100% glass sand as fine aggregate) mixtures perform favorably when compared to natural sand concrete mixtures. The results of mechanical and durability tests provided in this thesis show glasscrete may perform well in field conditions. The fresh properties of glasscrete also correlate well for use in field applications. Listed below are the major findings of this study:

- Glasscrete mixtures have a lower compressive strength than natural sand concrete mixtures at the same w/cm; therefore, it is necessary to reduce the w/cm in order to attain glasscrete mixtures that have comparable strengths to natural sand concrete mixtures at 7 days and 28 days. The need to reduce the w/cm may be due to the weakness of the glass particle-cement paste interface.
- Glasscrete mixtures require less super-plasticizer to achieve the same slump when compared to natural sand concrete. This may be due to smooth glass surfaces creating a less cohesive bond with the plastic cement paste.
- Glasscrete sets faster at the same design strength. This is due to glasscrete's lower w/cm creating a less porous cement matrix. More testing is necessary to quantify glasscrete's time of setting when compared to natural sand concrete at the same w/cm.
- Glasscrete tends to have a lower COTE and therefore lower tendency to crack at early ages due to thermal contraction. Temperature and moisture content play a key role the COTE values

- Glasscrete has a greater abrasion resistance than natural sand concrete only at similar design compressive strengths. However, at the same w/cm, glasscrete has a lower abrasion resistance. This may attributed to glass aggregates poor bond to cement paste.
- Glasscrete has a greater resistance to chloride penetration as well as a lower sorptivity at both similar design strengths and w/cm. This may be due to the glass sand creating a more impermeable matrix when compared to natural sand.
- Glasscrete requires the use of a supplementary cementitious material in order to mitigate ASR. This study used a Class F fly ash as a 20% replacement of cement by weight. Prior research (Shafaatian et al. 2012) proved this adequate in helping mitigate ASR.

## 5.2. Future Research

This study shows the viability of using glass as a 100% fine aggregate replacement in concrete systems. However, more research is necessary before field implementation. Below is a list gathered by this study:

- More testing should be completed comparing glasscrete and natural sand concrete at the same w/cm. Glasscrete strengths at 3000 lbs./in$^2$ and 6000 lbs./in$^2$ as well as w/cm of 0.30 and 0.60 will provide the Hawaii DOT more information on the strength development of glasscrete when compared to natural sand concrete.
- Fine glass production is a long and tedious task if done manually. Research is necessary to automate these processes in order to integrate glass processing equipment into concrete mixing plants. This will also reduce the transportation costs.
- The effect that washing of glass cullet has on the strength development needs to be examined. Past research shows it may have a substantial impact on the strength development (Polley et al. 1998).

- The glass particle-cement paste interface requires an in-depth examination. The absorption behavior and texture of glass sand plays a key role in the fresh and hardened properties of glasscrete and further testing on the microscopic scale may be necessary to quantify the effects. Macroscopic testing of the modulus of elasticity using ASTM C 469 as well microscopic testing of the modulus of elasticity using atomic force microscopy may help in better understanding the glass particle-cement paste interface.
- Other properties of glasscrete such as flexural strength, splitting tensile strength, and drying shrinkage need to be quantified. These will provide concrete designers a better understanding of field performance, especially with respect to pavements.
- A cost-benefit analysis will be useful to determine the cost of glasscrete when compared to natural sand concrete production. The cost associated with lowering the w/cm and creating glass sand productions plants will be weighed against environmental benefits of less landfilling and less use of virgin aggregate.

## References


ACI Committee 211, "Standard Practice for Selecting Proportions for Normal, Heavyweight, and Mass Concrete," ACI 211.1-91, Reapproved 2009.

ACI Committee 318, "Building Code Requirements for Structural Concrete", ACI 318-11.

American Society for Testing and Materials (ASTM), "Standard Test Method for Compressive Strength of Cylindrical Concrete Specimens," ASTM International, ASTM C 39-05.

American Society for Testing and Materials (ASTM), "Standard Test Method for Slump of Hydraulic-Cement Concrete," ASTM International, ASTM C 143-10.

American Society for Testing and Materials (ASTM), "Standard Test Method for Making and Curing Concrete Test Specimens in the Laboratory," ASTM International, ASTM C 192-07.

American Society for Testing and Materials (ASTM), "Standard Test Method for Air Content of Freshly Mixed Concrete by the Pressure Method," ASTM International, ASTM C 231-10

American Society for Testing and Materials (ASTM), "Standard Test Method for Mechanical Mixing of Hydraulic Cement Pastes and Mortars of Plastic Consistency," ASTM International, ASTM C 306-11.

American Society for Testing and Materials (ASTM), "Standard Test Method for Time of Setting of Concrete Mixtures by Penetration Resistance," ASTM International, ASTM C 403-08.

American Society for Testing and Materials (ASTM), "Standard Test Method for Linear Shrinkage and Coefficient of Thermal Expansion of Chemical-Resistance Mortars, Grouts, Monolithic Surfacings, and Polymer Concretes," ASTM International, ASTM C 531-00 (re-approved 2005).

American Society for Testing and Materials (ASTM), "Standard Test Method for Abrasion Resistance of Concrete or Mortar Surfaces by the Rotating-Cutter Method," ASTM International, ASTM C 944-99 (re-approved 2005).

American Society for Testing and Materials (ASTM), "Standard Test Method for Electrical Indication of Concrete's Ability to Resist Chloride Ion Penetration," ASTM International, ASTM C 1202-10.

American Society for Testing and Materials (ASTM), "Standard Test Method for Measurements of Rate of Absorption of Water by Hydraulic-Cement Concretes," ASTM International, ASTM C 1585-11.

Bartlett, F.M, MacGregor, J.G. (1994) "Effect of Core Length-to-Diameter Ratio on Concrete Core Strengths," *ACI Materials Journal*, 91(4) 339-348.

Bažant, Z.P., (1970) "Delayed Thermal Dilations of Cement Paste and Concrete Due to Mass Transport," *Nuclear Engineering and Design*, 14 308-318

Berke, N.S., Pfeifer, D.W., and Weil, T.G. (1988) "Protection Against Chloride-Induced Corrosion," *Concrete International*, 10 (12), 45-55.

Berry, M., Stephens, J., Cross, D. (2011) "Performance of 100% Fly Ash Concrete with Recycled Glass Aggregate," *ACI Materials Journal*, 108(4) 378-384.

Byars, EA, Zhu, HY, Morales, B. (2004) "ConGlassCrete 1 Project Final Report," The University of Sheffield Centre for Cement and Concrete, 1-54.

Byars, EA, Zhu, HY, Morales, B. (2004) "ConGlassCrete 2 Project Final Report," The University of Sheffield Centre for Cement and Concret, 1-29.

Castro, J., Bentz, D., Weiss, J., (2011) "Effect of Sample Conditioning on the Water Absorption of Concrete," *Cement and Concrete Composites*, (33) 805-813.

DeSouza, S.J., Hooton, R. D., Bickley, J.A., (1997) "Evaluation of Laboratory Drying Procedures Relevant to Field Conditions for Concrete Sorptivity Measurements," *Cement, Concrete, and Aggregates*, CCACDP, 10 (2), 59-63.

Dhir, R.K., Dyer, T.D., Tang, M.C., (2009) "Alkali-Silica Reaction in Concrete Containing Glass," *Materials and Structures* 42, 1451-1462.

Dossey, T., Salinas, J.V., McCullough, B.F., (1994) "Methodology for Improvement of Oxide Residue Models for Estimation of Aggregate Performance Using Stoichiometric Analysis," *Transportation Research Record* 1437 59-64.

Du, L., Folliard, K.J., (2005) "Mechanisms of Air Entrainment in Concrete," *Cement and Concrete Research* 35, 1463-1471.

Emanuel, J.H., Hulsey, J.L., (1977) "Prediction of the Thermal Coefficient of Expansion of Concrete," *ACI Journal,* 74-14 pp. 149-155.

Fraay, A.L.A, Bijean, J.M, De Hann, Y.M., (1989) "The Reaction of Fly Ash in Concrete: A Critical Examination," *Cement and Concrete Research*, 19 (2) 235-246.

Grasley, Z., (2003) "Internal Relative Humidity, Drying Stress Gradients, and Hygrothermal Dilation of Concrete," M.S. Thesis, University of Illinois at Urbana-Champaign, Champaign, IL.

Hall, C., (1989) "Water Sorptivity of Mortars and Concretes: A Review," *Magazine of Concrete Research*, 41 51-61.

Hall, C., Hoff, W.D., (2002) *Water Transport in Brick Stone and Concrete*, Spoon Press, New York, NY.

Hewlett, P.C., *Lea's Chemistry of Cement and Concrete*, 1998, John Wiley & Sons Inc, New York, NJ.

Hobbs, D.W., (1971) "The Dependence of the Bulk Modulus, Young's Modulus, Creep, Shrinkage, and Thermal Expansion of Concrete Upon Aggregate Volume Concentration," *Materials and Construction,* 4 (20) 107-114.

Jin W., Meyer C., Baxter S. (2000) "Glasscrete – Concrete with Glass Aggregate," *ACI Materials Journal,* 97(2) 208-213

Johnston, C.D., (1974) "Waste Glass as Coarse Aggregate for Concrete," *Journal of Testing and Evaluation,* 2 (5) 344-350

Kelham, S., (1988) "A Water Absorption Test for Concrete," *Magazine of Concrete Research,* 40 (143) 106-110.

Kou, S.C., Poon , C.S. (2009) "Properties of Self-Compacting Concrete Prepared with Recycled Glass Aggregate," *Cement & Concrete Composites* 31 107-113.

Leadership in Energy and Environmental Design (LEED®) for new Construction & Major Renovations, U.S. Green Building Council, October 2009.

Limbachiya, M.C., (2009) "Bulk Engineering and Durability Properties of Washed Glass Sand Concrete," *Construction and Building Materials* 23 1078-1083.

Malek, R.I.A, Roy, D.M., (1987) "The Permeability of Chloride Ions in Fly Ash-Cement Pastes, Mortars, and Concrete," MRS Symposium, Vol. 113, Materials Research Society, Pittsburgh, pp. 325-334.

Malhotra, V.M., Mehta, P.K., *High Performance, High Volume Fly Ash Concrete for Building Sustainable and Durable Structure*, Third Edition, 2008, Supplementary Cementing Materials for Sustainable Development Inc., Ottawa, Canada

Maraghechi, H. (2010) "Utilization of recycled glass as sand or cement replacement in concrete materials," M.S. Thesis, University of Hawai'i at Manoa, Honolulu, Hawai'i

Maraghechi, H., Shafaatian, S-M-H., Fischer, G., Rajabipour, F., (2012) "The Role of Residual Cracks on Alkali Silica Reactivity of Recycled Glass Aggregates," *Cement and Concrete Composites*, 34 41-47.

Martys, N.S., Ferraris, C.F., (1997) "Capillary Transport in Mortars and Concrete," *Cement and Concrete Research*, 27 (5) 747-760.

Meyer, C., "Recycled Glass – From Waste Material to Valuable Resource," *International Symposium on Recycling and Reuse of Glass Cullet*, 19-20 March, 2001. University of Dundee, Scotland.

Meyers, S.L, (1940) "Thermal Coefficient of Expansion of Portland Cement –Long Time Test," *Industrial and Engineering Chemistry*, 32 1107-1112 (Easton, PA).

Mindess, S., Young, J.F., Darwin, D., *Concrete, Second Edition*, 2003, Pearson Education, Inc. Upper Saddle River, NJ.

Municipal Solid Waste Generation, Recycling, and Disposal in the United States: Facts and Figures for 2010. US Environmental Protection Agency (EPA), Solid Waste and Emergency Response: www.epa.gov/osw, Washington, DC, November 2011.

Neville, A.M., *Properties of Concrete, Fourth Edition*, 1995, Pearson Education, Limited. Harlow, Essex, England.

Ozyildirim, C., Halsted., "Resistance to Chloride Penetration of Concrete Containing Fly Ash, Silica Fume, or Slag," in *Permeability of Concrete*, SP-108, American Concrete Institute, Detroit, MI, pp. 35-61.

Park, S.B, Lee, B.C., Kim, J.H., (2004) "Studies on the Mechanical Properties of Concrete Containing Waste Glass Aggregate," *Cement and Concrete Research* 34 2181-2189.

Philip, J.R., (1957) "The Theory of Infiltration: 4. Sorptivity and Alegebraic Infiltration Equations," *Soil Science*, 84 257-264.

Popovics, S., (1990) "Analysis of the Concrete Strength Versus Water-Cement Ratio Relationship," *ACI Materials Journal*, 87(5) 517-529.

PCA Cement Manufacturing Fact Sheet (2012), accessed 2012, <http://www.cement.org/briefingkit/pdf_files/ManufacturingFactSheet.pdf>

Popovics, S., (1987) "Attempts to Improve the Bond Between Cement Paste and Aggregate," *Materials and Structures*, 20 32-38.

Popovics, S., (1982) "Strength Relationships for Fly Ash Concrete," *ACI Journal*, 79 (5) 42-49.

Potter, P., E., (1978) "Petrology and Chemistry of Modern Big River Sands," *Journal of Geology*, 86 (4) 423-449.

Powers, T.C., Brownyard, T.L., (1960) "Studies of the Physical Properties of Hardened Portland Cement Paste," *Journal of the American Concrete Institute*, 18 (2) 101-131.

Quan, H., (2011) "The Effects of Change in Fineness of Fly Ash on Air-Entraining Concrete," *The Open Civil Engineering Journal*, 5 124-131.

Rajabipour, F., Maraghechi, H., Fischer, G. (2010) "Investigating the Alkali-Silica Reaction of Recycled Glass Aggregates in Concrete Materials," *ASCE Journal of Materials in Civil Engineering*, 22(12) 1201-1208

Rajabipour, F., Fischer, G., Sigurdardottir, p., Goodnight, S., Leake A., Smith, E., (2009) "Recycling and Utilizing Waste Glass as Concrete Aggregate," Proc., TRB Annual Meeting (CD-ROM), Paper No. 09-2195, Transportation Research Board, Washington, D.C.

Reindl, J, (2003) "Reuse/Recycling of Glass Cullet for Non-Container Uses," accessed April 2012. <http://www.epa.gov/osw/conserve/rrr/greenscapes/pubs/glass.pdf>

Rhoades, R., Mielenz, R.C., (1946) "Petrography of Concrete Aggregate," *Journal of the American Concrete Institute*, 17 (6).581-600.

Saccani, A., Bignozzi, M.,C., (2010) "ASR Expansion Behavior of Recycled Glass Fine Aggregates in Concrete," *Cement and Concrete Research*, 40 531-536.

Sakyi-Bekoe, K.,O., (2008) "Assessment of the Coefficient of Thermal Expansion of Alabama Concrete," M.S. Thesis, Auburn University, Auburn, Alabama.

Sellevold, E.J., Bjøntegaard, Ø., (2006) "Coefficient of Thermal Expansion of Cement Paste and Cocnrete: Mechanisms of Moisture Interaction," *Materials and Structures*, 39 809-815.

Shafaathian, S.M.H,. Akhavan, A., Maraghechi, H., and Rajabipour, F., "How Does Fly Ash Mitigate Alkali-Silica Reaction in Accelerated Mortar Bar Test?" *Cement and Concrete Composites*, in review (April 2012)

Shayan, A., Xu,A., (2003) "Value-Added Utilization of Waste Glass in Concrete," *Cement and Concrete Research*, 34, 81-89.

Stanish, K.D., Hooton, R.D., Thomas, M.D.A., "Testing the Chloride Penetration Resistance of Concrete: A Literature Review," FHWA Contract DTFH61-97-00022, Department of Civil Engineering, University of Toronto, Toronto, Ontario, Canada, 1997.

Tanesi, J., Crawford, G., Gudimettla, J., Ardani, A., (2012) "Coefficient of Thermal Expansion of Concrete," *Concrete International*, April, pp. 55-60.

Terro, M.,J., (2006) "Properties of Concrete Made with Recycled Crushed Glass at Elevated Temperatures," *Building and Environment*, 41.633-639.

Thomas, M.D.A., (2011) "The Effect of Supplementary Cementing Materials on Alkali-Silica Reaction: A Review," *Cement and Concrete Research*, 41 1224-1231.

Topcu, I.B., Canbaz, M. (2004) "Properties of Concrete Containing Waste Glass," *Cement and Concrete Research* 34 267-274.

Turgut, P., Yahlizade, E.S., (2009) "Research into Concrete Blocks with Waste Glass," *International Journal of Civil and Environmental Engineering* 1:4 203-209.

Walker, S., Bloem, D.L., (1960) “Effects of Aggregate Size on Properties of Concrete,” *Journal of the American Concrete Institute* 57-13 pp. 283-298.

Wartman, J., Grubb, D.G., Nasim, A.S.M., (2004) “Select Engineering Characteristics of Crushed Glass,” *Journal of Materials in Civil Engineering*, Nov-Dec, pp.526-539.

Whiting, D., (1988) “Permeability of Selected Concretes,” in *Permeability of Concrete, SP-108*, American Concrete Institute, Detroit, MI, pp. 195-222.

Won, M., (2005) “Improvements of Testing Procedures for Concrete Coefficient of Thermal Expansion,” *Transportation Research Record*, 1919, pp.23-28.

Zhu, H., Byars, E., (2005) “Potential for Use of Waste Glass in Concrete,” *Concrete*, 39 (2) 41-45.

Zoldners, C.G., (1971) “Thermal Properties of Concrete under Sustained Elevated Temperatures,” in *Temperature and Concrete, ACI SP-25*, pp. 1-32.